The functional role(s) of diaphanous related formins in protrusion

Von der Fakultät für Lebenswissenschaften
der Technischen Universität Carolo-Wilhelmina
zu Braunschweig
zur Erlangung des Grades einer
Doktorin der Naturwissenschaften
(Dr. rer. nat.)
genehmigte

D i s s e r t a t i o n

vorgelegt von

Jennifer Block

aus Friesoythe

1. Referent: Professor Dr. Jürgen Wehland

2. Referent: Professor Dr. Martin Korte

eingereicht am: 27.01.2010

mündliche Prüfung (Disputation) am: 01.04.2010

Druckjahr 2010

Vorveröffentlichungen der Dissertation

Teilergebnisse aus dieser Arbeit wurden mit Genehmigung der Fakultät für Lebenswissenschaften, vertreten durch den Mentor der Arbeit, in folgenden Beiträgen vorab veröffentlicht:

Publikationen

Koestler, SA, Rottner, K, Lai, F, **Block, J**, Vinzenz, M, Small, JV. F- and G-actin concentrations in lamellipodia of moving cells. PLoS One. 2009;4(3):e4810.

Lai FP, Szczodrak M, **Block J**, Faix J, Breitsprecher D, Mannherz HG, Stradal TEB, Dunn GA, Small JV, Rottner K. Arp2/3 complex interactions and actin network turnover in lamellipodia. EMBO J. 2008 Apr 9;27(7):982-92.

Block J, Stradal TEB, Hänisch J, Geffers R, Köstler S, Urban E, Small JV, Rottner K, Faix J. Filopodia formation induced by active mDia2/Drf3. J Microsc. 2008 Sep;231(3):506-17.

Tagungsbeiträge

Block J, Stradal TEB, Hänisch J, Geffers R, Köstler S, Urban E, Small JV, Rottner K, Faix J. The role(s) of diaphanous related formins in protrusion (2008). **Actin based motility course**, Institute Curie Paris (France); short talk

Für meine Eltern

Table of contents

1 Introduction

Many cellular processes such as cell migration, adhesion, mitosis, morphogenesis and endocytosis critically depend on a dynamic filament system. In mammalian cells this filament system is composed of three different kinds of cytoskeletal filaments - microtubules, intermediate filaments and actin filaments.

Microtubules consist of αβ-tubulin heterodimers and represent essential components of flagella and the mitotic spindle. *In vivo* microtubules are nucleated within the microtubule organising centre (MTOC) to which they remain attached with their minus ends while their plus ends grow into the cytoplasm. They form a distinct network that provides tracks for motor proteins that are engaged in intracellular transport, the organisation of organelles and cell division (Wade and Hyman, 1997).

Intermediate filaments are stable, rope-like filaments that most likely provide mechanical stability to cells or cell sheets. Data from animal models suggest that they have additional functions in a whole range of metabolic signalling and regulatory processes unrelated to their mechanical function (Pallari and Eriksson, 2006).

Over the last decades many studies have focused on unravelling the precise mechanisms of actin assembly and its regulation. It is evident today that actin polymerisation and depolymerisation is crucial for the formation of protrusive structures such as lamellipodia and filopodia, but the proteins and signalling pathways contributing to lamellipodia and filopodia formation are still under investigation. Lamellipodia formation critically depends on the actin nucleation activity of the Arp2/3-complex, but in terms of filopodia formation much less is known about the specific mechanism of initiation and nucleation.

Recently new classes of actin nucleators were found, one of them being the so called formin family. These proteins have been implicated in many actin-based processes such as cytokinesis, establishment and maintenance of cell polarity, stress fibre formation and cell migration. This protein family consists of 15 members, among them the well studied Diaphanous related formin 3 (mDia2/Drf3) and the yet insufficiently characterised formin FMNL2. In spite of significant efforts to unravel the precise cellular function of different formins, it is still highly controversial how exactly specific formins contribute to the formation of lamellipodia and filopodia.

1.1 Actin polymerization

The actin cytoskeleton is involved in many highly dynamic processes such as cell migration, abrupt or continuous changes and maintenance of cell morphology and tumor metastasis. To ensure that cells are able to respond to a large variety of signals leading to actin rearrangement, actin polymerization has to be fast and tightly regulated. Biochemically however, spontaneous actin polymerisation requires a slow nucleation process. Self assembly of monomeric globular actin (G-Actin) to an actin dimer or trimer is thermodynamically unfavoured, which is why actin nucleators are required to overcome these kinetic barriers (see 1.3.1).

Once a nucleation seed is formed, e.g. triggered by an actin nucleator, it becomes more favourable to add another monomer than to return to a dimer. ATP-Actin is incorporated at both sides of the growing actin filament in a process termed polymerisation to form helical filaments called F-actin (filamentous actin). Electron microscopy experiments of these actin filaments decorated with HMM (heavy mero myosin) revealed that actin filaments are polarized with a fast growing barbed and a slow growing pointed end (Huxley, 1963). As the monomers are shifted within the filament towards the pointed end, ATP-actin is slowly hydrolysed to ADP-actin. ADP-actin has a lower affinity for the growing filament than ATP-actin resulting in dissociation from the filament, a process called depolymerisation. Since ATP hydrolysis lowers the affinity of ADP-bound actin within an actin filament as compared to ATP-bound actin (Korn *et al.*, 1987), it generates a difference in the critical concentration (Cc) between the barbed and the pointed end. Net polymerisation at either end occurs when the G-actin concentration is higher than the critical concentration, and net depolymerisation occurs when the G-actin concentration is lower than Cc. When equilibrium is established (steady state) pointed ends undergo constant disassembly which is exactly compensated by actin association to the barbed end, a process termed treadmilling (Figure 1). In this case actin filaments move forward while keeping a constant length (Pollard, 1986). ADP-actin disassembly from the pointed end constitutes the rate limiting step and determines the concentration of monomeric actin and thereby the rate of barbed end growth (Kirschner, 1980; Wegner, 1976; Wegner, 1977). Continuous incorporation of actin monomers at the barbed end generates a force sufficient to push the membrane forward to form structures such as lamellipodia and filopodia. To couple membrane protrusion and retraction to extracellular signals, actin polymerisation and depolymerisation are tightly regulated by a huge variety of actin binding proteins such as formins and signalling proteins such as Rho-GTPases.

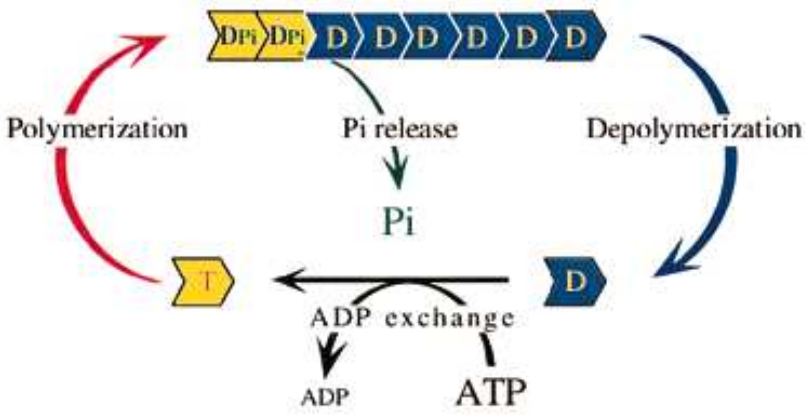

Figure 1: Actin treadmilling at steady state

Actin monomers are incorporated in the barbed end and dissociate at the pointed end. Maturation of the filament leads to the hydrolysis of ATP-actin to ADP-actin and the release of P_i. Subsequently ADP-actin is exchanged to ATP-actin which can reincorporate into the barbed end (from Carlier and Pantaloni, 1997).

1.2 Cellular organisation of the actin cytoskeleton

Cell motility is a prerequisite for many cellular processes such as embryonal development, proper immune response and the abnormal behaviour of metastasizing cancer cells. As a first step in migrating towards certain extracellular stimuli, cells exhibit a characteristic polarized morphology. At the cell front, actin assembly drives the formation of a flat membrane protrusion called lamellipodium and finger like projections termed filopodia (Figure 2). Focal adhesions are formed at the leading edge to anchor the protrusion to the extracellular matrix. Finally, to move forward, the cell retracts its trailing edge by combining actomyosin contractility and disassembly of adhesions at the rear. Dynamic actin structures like lamellipodia, filopodia and stress fibres (Figure 2) are crucial for fundamental processes such as cell migration.

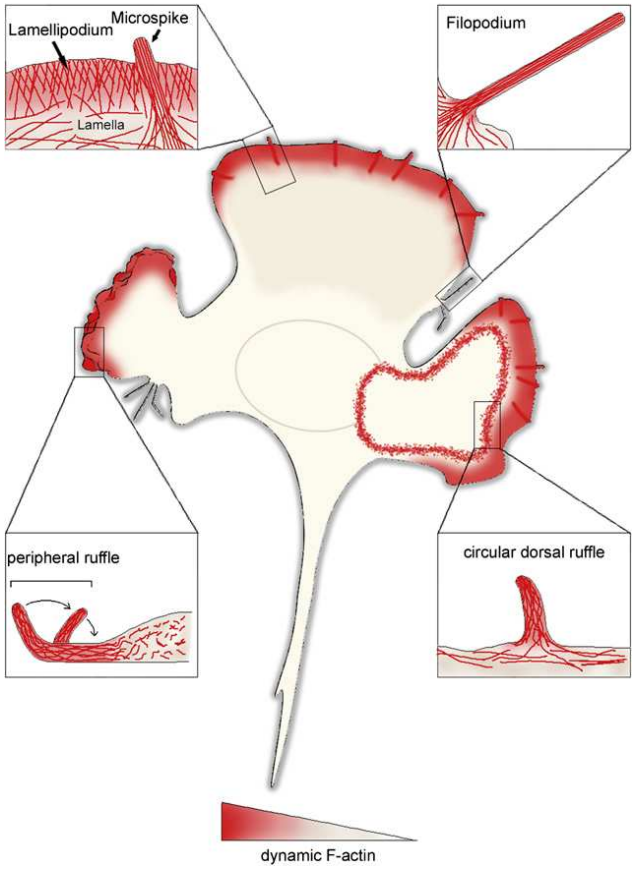

Figure 2: Migrating fibroblast showing different types of membrane protrusions

Main protrusive structures frequently found in migrating cells are lamellipodia, filopodia, peripheral and dorsal ruffles. Microspikes, which remain embedded in the lamellipodium, and filopodia, which protrude beyond the cell periphery, consist of parallel bundles of actin filaments. Lamellipodia are characterised by their crisscross arrangement of actin filaments. By folding up- and backwards in a process termed ruffling lamellipodia generate peripheral or circular dorsal ruffles (bottom), the latter of which are implicated into macropinocytosis. Concentration of dynamic actin filaments (F-actin) at the cell periphery is indicated by the gradient of red intensity (from Ladwein and Rottner, 2008).

1.2.1 Lamellipodia/membrane ruffles

Ingram and Abercrombie were among the first to systematically investigate the leading edge of motile cells (Ingram 1969; Abercrombie 1970). When this structure was moving parallel to the substrate it was referred to as lamellipodium when it turned upward it was designated as membrane ruffle. Subsequent analyses revealed that the lamellipodium consists of a dense array of actin filaments and demonstrated that protrusion was based on actin polymerisation. By injecting fluorescently labelled actin molecules into the cell body, the lamellipodium was discovered to be the primary site of actin incorporation (Glacy, 1983). The fast growing barbed end of the actin filament is orientated towards the plasma membrane (Small *et al.*, 1978) pushing the membrane

forward by incorporation of actin at the barbed end and depolymerisation at the pointed end in a treadmilling fashion.

By applying critical-point-drying-replica technique Svitkina and colleagues observed multiple branches in the lamellipodium, giving rise to the dendritic nucleation model (Svitkina and Borisy, 1999; Mullins *et al.*, 1998). In this model the Arp2/3-complex nucleates new actin filaments, caps their pointed ends and anchors them in a 70° angle to the sides of pre-existing filaments. This is supported by *in vitro* data showing that the Arp2/3-complex nucleates branched actin filaments with a characteristic angle of 70° (Blanchoin *et al*,. 2000; Pantaloni *et al.*, 2001). However, recent data suggest that the critical point drying technique introduces distortions into actin networks, such that crossing filaments may appear branched (Small and Auinger, 2008). Actual negative staining and preliminary cryo electron tomography studies showed no indication for actin filament branching in the lamellipodium, showing that the lamellipodium is a distinct protrusive entity composed of a network of primarily unbranched actin filaments (Koestler *et a*l., 2008; Small and Auinger, 2008). To fully understand the ultrastructure of the lamellipodium, additional electron tomography studies are required.

1.2.2 Filopodia/microspikes

Another type of cellular protrusion is termed filopodium. Filopodia are highly dynamic structures that can be found in many different cell types and were most intensely studied in motile cells such as fibroblasts and the neuronal growth cone. Filopodia are finger-like membrane projections filled with tight bundles of parallel actin filaments. They serve as pioneers during protrusion by sensing the environment e.g. for directed cell migration. Filopodia contain receptors for diverse signalling molecules and extracellular matrix molecules (Galbraith *et al.*, 2007; Vasioukhin *et al.*, 2000). In addition, they play a role in cell-cell adhesion in epithelial cells, wound closure in *Drosophila* (Wood *et al.*, 2002) and in guiding axons and dendrites towards their proper targets in the neuronal growth cone (Gallo and Letourneau, 2004). Similar to lamellipodia, the fast growing ends of actin bundles within the filopodium are oriented towards the plasma membrane and push the membrane forward by continuous elongation.

Lamellipodia frequently contain tight parallel bundles of actin filaments called microspikes, which remain embedded within the lamellipodium upon continuous protrusion. By protruding beyond the leading edge microspikes can develop into filopodia, however microspikes are no essential precursors for filopodia formation.

It is still highly controversial how filopodia are nucleated and so far two alternative models of filopodia formation have been presented. As filopodia are often associated with lamellipodia Svitkina and colleagues proposed that filopodia initiation and maintenance critically depends on Arp2/3-complex nucleated lamellipodial actin filaments (Svitkina *et al.*, 2003). In this so called convergent elongation model the elongation of some barbed ends in the network is terminated by capping, whereas other filament barbed ends are bound by a tip-complex that allows continuous elongation and clustering of several barbed ends. This privileged barbed ends continue to elongate together and are subsequently crosslinked by the actin bundling protein fascin to generate the typical filopodial architecture of actin filaments (Gupton and Gertler, 2007).

However, several independent studies failed to establish the requirement of lamellipodial filaments in filopodia formation (Nicholson-Dykstra and Higgs, 2008; Steffen et al, 2006). These observations led to an alternative model of filopodia formation by *de novo* nucleation. Here, actin filaments in filopodia do not derive from the underlying lamellipodial network, but are nucleated at filopodial tips by actin nucleators such as formins independent of the Arp2/3-complex (Faix and Rottner, 2006). In this case, lamellipodia and filopodia are initiated and maintained by separable core machineries regulated by distinct signalling pathways (Faix *et al.*, 2009). This hypothesis has been supported by recent findings in *Dictyostelium* showing that the formin dDia2 is essential for initiation and maintenance of filopodia in this cell type (Schirenbeck *et al*., 2005). In mammalian cells, increasing evidence suggests that filopodia formation is accomplished by formins such as mDia2 (Yang *et al.*, 2007; Beli *et al.*, 2008; see 1.3.1.2.2).

1.2.3 Stress fibres

Stress fibres were initially identified as thick actin filaments (Lewis and Lewis, 1924; Byers *et al.*, 1984). Nowadays, it is well established that they are thick bundles of actin filaments containing contractile α-actinin-myosin structures, which allows them to produce contractile forces important to maintain tension and cell shape. Stress fibres often terminate at least with one end in focal contacts, which represent regions of very close contact between the ventral cell surface and the substratum (Izzard and Lochner, 1976). A second type of adhesion structure termed focal complexes are defined as smaller adhesion sites residing at the base of lamellipodia, which can mature into focal contacts (Rottner *et al.,* 1999b; Zaidel-Bar *et al.,* 2003).

1.3 Regulation of actin assembly

In vitro, actin polymerisation is too slow to account for the rapid morphological changes and fast protrusion in response to extracellular signals. To accelerate actin assembly *in vivo,* polymerisation is highly regulated by many different actin binding proteins. As mentioned earlier, nucleation, which represents the first step of *de novo* filament formation, is energetically unfavourable for which reason actin nucleators are necessary to catalyse formation of the actin seed. In addition, several other proteins are required to control polymerisation and depolymerisation, terminate filament growth by capping and for stabilisation, bundling and severing of the growing filaments (dos Remedios *et al.*, 2003). A subset of these actin binding proteins has emerged to be essential for actin-based motility *in vitro* by reconstitution of actin-mediated motility on either bacteria or functionalised beads (Loisel *et al.*, 1999; Wiesner *et al.*, 2003). Actin-based motility could be initiated and maintained in minimal motility medium containing an actin nucleator (Arp2/3-complex), an Arp2/3-complex activator (nucleating promoting factor e.g. N-WASP), an actin depolymerisation factor (ADF/cofilin) and a capping protein (Wiesner *et al.*, 2003). Similar experiments in a more recent study revealed an Arp2/3-independent process, where actin-based motility is mediated by actin, profilin and the FH1-FH2-domain of a formin (Romero *et al.*, 2004).

1.3.1 Actin nucleators

A *bona fide* actin nucleator can be defined as a factor that stimulates formation of a filament that grows rapidly at its barbed end. Additionally it is able to efficiently seed polymerization from a pool of profilin-bound actin monomers (profilin–actin), since this may be the dominant species of available ATP-actin monomers in eukaryotic cells (Chesarone and Goode, 2009). Over the last years an increasing number of actin nucleators have been identified and characterized. The first identified and very well characterised actin nucleator was the Arp2/3-complex. Other prominent actin nucleators are members of the formin family and WH2-domain-containing actin nucleators including Leiomodin (Lmod), Cordon bleu (Cobl) and Spire proteins. All of these proteins are proposed to nucleate actin filament networks with distinct properties.

1.3.1.1 Arp2/3-complex

1994 Machesky and colleagues initially purified the Arp2/3-complex from *Acanthamoeba castellanii* using its affinity for the actin-binding-protein profilin (Machevsky *et al.*, 1994). Subsequently, the complex could be isolated from several other organisms including humans (Welch *et al.*, 1997). The complex consists of seven

polypeptides including two actin-related-proteins Arp2 and Arp3, giving the complex its name. The remaining five subunits are referred to as ArpC1, ArpC2, ArpC3, ArpC4 and ArpC5 (Machesky *et al.*, 1994; Higgs and Pollard, 1999). Sequence alignments (Kelleher *et al.*, 1995) and the crystal structure of the bovine complex (Robinson *et al.*, 2001; Nolen *et al.*, 2004) revealed that the subunits Arp2 and Arp3 possess strong structural similarity to actin and function as an actin-like heterodimer to template the nucleation of a daughter filament. Thus, the Arp2/3-complex bypasses the critical step of actin dimer formation and allows further addition of actin monomers to form a filament. Within the Arp2/3-complex, Arp2 and Arp3 constitute the core of the complex with the other subunits organised around them.

The purified Arp2/3-complex possesses little activity on its own. In the crystal structure Arp2 and Arp3 are too far apart to form a pseudo actin dimer that nucleates actin filaments (Robinson *et al.*, 2001). To enable actin nucleation the Arp2/3-complex needs to be activated which is achieved by so called nucleation promoting factors (NPFs) such as WASP/WAVE family proteins. Electron microscopy analyses of the Arp2/3-complex bound to WASP indicate that a major conformational change takes place upon activation bringing Arp2 and Arp3 in close contact to enable filament nucleation (Rodal *et al.*, 2005). Recent data revealed that phosphorylation is crucial for binding of the Arp2/3-complex to the pointed end of actin filaments and nucleating actin filaments, although it is dispensable for binding of NPFs or the sides of actin filaments (LeClaire *et al.*, 2008).

Once activated, the Arp2/3-complex initiates the formation of a new daughter filament that emerges from an existing (mother) filament in a y-branch configuration with a regular 70° branch angle *in vitro* (Mullins *et al.*, 1998; Amann and Pollard, 2001). However recent data failed to detect branched actin filaments within the lamellipodium (Koestler *et al.*, 2008; see 1.2.1), suggesting that additional yet unknown factors regulate the structural organisation of Arp2/3-complex-nucleated actin filaments *in vivo*.

1.3.1.2 Formins

The first identified member of the formin family was Formin1, named on the basis of the hypothesis that this gene was disrupted in mice with limb deformity defects (Woychik *et al.*, 1990). Although a later study showed that the limb defects arose from disruption of an adjacent gene (Zuniga *et al.*, 2004), the name formin has persisted. Formins can be found in a wide range of species including slime molds, plants, yeast, animals and humans (Higgs and Peterson, 2005; Rivero *et al.*, 2005). Bioinformatic studies showed

that eukaryotic species have multiple formin genes, e.g. 15 formin genes were found in mammals.

All formins share the typical formin homology 2 (FH2) domain, which is the most conserved part of these proteins. Crystallographic studies have now yielded structures of the FH2-domains of yeast Bni1 in complex with and without actin (Xu *et al.*, 2004; Otomo *et al.*, 2005b), mouse mDia1 (Shimada *et al.*, 2004) and DAAM1 (Yamashita *et al.*, 2007). All structures indicate that the FH2-domain is capable of dimerisation and is arranged in a donut-like structure, in which the two FH2 polypeptides associate such that the head of each subunit contacts the tail of the other subunit (Figure 4).

In addition to the FH2-domain most formins contain a formin homology 1 (FH1) domain, which is typically located N-terminally to the FH2-domain and comprised of discrete tracks of contiguous proline residues (Higgs and Peterson, 2005; Rivero *et al.*, 2005). The number of polyproline tracks within the FH1-domain is highly variable - Fus1p from *S. pombe* contains a single polyproline track, while mouse mDia1 contains 14 such tracks. Polyproline residues in the FH1-domain are well established to bind the actin-binding protein profilin (see 1.3.1.2.1) (Paul and Pollard, 2008; Neidt *et al.*, 2009).

The predominant class of formins in fungi and mammalian cells are diaphanous related formins (Drfs). Additionally to the FH1 and FH2-domain they are characterised by well-defined intramolecular interactions between the N- and the C-terminus to maintain Drfs in an autoinhibited state. The Drfs include Dia (1, 2 and 3), DAAM (1 and 2), FMNL/FRL (1, 2 and 3), and FHOD (1 and 3) in mammalian cells and Bni1, Bnr1 and sepA in yeast. The N-terminal half of a Drf contains the GTPase-binding domain (GBD), the Diaphanous inhibitory domain (DID), the dimerisation domain (DD) and the coiled-coil domain (CC) (Figure 3A). C-terminally to the FH2-domain Drfs bear a Diaphanous autoinhibitory domain (DAD), which binds to the DID domain to keep the protein in an inactive conformation (Alberts *et al.*, 2001; Watanabe *et al.*, 1999) (Figure 3). Drfs act as effectors of Rho-GTPases, which bind to the GBD and release autoinhibition (Alberts, 2001; Li and Higgs, 2003; Watanabe *et al.*, 1999) (Figure 3B). Crystal structures of either the DAD- or Rho-bound N-terminus of mDia1 indicate that binding of Rho and DAD to the N-terminus is mutually exclusive, although the binding sites are only partially overlapping (Rose *et al.*, 2005b; Lammers *et al.*, 2005; Nezami *et al.*, 2006). Remarkably, binding of RhoA to the N-terminus of mDia1 and binding of Cdc42 to the N-terminus of FRLα, respectively, is not sufficient to fully activate the respective formin (Li and Higgs, 2005; Seth *et al.*, 2006). Therefore it is assumed that additional yet unknown factors are required to fully activate Drfs.

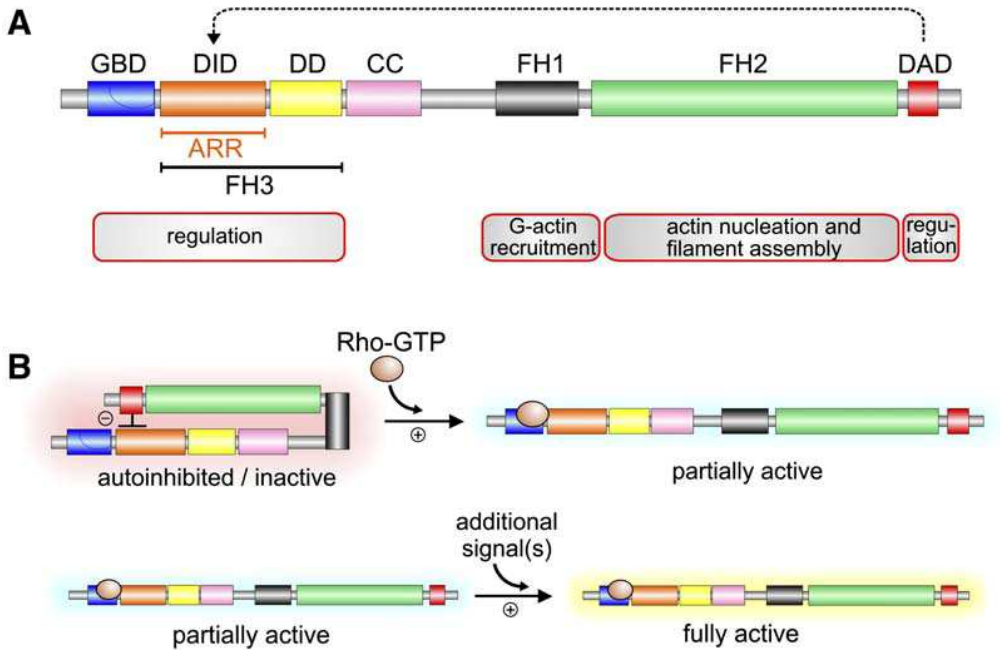

Figure 3: Domain organisation and molecular regulation of diaphanous related formins

(A) Schematic representation of the domain organization of a representative DRF such as mDia1. Abbreviations: GBD, GTPase binding domain; DID, Diaphanous-inhibitory domain; DD, dimerisation domain; CC, coiled coil; FH1, formin homology 1 domain; FH2, formin homology 2 domain; FH3 formin homology 3 domain; ARR, armadillo-repeat region. (B) The interaction of DAD with DID causes autoinhibition of DRFs. This is partly relieved by association of an active, GTP bound Rho-GTPase to GBD, resulting in dissociation of the DAD from the DID domain, leading to a partial activation of the DRF. An unknown additional signal(s) is required to fully activate the DRF (from Faix and Grosse; 2006).

Little is known about how formins are inactivated. It has been assumed that formins can cycle between activated, partially active and inactivate states due to GTP hydrolysis upon Rho binding to GTPase-activating proteins (GAPs, see 1.3.7) (Martin and Chang, 2006; Kovar, 2006). In *S. cerevisiae,* the formin Bnr1 is replaced from the pointed end by a protein called Bud14 *in vitro*, but it remains unclear whether the Bnr1-Bud14 interaction is subsequently disrupted to recycle Bnr1 for new actin assembly (Chesarone *et al.*, 2009). Recent data reported another mechanism of inactivation for mammalian mDia2 during cytokinesis, which is mediated by a posttranslational modification. Activity of mDia2 is regulated by ubiquitin-mediated proteolysis, which is a well-characterised mechanism to degrade proteins via the proteasome. Subsequently, this is thought to contribute to the disassembly of the cytokinetic ring, especially considering that mDia2 is essential for proper ring assembly (DeWard and Alberts,

2009). Whether a general mechanism of formin inactivation exists or if every formin has a specific way of becoming inactive will have to be investigated in the future.

1.3.1.2.1 Formin activities on actin

Formins are well characterised actin nucleators. Initial studies investigated the biochemical effects of isolated FH1-FH2 and FH2-domains of the yeast formin Bni1 on actin, which revealed that nanomolar concentrations directly nucleate actin assembly (Pruyne *et al.*, 2002; Sagot *et al.*, 2002a). Both studies found that actin filaments nucleated by Bni1 are linear (unbranched) and grow by polymerisation at their barbed ends. Additionally, it was reported that intact FH1-profilin interactions are required for Bni1-FH1-FH2 to efficiently assemble filaments from profilin-bound actin monomers.

Up to date, many FH2 and FH1-FH2 fragments have been characterised including mDia (Li and Higgs, 2003; Harris *et al.* 2006a), FRL (Harris *et al*., 2004; 2006a), DAAM1 (Moseley *et al.*, 2006), INF2 (Chhabra and Higgs, 2006) and many others. It is evident that FH2-domains almost universally nucleate actin polymerisation although they vary considerably in their actin assembly promoting potencies. Additionally these studies revealed that all formins nucleate unbranched actin filaments and remain associated with the barbed end as has been initially reported for Bni1. In contrast to the Arp2/3-complex formins lack structural similarity to actin. Kinetic modelling suggested that the FH2 dimer interacts directly with the polymerisation intermediate and stabilises it (Shimada *et al.*, 2004; Xu *et al.*, 2004).

Most FH2-domains maintain a high affinity and persistent association with the barbed end of the filament. As they are processively moving with the growing filament and thereby preventing it from capping proteins (see 1.3.6) while allowing continuous elongation, they are often referred to as processive or leaky cappers (Zigmond *et al.*, 2003). To efficiently nucleate actin filaments, profilin-actin complexes must be inserted between the FH2-domain and the barbed end of the filament (Figure 4). Initially, it has been proposed that the formin is “stair stepping” on the elongating barbed ends, implying that the FH2 dimer equilibrates between alternating open and closed conformations to allow or prevent monomer addition (Xu *et al.*, 2004). In the open state prior to subunit addition one FH2-domain partially dissociates from the actin filament, allowing subunit addition from the solution and thereby re-establishing the attached formin in the closed state. This model has been revised recently leading to a so called “stepping second” mechanism in which actin subunit addition onto the barbed end precedes translocation and dissociation of the formin dimer, meaning that dissociation depends on elongation (Paul and Pollard, 2008; 2009).

In most eukaryotic cells, profilin-actin is the predominant form of monomeric actin available for polymerisation (Pollard *et al.*, 2000; Kaiser *et al.*, 1999). The FH2-domain only poorly assembles filaments from profilin-actin. In contrast, FH1-FH2 is much more efficient in assembling actin filaments from either actin or profilin-actin. The polyproline stretches in the FH1-domain are capable of interacting with profilin-actin and concentrating profilin-actin near the filament barbed ends. In the current model, the FH1-domain forms a flexible rope-like structure (Figure 4) that allows rapid collisions between profilin-actin and the FH2-bound actin filament. After incorporation of the actin monomer into the filament the FH1-domain dissociates from the actin subunit and completes the elongation cycle (Vavylonis *et al.*, 2006).

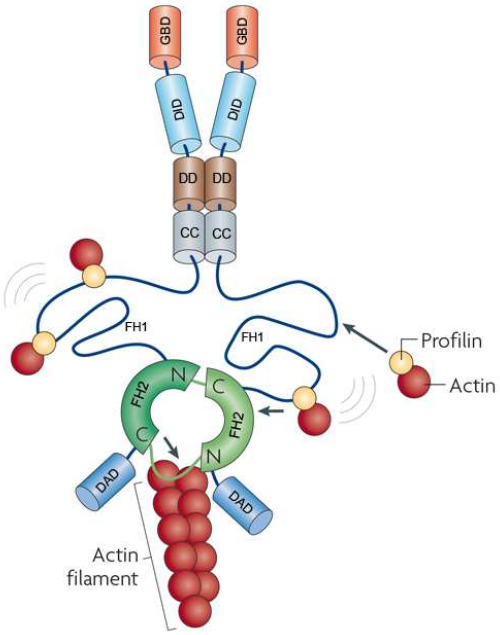

Figure 4: Schematic of a formin in action

The FH2-domain and the dimerisation-domain mediate formin dimerisation. The FH1-domain recruits profilin-actin complexes and delivers them to the FH2-domain for incorporation into the growing filament. The growing actin filament sits inside the dimeric FH2-domains which dynamically move with the growing filament. Grey lines emphasize the dynamic motion of the formin on the barbed end (modified from Chesarone *et al.*, 2009).

Although nucleation, elongation and capping appear to be activities conserved in most formins, these proteins can have additional, more specialised effects on actin filaments including bundling, severing and depolymerisation. Actin bundling activity has been described for the formins INF2 (Chhabra and Higgs, 2006), FRL1 and mDia1 (Esue *et al.*, 2008). FRL1 and INF2 have additionally been implicated in filament severing and

depolymerisation (Harris *et al.*, 2004; Chhabra and Higgs, 2006), but the physiological consequences of these activities remain elusive at this stage.

1.3.1.2.2 Formin functions in cell migration

Formin function has been linked to a wide variety of cellular processes in different cell types and tissues. They are considered to be involved in cytokinesis, endocytosis, cell polarity, morphogenesis, transcription and the stabilisation of microtubules.

Furthermore, mammalian formins have been shown to be critically involved in cell adhesion and motility. In regard to this issue, mDia1 is the most thoroughly studied formin. It functions downstream of Rho in assembling stress fibres (Watanabe *et al.*,1999; Peng *et al.*, 2003; Hotulainen and Lappalainen, 2006), which modulate cell adhesion to the substratum, and are essential for retraction of the trailing edge during cell migration. Several studies utilising active mDia1 variants reported the induction of massive thin actin fibres reminiscent of Rho-induced stress fibres (Higashida *et al.*, 2004; Copeland and Treisman, 2002; Satoh and Tominga, 2001; Tominaga *et al.*, 2000; Watanabe *et al.*, 1999). The fact that depletion of mDia1 does not result in a loss of stress fibres might indicate that other formins can at least partially rescue the effect of mDia1 removal (Chhabra & Higgs, 2007; Peng *et al.*, 2003). A possible candidate affecting stress fibre formation besides mDia1 may be the Drf FHOD1, since active variants have also been described to induce thick F-actin bundles (Gasteier *et al.*, 2003; Takeya *et al.*, 2008; Koka *et al.,* 2003).

Besides its effects on stress fibre formation, active mDia1 elicited the formation of filopodia with the EGFP-tagged formin localising at their tips in several cell types (Sarmiento *et al.*, 2008; Copeland *et al.*, 2007; Higashida *et al.*, 2004). Furthermore, RNA interference of mDia1 efficiently reduced fibroblast migration in scratch-wound assays (Goulimari *et al.*, 2005). Additional data supporting the requirement of mDia1 in cell migration have been provided by Yamana and colleagues, who depleted mDia1 expression in rat glioma cells (Yamana *et al.*, 2006), and Eisenman *et al.*, who analysed T-cells derived from *Drf1*-targeted mice (Eisenman *et al.*, 2007). In both studies, the loss of mDia1 resulted in impaired cell migration. However, it is not clear if the effect of mDia1 on cell migration depends on its impact on actin polymerisation, microtubule stabilisation or is mediated by possible effects on cell polarity. Further studies will be needed to clarify this issue.

Ablation of mDia1 in murine fibroblast cells resulted in an elevated mDia2 (human homolog=Drf3) expression and an increased formation of lamellipodia and filopodia. Microinjection of anti-mDia2 antibody or the expression of a dominant-negative mDia2 blocked Cdc42-induced actin reorganization, suggesting a potential role of mDia2 as an effector of Cdc42 (Peng *et al.*, 2003). Another pathway leading to the formation of filopodia via mDia2 involves the Rho-GTPase Rif, indicating that filopodia formation via mDia2 can be induced by two distinct pathways (Pellegrin and Mellor, 2005). In multiple species, mDia2 localises to the tips of protruding filopodia and has been reported to be required for their formation, as shown for its *Dictyostelium* ortholog dDia2 (Yang *et al.*, 2007; Peng *et al.*, 2003; Pellegrin and Mellor, 2005; Schirenbeck *et al.*, 2005). These findings suggest that the basic principle and mechanism of filopodia formation are conserved in many eukaryotes (Faix and Grosse, 2006). However, it is quite likely that other formins beside mDia2 are involved in filopodia formation, as NIH3T3 and Swiss3T3 cells are well known to form these protrusive structures but only express minute amounts of mDia2 (Block *et al.*, 2008; Tominga *et al.*, 2002).

The haematopoietic FMNL1 (FRL1) has been described to interact with Rac in a nucleotide dependent manner. Over-expression of a truncated FMNL1 variant strongly inhibited cell adhesion and cell migration in macrophages, suggesting a role for FMNL1 in reorganisation of the actin cytoskeleton (Yayoshi-Yamamoto *et al.*, 2000). However, a more recent study observed release of the autoinhibited state only by active Cdc42 but not by Rac (Seth *at al.*, 2006). Other formins such as FMNL2 (Zhu *et al.*, 2008) and FHOD1 (Koka *et al.*, 2003; Westendorf, 2001) have been described to enhance cell motility, but how they influence the actin cytoskeleton needs to be investigated.

1.3.1.3 WH2-domain-containing actin nucleators

Recent studies revealed a third group of actin nucleators comprising Spire, Leiomodin (Lmod) and Cordon bleu (Cobl). They all contain the Wiskott-Aldrich syndrome protein homology 2 (WH2)-domain for actin nucleation, but seem to serve distinct cellular functions and mechanisms. WH2-domains can be found in many proteins involved in motility and they are capable of binding G-actin via their amphipathic N-terminal α-helix.

Spire contains four central WH2-domains, which are all required for maximal nucleation activity (Quinlan *et al.*, 2005). The rate of actin filament nucleation mediated by spire is similar to formins, but much slower than observed for activated Arp2/3-complex. To nucleate new actin filaments, each WH2-domain binds an actin monomer thereby generating a prenucleation complex. The monomers are arranged in a way reminiscent

of a single short stranded actin filament to which actin monomers from the cytosolic pool can attach (Bosch *et al.*, 2007; Quinlan *et al.*, 2005). After nucleation, Spire proteins remain associated with the slow-growing pointed end of the new filament. Spire has been shown to work closely together with the fly formin cappuccino and the mammalian homolog FMN2 (Pechlivanis *et al.*, 2009; Quinlan *et al.*, 2007; Quinlan *et al.*, 2005, Bosch *et al.*, 2005). In the initial study, Spire did not affect the nucleation ability of Cappucino. However, more recent data suggest that the Spire/formin interaction blocks the FH2-driven actin nucleation, and leads to an increased actin nucleation by Spire (Quinlan *et al.*, 2007).

In contrast to Spire, which is widely expressed in higher eukaryotes, Cobl has been found in vertebrates only (Ahuja *et al.*, 2007). It comprises three WH2 domains, which create a cross-filament trimer upon binding of three actin monomers. This trimer can then rapidly elongate and give rise to non-bundled, unbranched actin filaments. All three WH2 domains are crucial for actin nucleation *in vitro.* Cobl-mediated nucleation is very efficient, it reaches the performance of N-WASP-WA-Arp2/3-complex-mediated actin nucleation already at low nanomolar concentrations. In contrast to Arp2/3-complex, Cobl does not shield the pointed end from depolymerisation. Cobl has been described to control neuronal morphology and development.

The third member of WH2-containing actin nucleators is Leiomodin, which seems to be restricted to muscle tissue (Chereau *et al.*, 2008) that apparently lacks Spire and Cobl (Schumacher *et al.*, 2004; Ahuja *et al.*, 2007). Leiomodin comprises just one WH2 domain but is capable of recruiting 3 actin monomers via two additional actin binding sites, thereby enabling nucleation. As knockdown of leiomodin severely compromised sarcomere assembly in cultured muscle cells, a role for leiomodin in the nucleation of tropomyosin-decorated filaments in muscles has been suggested.

1.3.2 Nucleation promoting factors

As mentioned previously, the Arp2/3-complex needs to be activated by nucleation promoting factors. Most prominent members of this group are the Wiskott-Aldrich syndrome protein (WASP) (Winter *et al.* 1999; Yarar *et al.*, 1999), N-WASP (Rohatgi *et al.*, 1999) and the suppressor of cyclic AMP repressor Scar/WASP-family verprolin-homologous (WAVE) proteins (Machesky *et al.*, 1999). More recent studies have uncovered even further Arp2/3-complex activators, such as WASH (Linardopoulou *et al.*, 2007), WHAMM (Campellone *et al.*, 2008) and JMY (Zuchero *et al.*, 2009).

All NPFs share a conserved CA region capable of binding the Arp2/3-complex. Via this region, NPFs interact with four subunits within the Arp2/3-complex – Arp3, Arp2,

ARPC1 and ARPC4 (Zalevsky *et al.,* 2001a, b). The CA region is necessary and sufficient to bind Arp2/3-complex, but it is not sufficient to activate Arp2/3-complex *in vitro* (Hüfner *et al.*, 2001; Marchand *et al.*, 2001; Weaver *et al.*, 2001). To cause activation of the Arp2/3-complex, NPFs require an actin-binding site in addition to the CA-region. This actin-binding site can either bind G-actin in case of class I NPFs or F-actin in case of class II NPFs.

Class I NPFs, which include ActA, WASP, N-WASP, WASH, WHAMM, JMY and Scar, have one or two WH2-domains capable of G-actin binding. These WH2-domains are often referred to as V-domains (verprolin homology domain), which can normally be found N-terminal to the CA region, but can be positioned differently (Skoble *et al.,* 2000; Zalevsky *et al.*, 2001a). Class I NPFs bind to the inactive Arp2/3-complex and G-Actin, thus forming a NFP*ARP2/3*G-actin assembly. Within this assembly, the interaction between the Arp2/3-complex and the CA-region of the NPF may cause an activating conformational change in the complex (Robinson *et al.*, 2001; Zalevsky *et al.*, 2001b). Simultaneous binding of the Arp2/3-complex and G-Actin by the NPF probably supports the generation of a nucleation core. According to the current model, this ternary assembly interacts with a pre-existing “mother filament” (Machesky *et al.*, 1999) resulting in the complete activation of the Arp2/3-complex and nucleation of a new daughter filament.

Class II NPFs include mammalian cortactin and yeast Abp1p. In contrast to class I NPFs, they are capable of binding actin filaments and Arp2/3-complex simultaneously, since they exhibit a F-actin binding FAB domain instead of the G-actin binding WH2-domain in class I NPFs. This FAB domain is crucial for Arp2/3-complex activation (Goode *et al.*, 2001; Uruno *et al.*, 2001; Weaver *et al.*, 2001). The precise mechanism of Arp2/3-complex activation mediated by class II NPFs is not well understood. The fact that they bind F-actin instead of G-actin might provide a functionally relevant distinction, as these NPFs were shown to be less potent than class I NPFs *in vitro*. Cortactin lacks a central region and fails to promote an activating conformational change in the Arp2/3-complex (Goley *et al.*, 2004), perhaps explaining its weak NPF activity. Notably, cortactin and N-WASP can bind to the Arp2/3-complex simultaneously, but whereas N-WASP is released after actin filament branching, cortactin remains associated with the nucleator (Egile *et al.*, 2005; Weaver *et al.*, 2002). Cortactin might therefore predominantly serve to stabilize the branch rather than initial induction of nucleation. Accordingly, its lamellipodial turnover was found to be largely uncoupled from that of the Arp2/3-complex and class I NPFs (Lai *et al.*, 2008).

1.3.2.1 WASP and WAVE proteins

Very well characterised Arp2/3-complex activators are WASP and WAVE (also Scar = suppressor of cyclic AMP repressor) proteins. This family comprise the haematopoietic-specific WASP, ubiquitous N-WASP and three WAVE isoforms (1, 2 and 3) in mammals.

WASP and N-WASP are predominantly found in an autoinhibited conformation caused by interaction between the C- and the N-terminus. In addition to the previously described VCA motif, WASP proteins exhibit a CRIB-motif (for Cdc- and Rac-interactive binding), which binds to the Rho-GTPase Cdc42. Binding of Cdc42 to the CRIB-motif and the second messenger PIP_2 to an adjacent basic region activates WASP proteins by releasing its autoinhibition (Prehoda *et al.*, 2000; Kim *et al.*, 2000; Stradal *et al.*, 2004). Further, WASP interacting proteins such as WIP (WASP interacting protein) (Ramesh *et al.*, 1997), Toca-1 (transducer of Cdc42-dependent actin assembly 1) (Ho *et al.*, 2004) and WISH (Takenawa and Miki, 2001) have been reported to additionally regulate their activity. Recent data demonstrated an additional level of regulation via dimerisation, which increases the affinity of active WASP species for Arp2/3-complex and thereby enhancing actin assembly (Padrick *et al.*, 2008). The function of WASP proteins has been linked to receptor mediated endocytosis, PIP_2-induced vesicle movement and actin tail or pedestal formation induced by *Vaccinia virus*, *Shigella* or pathogenic *E. coli* (Benesch *et al.*, 2002; Linder *et al.*, 2000; Lommel *et al.*, 2001; Frischknecht *et al.*, 1999; Snapper *et al.*, 2001; Lommel *et al.*, 2004; Egile *et al.*, 1999).

Since N-WASP acts downstream of Cdc42, which is well established to induce filopodia although it is not required for their formation (Czuchra *et al.*, 2005), it had appeared intuitive to assume that filopodia are nucleated by a complex of Cdc42-N-WASP-Arp2/3 (Bu *et al.*, 2008; Martinez-Quiles *et al.*, 2001). However this assumption turned out to be wrong, as N-WASP could not be detected in filopodia by using either GFP-tagged fusion proteins or antibodies specific for endogenous protein (Faix and Rottner, 2006). Finally, deletion of the N-WASP gene in murine cells (Lommel *et al*., 2001; Snapper *et al.*, 2001) and knockdown of N-WASP in *Drosophila* cells (Biyasheva *et al.*, 2004) did not abolish filopodia formation, indicating that N-WASP is dispensable for this process.

In contrast to WASP-proteins, recombinant purified WAVE proteins are constitutively active (Lebensohn and Kirschner, 2009; Machesky *et al.*, 1999). WAVE-proteins are naturally integrated in heteropentameric complexes with Sra-1 (Pir121), Nap 1, Abi-1,

and HSPC300 or their homologs (Eden *et al.*, 2002; Gautreau *et al.*, 2004). Individual depletion of single WAVE-complex components leads to downregulation of the other components as well, demonstrating stability and integrity of the complex as a whole (Innocenti *et al.*, 2004; Kunda *et al.*, 2003; Steffen *et al.*, 2004). Over the last years, a matter of discussion has been whether the WAVE-complex is intrinsically active or inactive (Eden *et al.*,2002; Innocenti *et al.*,2004; Kim *et al.*, 2006; Derivery *et al.*, 2009). Reports showing that WAVE-complex is constitutively active have recently been challenged by Lebensohn and Kirschner claiming that previous data of constitutive activity are artefacts of *in vitro* manipulation and purified WAVE-complex is basally inactive (Lebensohn and Kirschner, 2009). This conclusion is in line with several other studies reporting basal inactivity of the WAVE-complex (Ismail *et al.*, 2009; Derivery *et al.*, 2009; Eden *et al.*, 2002). It can be activated by the Rho-GTPase Rac and acidic phospholipids as well as by a specific state of phosphorylation (Lebensohn and Kirschner, 2009; Ismail *et al.*, 2009). Whether activation of the WAVE-complex results in the dissociation of the subunits Sra-1 and Nap1 (Eden *et al.*, 2002), recruitment of the active complex to sites of actin assembly (Steffen *et al.*, 2004; Innocenti *et al.*, 2004), an allosteric change that exposes the VCA domain of WAVE (Lebensohn and Kirschner, 2009) or a combination of these models awaits further investigation. The WAVE-complex has been shown to be crucial for the formation of lamellipodia and membrane ruffles in mammals and *Drosophila*, since these structures are abolished upon removal of different subunits (Innocenti *et al.*, 2004; Kunda *et al.*, 2003; Steffen *et al.*, 2004).

1.3.3 ADF/cofilin

The effects of ADF/cofilins are diverse and their regulation is complex. ADF/cofilins have been shown to enhance the turnover of actin filaments *in vitro* (Carlier *et al.*, 1997). They crucially contribute to actin dynamics since they are part of the minimal machinery that is required for actin-based propulsion of beads or *Listeria* (Loisel *et al.*, 1999, see 1.3). ADF/cofilins have a higher affinity for ADP-bound F-actin and promote dissociation of ADP-actin from the pointed end of an actin filament. These actin monomers can subsequently be recycled for new actin polymerisation. Besides increasing the depolymerisation rate ADF/cofilins are capable of severing pre-existing filaments. In one model, this is thought to generate new barbed ends capable of elongation and to promote actin-based motility (Bamburg and Wiggan, 2002). ADF/cofilins are regulated by multiple mechanisms, including inactivation by

phosphorylation and polyphosphoinositide interaction, the effects of pH and the synergistic or competitive interactions of ADF/cofilins with other actin binding proteins (Van troys *et al.*, 2008)

1.3.4 ENA/VASP

Enabled/Vasodilator-stimulated phosphoproteins (Ena/VASP) play a crucial role in cell movement and shape changes in vertebrates. They localise to sites of active actin assembly including focal adhesions, stress fibres, lamellipodia and filopodia (Reinhard *et al.*, 1992; Gertler *et al.*, 1996; Rottner *et al.*, 1999a; Svitkina *et al.*, 2003). Three Ena/VASP proteins are expressed in vertebrates, namely Mena, Evl and VASP. All members of the Ena/VASP family share the N-terminal EVH1-domain required for subcellular localization, followed by a central proline-rich region (PRD), and finally a C-terminal EVH2-domain mediating interactions with actin as well as the multimerisation of the molecule. *In vitro,* VASP binds G- and F-actin and nucleates and bundles actin filaments (Schirenbeck *et al.*, 2006; Laurent *et al*., 1999). It is capable of binding profilin and profilin-actin through a central prolin rich domain (Ferron *et al*., 2007; Kursula *et al*, 2008). Controversy arises concerning the capping activity of VASP, as some studies indicated that VASP can compete with capping proteins, whereas others reported the contrary (Trichet *et al.*, 2008, Bear and Gertler, 2009). Meaningful data supporting the anti-capping activity of VASP was recently provided by Breitsprecher *et al.* (Breitsprecher *et al.*, 2008). Using VASP immobilized on beads they showed that actin filaments elongated continuously even in the presence of high concentrations of capping protein. Additionally, they reported that VASP accelerated filament elongation independently of profilin.

The *Dictyostelium* VASP is a binding partner of dDia2 and cooperates with the formin in filopodia formation in this cell type. *Dictyostelium* cells lacking either the single VASP member or dDia2 failed to form filopodia, suggesting a critical role of VASP and dDia2 in filopodia formation (Schirenbeck *et al.*, 2005). The crucial role of VASP in filopodia formation is suggested to be its bundling activity, which is restricted to the tip of nascent filopodia before other actin bundling proteins like fascin stabilise the filopodia shaft (Schirenbeck *et al.*, 2006). Similar results were obtained in neurons, showing that Ena/VASP-deficient cortical neurons lack filopodia and failed to elaborate neuritis (Kwiatkovski *et al.,* 2007). In contrast to *Dictyostelium* cells, which require both VASP and dDia2 for filopodia formation, ectopic expression of mDia2 in neurons is sufficient to restore the formation of filopodia independently of VASP (Dent *el al*., 2007). Whether

this indicates cell type-specific mechanisms for the initiation of filopodia requires further investigation.

1.3.5 Profilin

Profilin is a small abundant protein capable of binding and sequestering G-actin. It is best known for its ability to promote the exchange of ADP for ATP in actin monomers released from filaments and thereby replenishing the pool of ATP-actin in the cell (Mockrin *et al.*, 1980; Goldschmidt *et al.*, 1992). By binding to actin monomers, profilin decreases the concentration of free actin monomers available for filament elongation. Thus, it prevents spontaneous nucleation in the absence of F-actin barbed ends and facilitates controlled polymerisation.

Profilin can bind simultaneously to G-actin and to prolin-rich region as e.g. in the FH1-domain of formins. In case of formin-mediated actin nucleation, profilin-actin binds to the FH1-domain and is transferred to the FH2-domain for incorporation into a growing filament, thus increasing the elongation rate of filaments associated with the formin FH1FH2-domain (Kovar *et al.*, 2006) At high profilin concentrations, free profilin competes with actin-bound profilin for binding the FH1 polyproline tracks and thereby inhibits profilin-actin transfer onto barbed ends (Kovar *et al.*, 2006; Vavylonis *et al.*, 2006). A recent study suggests that formins preferentially select specific isoforms of profilin-actin, which may provide an important mechanism to specialise formins for specific cellular processes (Neidt *et al.*, 2008).

1.3.6 Capping protein

The heterodimeric capping protein (CP) is an essential element of the actin cytoskeleton regulating the polymerisation of actin filaments. It can be found in every eukaryotic organism and every metazoan cell type (Cooper and Sept, 2008). The functional unit comprises an α/β-heterodimer and although the two subunits lack any sequence similarity their secondary structure is very similar (Yamashita *et al.*, 2003). The two subunits bind very tightly to each other and both are required for actin binding activity *in vitro* and stability *in vivo* (Amatruda *et al.*, 1992).

Capping protein binds with high affinity to the barbed end of actin filaments, thereby preventing the addition and the loss of actin monomers and at the same time leaving the pointed end unaffected (Caldwell *et al.* 1989; Casella *et al.*, 1989). Capping protein is essential to reconstitute Arp2/3-mediated motility *in vitro* (Loisel *et al.*, 1999) (see 1.3). Knockdown of capping protein abrogated lamellipodia formation (Iwasa and Mullins, 2007; Mejillano *et al.*, 2004), and was accompanied by an increase in filopodia

formation (Mejillano *et al.*, 2004; Hug *et al.*, 1995). This supports the crucial role of capping protein for Arp2/3-mediated actin assembly *in vivo*.

1.3.7 Rho-GTPases

The actin cytoskeleton is highly regulated by a family of small proteins named Rho-GTPases. They are found in all eukaryotic cells and in mammalian cells 20 genes encoding Rho-GTPases have been identified. Based on sequence similarity and functions these Rho-GTPases can be divided into five main subgroups, the Rho-like, Rac-like, Cdc42-like, Rnd and RhoBTB like (Figure 5). Among them the Rho-like, Rac-like and Cdc42-like are the best studied Rho-GTPases so far.

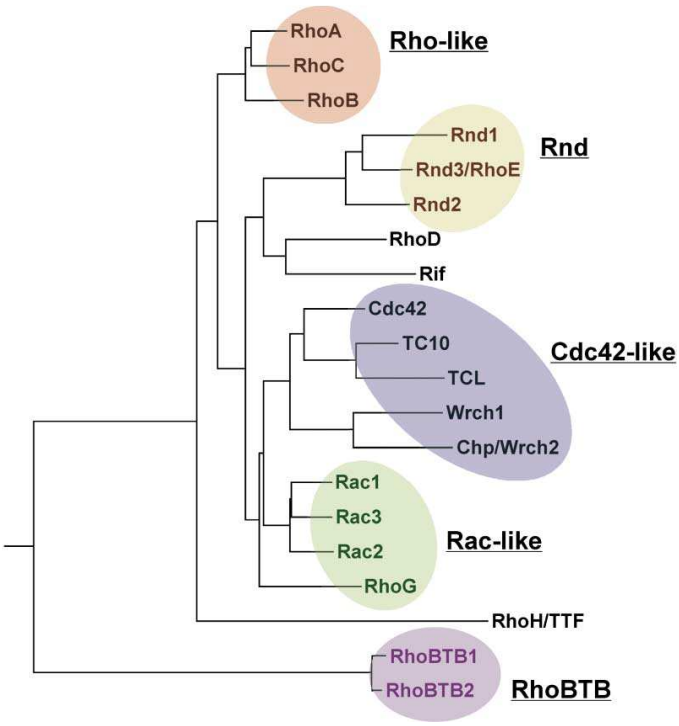

Figure 5: The Rho- family of proteins

Mammalian cells exhibit 20 Rho family members. These protein family is devided into 5 main subgroups, namely Rho-like, Rnd, Cdc42-like, Rac like and RhoBTB (from Burridge and Wennerberg, 2004).

Rho GTPases act as key molecular switches regulating the formation of cellular protrusions. Their activity is tightly controlled by alternating between an active GTP-bound and an inactive GDP-bound status (Figure 6). Guanine nucleotide exchange factors (GEFs) catalyse the exchange of GDP for GTP and thereby activate the Rho-GTPase (Raftopoulou and Hall, 2004; Rossman *et al.*, 2005). The active, GTP-loaded GTPase is capable of interacting with downstream effectors such as formins to mediate a specific response. Guanine activating proteins (GAPs) stimulate the intrinsic GTPase

activity which hydrolyses GTP to GDP thus inactivating the protein (Bernards, 2003). GDP dissociation inhibitors (GDIs) inhibit the dissociation of GDP from Rho-GTPases and block the intrinsic and GAP-catalysed GTPase activity to prevent spontaneous activation (DerMardirossian and Bokoch, 2005; Dovas and Couchman, 2005). Additionally, GDIs interact only with prenylated Rho-GTPases, extract them from membranes and sequester them in the cytoplasm away from their regulators and targets (Dovas and Couchman, 2005).

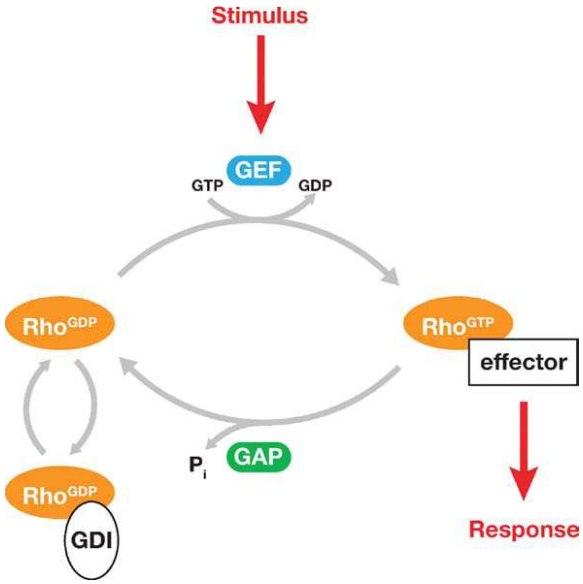

Figure 6: The GTPase cycle

Rho GTPases cycle between an active (GTP-bound) and an inactive (GDP-bound) state. In mammalian cells, a large family of 85 Guanine exchange factors (GEFs) catalyse the exchange of GDP for GTP, thereby activating Rho-GTPases. Activated Rho-GTPases interact with downstream effectors to elicit specific responses. GTPases activating factors (GAPs), comprised of 80 members in mammals, stimulate GTP hydrolysis, thus inactivating the protein (from Jaffe and Hall, 2005).

Membrane binding and thus proper targeting is achieved by posttranslational addition of a prenyl moiety (e.g. geranylgeranyl) to the C-terminus of Rho-GTPases. Finally, Rho-GTPases are regulated by phosphorylation and ubiquitination; however, the contribution of these modifications to the physiological behaviour is unclear.

Our knowledge about the cellular functions of Rho-GTPases has been improved by over-expression studies in cell lines using either dominant negative or constitutively active Rho-GTPases, which inhibit or overstimulate Rho-GTPase signalling. Additional understanding has been provided by loss of function studies using transient

approaches like RNA interference and conditional knockout mice and cell lines, respectively.

The Rho-GTPase Cdc42 has a crucial role in the regulation of cell polarity, vesicle trafficking and early cell development in *D. melanogaster* and *C. elegans*. By activating the nucleation promoting factor N-WASP, Cdc42 promotes Arp2/3-mediated actin nucleation e.g. in endocytosis. In many cell types, constitutively active and dominant negative Cdc42 influence the formation of filopodia, but the molecular mechanism of Cdc42-induced filopodia formation is still controversial, since one of its direct effectors N-WASP is dispensable for the formation of these protrusive structures (see 1.3.2.1). Over the last years, Diaphanous related formins (e.g. mDia2), whose activity is controlled by Rho-GTPases such as Cdc42, emerged as key regulators of filopodia. However, Cdc42-deficient cell lines are still capable of forming these finger like projections (Czuchra *et al.*, 2005). This indicates that other Rho-GTPases can contribute to the formation of filopodia, given that besides Cdc42 other Rho-GTPases such as Rif (Rho in filopodia), Wrch1 and RhoD can trigger the initiation of these structures (Aspenström *et al.*, 2009; Burridge and Wennerberg, 2004; Ellis and Mellor, 2000).

The Rac protein family comprises Rac1, Rac2 and Rac3 and RhoG. Rac1 is ubiquitously expressed in human tissue, Rac2 is restricted to the haematopoietic system and Rac3 is most abundant in the brain. Data from knockout mice indicate that although the three Rac isoforms share a high sequence similarity, they have non-redundant functions (Wheeler *et al.*, 2006). Rac1 is a key regulator of lamellipodia and membrane ruffles in a variety of cell types including fibroblasts and epithelial cells (Ridley, 2001). Activation of the WAVE-complex by binding of Rac to the subunit Sra-1 results in Arp2/3-complex mediated actin nucleation (see 1.3.2.1), stimulating the formation of lamellipodia and membrane ruffles. Local activation of a photoactivatable Rac is sufficient to induce cell motility and controls the direction of cell migration (Wu *et al.*, 2009), supporting the critical role of Rac in protrusion.

Stress fibre formation is regulated by the Rho-family comprising three isoforms RhoA, RhoB and RhoC. Rho activates Rho-associated-kinase (Rock), which inhibits myosin light chain phosphatase and phosphorylates myosin light chain thereby stimulating actomyosin II contractility in stress fibres (Chrzanowska-Wodnicka and Burridge, 1996; Kimura *et al.*, 1996). Additionally, RhoA is well established to activate the formin mDia1, which may promote the formation of stress fibres (see 1.3.1.2.2) and to activate LIM kinase, which in turn inhibits the depolymerisation factor ADF/cofilin resulting in

more stable actin filaments e.g. in stress fibres (Amano *et al.*, 2001; Maekawa *et al.*, 1999; Pritchard *et al.*, 2004).

Rho-GTPases are also capable of influencing the activity of each other. The crosstalk between them employes activation and suppression e.g. by interacting with specific GEFs and GAPs or interactions between their respective downstream signalling pathways (Burridge and Wennerberg, 2004). It is well established that Cdc42 can activate Rac (Nobes and Hall, 1995), resulting in the formation of lamellipodia and membrane ruffles. RhoG has been described to activate Rac via binding to ELMO1, which activates the unconventional Rac GEF Dock180 (Katoh and Negishi, 2003). Furthermore, downregulation of the Rac1 pathway promotes the enlargement of focal contacts, whereas inhibition of the RhoA pathway stimulates membrane ruffling, revealing an antagonism between Rac1 and RhoA (Rottner *et al.*, 1999b). This antagonism is supported by data showing that Rock, which is a well established downstream effector of RhoA, phosporylates the Rac specific GAP, FilGAP, thereby inactivating Rac and suppressing cell spreading (Ohta *et al.*, 2006).

1.3.7.1 Rho-GTPases and Formins

Diaphanous-related formins are well established effectors of Rho-GTPases. Binding of Rho-GTPase to the GTPase binding domain releases the autoinhibited state (see 1.3.1.2) and thereby enables actin polymerisation mediated by formins. Each formin is activated by a distinct subset of Rho-GTPases, e.g. mDia1 by RhoA, RhoB and RhoC (Rose *et al.*, 2005a; Watanabe *et al.*, 1999), mDia2 by Cdc42 and Rif (Peng *et al.*, 2003; Pellegrin and Mellor, 2004) and DAAM1 by RhoA and Cdc42 (Aspenström *et al.*, 2006). For others like FMNL2 and -3 it is still unclear which Rho-GTPases are able to release the autoinhibiton in these formins.

In addition to the Rho-GTPase-mediated activation of formins, increasing evidence suggests a possible positive feedback regulation. mDia1 activates RhoA via binding of the Rho GEF LARG, which in turn is controlled by RhoA-induced release of mDia1 autoinhibition (Kitzing *et al.*, 2007). The Drfs DAAM1 and mDia2 have been shown to activate RhoA probably also by interacting with a Rho-GEF (Habas *et al.*, 2001), suggesting that at least some formins are capable of promoting Rho-activation.

1.4 Aims of this thesis

The work presented here aimed at shedding light on the influence of diaphanous related formins on cell migration especially on the formation of lamellipodia and

filopodia. In this context the Drfs Drf3 and FMNL2 where of main interest, as they are widely expressed and abundant in various tissue culture cell lines. To characterise Drf3 and FMNL2, both proteins were cloned and the dynamic localisation of the EGFP-tagged proteins analysed in motile cells. A constitutively active Drf3 construct was used as a tool to study the ultrastructure of formin-induced filopodia, and to determine the mechanism of filopodia formation. Additionally, the requirement of Drf3 for the formation of filopodia and lamellipodia was investigated.

In the second part of this thesis, the diaphanous related formin FMNL2 was subject of functional characterisation, including biochemical interaction studies, cellular localisation analyses and –in collaboration- *in vitro* nucleation and TIRF experiments. Finally, I explored the contribution of FMNL2 to cell migration by employing RNA interference.

2 Material and Methods

2.1 Chemicals, Media, Buffers

If not stated otherwise, all chemicals were purchased from the following companies: Amersham, Bioscience, BioRad, Boehringer Mannheim, Fermentas, Fluka, GE Healthcare, Invitrogen, Life Technologies, Merck, Macherey-Nagel, Millipore, New England Biolabs, PAA, Promega, Qiagen, Riedel de Haen, Roche, Roth, Sigma-Aldrich, Serva and TaKaRa.

The quality standard was p.a. (*per analysis*).

All buffers were prepared in deionised water, which has been purified by a milli-Q-system (Millipore).

2.2 Cell Culture Reagents and Plasticware

Cell culture media and additives were from Gibco, Invitrogen, PAA or Sigma unless stated otherwise. Plasticware was obtained from Corning, Falcon and Nunc.

2.3 Enzymes und Reagents for Molecular Biology

Enzymes were from New England Biolabs, MBI Fermentas or Roche. T4-DNA Ligase and alkaline phosphatase were obtained from Roche. Phusion DNA Polymerase was purchased from Finnzymes. Oligonucleotides were from Biosprings or MWG-Biotech. DNA-standards were from Eurogentec and protein markers from MBI Fermentas.

2.4 Vectors

For generation of EGFP-fusion constructs, pEGFP-C1, -C2, -C3 and -N1, -N2, -N3 vectors were used (Clontech). The pGEX-6P-1, -2 and -3 vectors for the production of GST (glutathione-S-transferase) fusion proteins were purchased from Amersham Biosciences.

2.5 Bacteria culture:

Escherichia coli TG2 (Stratagene) for amplification of plasmids: Genotype: *supE hsd*Δ5 *thi* Δ(*lac-proAB*) Δ(*srl-recA*)306::Tn*10(tet^r)* F[*tra*D36 *proAB*$^+$ *lacI*^{q} *lacZ*ΔM15].

Escherichia coli JM110 (Stratagene) for amplification of plasmids: Genotype**:** *rpsL* (Strr) *thr leu thi-1 lacY galK galT ara tonA tsx dam dcm supE44* Δ(*lac-proAB*) [F´ *traD36 proAB lacI*q*ZΔM15*].

Escherichia coli GM2163 (Fermentas) for amplification of plasmids: Genotype: F⁻*ara-14 leuB6 fhuA31 lacY1 tsx78 glnV44 galK2 galT22 mcrA dcm-6 hisG4 rfbD1 rpsL136 dam13::Tn*9 *xylA5 mtl-1 thi-1 mcrB1 hsdR2.*

2.5.1 Media for bacterial culture:

LB-medium (**L**uria **B**ertain broth):

bacto-tryptone	10 g/l
bacto-yeast extract	5 g/l
NaCl	120 mM

SOB-medium:

bacto-tryptone	20 g/l
bacto-yeast extract	5 g/l
NaCl	0,6 g/l
KCl	0,1 g/l

SOC-medium:

SOB – Medium	
+ $MgCl_2$	10 mM
+ $MgSO_4$	10 mM
+ Glucose	20 mM

2.6 Molecular biological standard techniques:

2.6.1 Plasmids

Plasmid	Origin	Source
EGFP-N2-DRF3 ΔN	human	Jan Faix, Hannover Medical School, Hannover, Germany
EGFP-C1-Drf3ΔN	human	Jan Faix, Hannover Medical School, Hannover, Germany
EGFP-N2-Drf3 full length	human	this thesis
EGFP-C1-Drf3 full length	human	Jan Hänisch, HZI, Braunschweig, Germany
EGFP-C1-DRf3ΔDAD	human	Jan Faix, Hannover Medical School, Hannover, Germany
EGFP-C1-mDia 1ΔDAD	mouse	Jan Faix, Hannover Medical School, Hannover, Germany
EGFP-C1-mDia 1 full length	mouse	Jan Faix, Hannover medical school, Hannover, Germany
EGFP-C1-DAAM1	human	this thesis
EGFP-C1-DAAM1ΔC50	human	this thesis
EGFP-C3-FMNL2C full length	human	this thesis
EGFP-N1-FMNL2C full length	human	this thesis
EGFP-N1-FMNL2ΔDAD	human	this thesis
EGFP-N1-FMNL2ΔDAD G2A	human	this thesis
EGFP-C1-FMNL2ΔDAD	human	this thesis
EGFP-FMNL2-GBD	human	Christine Standfuß-Gabisch, Theresia Stradal, HZI, Braunschweig, Germany
EGFP-FMNL2-Arr	human	this thesis
EGFP-C3-FMNL2A	human	this thesis
EGFP-C3-FMNL2B	human	this thesis
EGFP-N1-FMNL2A	human	this thesis
EGFP-N1-FMNL2B	human	this thesis
EGFP-N1-FMNL2C-G2A	human	this thesis

EGFP-N1-FMNL2A-G2A	human	this thesis
EGFP-N1-FMNL2B-G2A	human	this thesis
EGFP-C3-FMNL3	mouse	this thesis
EGFP-C3-FMNL3-Arr	mouse	this thesis
Prk5-myc cdc42L61	human	Laura Machesky (Beatson Institute, Glasgow, UK)
Prk5-myc-RacL61	human	Laura Machesky (Beatson Institute, Glasgow, UK)
GST-cdc42L61	human	Alan Hall (University College, London, UK)
GST-cdc42N17	human	Alan Hall (University College, London, UK)
GST-Rac1L61	human	Alan Hall (University College, London, UK)
GST-Rac1N17	human	Alan Hall (University College, London, UK)
GST-RhoAL63	human	Petra Hagendorff, Theresia Stradal, HZI, Braunschweig, Germany
MBP-RifL77	human	Petra Hagendorff, Theresia Stradal, HZI, Braunschweig, Germany
MBP-RhoGV12	human	Petra Hagendorff, Theresia Stradal, HZI, Braunschweig, Germany
MBP-RhoDV26	human	Petra Hagendorff, Theresia Stradal, HZI, Braunschweig, Germany

Table 1: List of constructs used in this work.

2.6.2 Oligonucleotide primers

	Name	Sequence 5´to 3´	Purpose
1	DAAM1 BamH1 fwd	GAGAGGATCCATGGCCCCAAGAAAGAGAGGTG	Cloning of DAAM1
2	DAAM1 Sal1 rev (mut)	GAGAGTCGACTTAGAAATTAAGGTTTGTGATTG	Cloning of DAAM1
3	DAAM1 seq fwd	AGTCTCAAGACTGCCATCA	Sequencing
4	DAAM1 seq rev	TCTGAGCCAGAACGAATTG	Sequencing

5	DAAM1 DAD Sal I rev	GAGGTCGACACTTTTACGTTCCCTTTCAC	Cloning of DAAM1 ΔDAD
6	DAAM1 delta C50 Sal I rev	GAGGTCGACTTCTTCACTATTCTCTTTAGC	Cloning of DAAM1ΔC50
7	FMNL2 Sal I fwd	GAGGTCGACATGGGCAACGCAGGGAGCA	Cloning of FMNL2
8	FMNL2 1316 rev	TCCCGAACGACATCCAGCTC	Cloning of FMNL2
9	FMNL2 1084 fwd	GACAAGCTTCAAGTCCAGATCC	Cloning of FMNL2
10	FMNL2 1492 rev	ATGGACAATGTGCCAGAAGC	Cloning of FMNL2
11	FMNL2 1903 fwd	AAGCCCAATCAGATCAATGG	Cloning of FMNL2
12	FMNL2 Sac II rev	GAGACCGCGGTCACATTGTTATTTCGGCA	Cloning of FMNL2
13	FMNL2 seq fwd	TTATGGTGGCTTCTATGCAG	Sequencing
14	FMNL2 seq rev	TTGACTTTGTATCTAAGAGC	Sequencing
15	FMNL2 DAD SacII	GAGCCGCGGTTGCTGCTGCCTCTTTGATTTATG	Cloning of FMNL2 ΔDAD
16	FMNL2-GBD Not1rev Stopp	GAGCGGCCGCTTATCTGACAAGACAAACGGC	Cloning of FMNL2-GBD
17	FMNL2-ARR_{stop} Sac2 rev	GAGAGACCGCGGTTACATGAGTTGCTTTTCCAG	Cloning of FMNL2-Arr
18	FMNL2 A2 fwd	TGCAGTCGACATGGCCAACGCAGGGAGCATGG	Mutagenesis of FMNL2
19	FMNL2 A2 rev	CCATGCTCCCTGCGTTGGCCATGTCGACTGCA	Mutagenesis of FMNL2
20	mFMNL3 192 fwd	GGATCTGATCTGTGACCAGG	Cloning of FMNL3
21	mFMNL3 BamH1 w/o stopp rev	GAGAGGATCCACAGTTTGACTCGTC	Cloning of FMNL3

22	mFMNL3 Xho fwd	GAGACTCGAGATGGGCAACCTGGAGAGC	Cloning of FMNL3
23	mFMNL3 rev	TCTCCTCCGGAACTTCTTCC	Cloning of FMNL3
24	FMNL3 seq fwd 942	CAGCAACATTGACTTCATGG	Sequencing
25	FMNL3 seq rev 2021	GTTTGACTTACAGACACTACC	Sequencing
26	FMNL3-Arr SalI rev	GAGAGTCGACTAGCAGCTGCTTCTCCAG	Cloning of FMNL3-Arr

Table 2: List of primers for amplifying, sequencing and site directed mutagenesis used in this thesis.

Oligonucleotides used in this thesis were synthesised either by Biospring or MWG Eurofins. Oligonucleotides were designed with Primer 3 webinterface (http://frodo.wi.mit.edu/primer3) or Vector NTI Suite 8 and 10 (Invitrogen).

2.6.3 Generation of constructs

EGFP-fusion constructs were generated by polymerase chain reaction (PCR) introducing the respective cutting sites at the C- and N-terminus of the appropriate fragment. Phusion DNA Polymerase was used according to the manufacturer´s protocol. Annealing temperature and extension time were adapted according to the used primers (annealing temperature calculated with Vector NTI Suite 8) and the size of the expected product, respectively. If suitable native cutting sites were used to fuse the fragment to the respective vectors, EGFP-vectors and fragments were cut with similar enzymes or enzymes producing compatible ends and subsequently ligated using T4-DNA-ligase.

Human DAAM1 full length constructs were generated using the Image Clone IRATp970B1285D and IRAKP96141452Q (imaGenes, Germany) as template and the primers 1 and 2 in the PCR reaction. For the generation of the ΔC50 construct lacking the DAD-domain, primers 1 and 6 were used. Both PCR fragments were cut with BamH1 and Sal1 and ligated in an EGFP-C1 vector (Clontech) cut the same way.

The generation of the human FMNL2 full length construct was performed in several steps including a number of intermediates constructs, generation of which is shown in Table 3.

Name	Fragments	Vector	Fragment source
Intermediate 1	FMNL2 SalI/HindIII (1 -1088bp; Primers 7&8)	EGFP-C3 SalI/HindIII	IMAGEClone IRALp962K1959Q2 (imaGenes, Germany)
Intermediate 2	FMNL2 HindIII/EcoRV (1088-1471bp; Primers 9&10)	pBluescript SK II HindIII/EcoRV	Hela S3 cDNA
Intermediate 3	FMNL2 EcoRV/EcoRI (1471-1953bp)	Intermediate 2 EcoRV/EcoRI	fragment synthesised by GenScript (GenScript USA Inc., USA)
Intermediate 4	Intermediate 3 (1088-1953) HindIII/EcoRI	Intermediate 1 HindIII/EcoRI	-
EGFP-C3-FMNL2	FMNL2 EcoRI/SacII (1953-3278bp; Primers 11&12)	Intermediate 4 EcoRI/SacII	Hela S3 cDNA

Table 3: Generation of EGFP-FMNL2 fusion protein.

For cloning of FMNL2 isoforms A and B, C-terminal sequences encompassing the isoform-specific sequences were synthesized by GenScript (GenScript USA Inc., USA) and exchanged with the C-terminus of FMNL2C using internal BamH1 and C-terminal SacII cutting sites.

The FMNL3ΔN construct was generated using the IMAGE Clone IRAKp961L0355Q (imaGenes, Germany) encoding the murine FMNL3 sequence (residues 63-1028). For generation of FMNL3 full length the N-terminus (aa 1-103) was amplified from mouse B16-F1 cDNA (see 2.6.13) and fused to the FMNL3ΔN sequence by using an internal BspEI cutting site.

All constructs were verified by restriction digest, sequencing and expression tests.

2.6.4 Site directed mutagenesis:

In this thesis, the Quick change site-directed mutagenesis kit (Stratagene) was used to switch the amino acid glycin2 of FMNL2 into alanine in order to obtain a FMNL2 mutant that cannot be myristoylated. The reaction was performed as described in the Quick change site directed mutagenesis manual.

2.6.5 DNA Sequencing

For sequencing, DNA samples were sent to MWG Operon (Martinsried, Germany). ABI sequence files were edited and aligned with Vector NTI Suite 8 and 10.

2.6.6 Restriction Digest and Dephosphorylation

2-15 µg plasmid DNA were restriction digested in a total volume of 10-100 µl in the appropriate restriction buffer containing 10 U restriction enzyme for 1-2 hours at 37°C.
To prevent cutted DNA vectors from religating they were dephosphorylated using 1 U alkaline phosphatase (Roche) for 5 minutes at 50°C. Afterwards restricted fragments were analyzed by gel-electrophoresis.

2.6.7 DNA Extraction from Agarose Gels

DNA fragments for subcloning were extracted from agarose gels using the NucleoSpin Extract II Kit from Machery&Nagel (Macherey-Nagel, Düren, Germany) according to manufacturers´ instructions.

2.6.8 Ligation

T4-DNA ligase (Roche) was used to covalently link DNA fragments with required vectors as recommended by the manufacturer. 10 - 100ng of the vector was mixed with 3x molar excess of the fragment and incubated either for 30min - 4h at room temperature or overnight at 4°C. Afterwards, the reaction was transformed into competent TG2 *E. coli.*

2.6.9 Generation of $CaCl_2$-competent *E. coli*

To generate competent *E. coli* that are highly efficient in taking up DNA, the protocol was as follows: an overnight culture of TG2 was diluted 1:100 into SOB medium and incubated under agitation at 37°C until OD 600 reached 0.5. The bacteria were harvested by centrifugation (5000 x g, 10 min, 4°C) . The pellet was resuspended in 1/5 of the culture volume of ice-cold 0.1 M $CaCl_2$ and incubated for 20 minutes on ice. After centrifugation (5000 x g, 10 min, 4°C), bacteria were resuspended in 1/100 to 1/200 of the culture volume of ice-cold 0.1 M $CaCl_2$ and incubated for 3 hours on ice. The bacteria were supplemented with glycerine to a final concentration of 10% (v/v), snap-frozen in liquid nitrogen and stored at –80°C.

2.6.10 Transformation of *E. Coli*

For transformation, 50 - 100µl aliquots of competent *E. coli* were thawn on ice, mixed gently with 100 ng Plasmid-DNA or 10 - 15µl of a ligation reaction and incubated on ice

for 30 min. Bacteria were then heat shocked at 42℃ for 1min, left on ice for 1min and resuspended in 250µl of SOC-Medium. Bacteria were gently shaken at 37℃ for 1 hour and plated on agarplates containing the appropriate antibiotic and incubated for 12 - 16h at 37℃.

2.6.11 Preparation of plasmids from *E. Coli*

Plasmid midi and maxi preparations were performed using the Nucleo Bond plasmid purification kit 100 and 500 from Macherey&Nagel, respectively.

For plasmid mini preparations, 1-1.5 ml LB-medium containing the appropriate antibiotic were inoculated with single colonies and incubated at 37℃ o/n. Bacteria were harvested by centrifugation and resuspended in 100 µl buffer 1 with RNAse A. After adding 200µl of buffer 2 and 150 µl of ice-cold buffer 3, the bacterial suspension was incubated 3-5 minutes on ice. The bacterial lysate was harvested after centrifugation of the suspension at 12000 g for 5 minutes and mixed with 400 µl isopropanol to precipitate the eluted plasmid DNA. This mixture was incubated at room temperature for 2 minutes and centrifuged at 12000 g for 5 minutes. The DNA pellet was washed with 70% Ethanol several times and dried at 37℃ for approximately 30 minutes. The DNA pellet was redissolved in 50 µl Baker H_2O.

2.6.12 RNA Purification

For the purification of total RNA from tissue culture cells all solutions were prepared in DEPC treated water. RNA free plastic ware was purchased from Roth (Karlsruhe, Germany).

To prepare total RNA from tissue culture cells a confluent 10cm dish was washed once with PBS and then lysed in 1ml peqGOLD TriFast™ reagent. Probes were then incubated for 10 min at room temperature. 100µl of 1-Bromo-3-chloropropane was added for each ml of tissue culture lysate, and mixed for 15sec. The mixture was incubated at room temperature for 10-15min and subsequently centrifuged for 15min at 12000g at 4℃. The upper aqueous phase was transferred into a new Eppendorf tube, and an equal amount of isopropanol was added and mixed gently. After 15min of incubation at room temperature, the sample was centrifuged at 14000g for 15min at 4℃. The supernatant was transferred into a new Eppendorf tube and washed with 1ml 75% EtOH and centrifuged at 7500g for 8min at 4℃. The RNA pellet was dried at 37℃ and solved in an appropriate amount of DEPC-treated water under agitation at 56℃ for 10min.

2.6.13 cDNA Synthesis

cDNA synthesis has been carried out using the Omniscript reverse transcriptase kit (Qiagen) according to the manufacturer´s instruction.

For the reverse transcriptase reaction, the following primers were used:

Fragment	Used primer sequence 5´to 3´	cDNA source
FMNL2	TTTTTTTTTTTTTTTTTTTT	Hela S3
FMNL2	TTTTTTTTTTTTTTTTTTTT	Hela S3
FMNL3	TCTCCTCCGGAACTTCTTCC	B16-F1

Table 4: Primers used for cDNA synthesis

2.6.14 Quantification of DNA and RNA

The photometric absorption of DNA and RNA in solution has a maximum at a wavelength of λ = 260 nm. To determine the concentration of nucleic acid, an aliquot of the solution was diluted to an extinction of the optical density (OD) OD_{260} = 0.1- 1.0, which corresponds to a concentration range, in which the absorption in still linear. The concentration of the DNA and RNA can be calculated by including the molar extinction coefficient (ε) of RNA or DNA (40 or 50 µg/µl, respectively) as follows: OD_{260}• dilution factor • ε µg/µl = cDNA µg/µl

2.7 Protein Biochemistry

2.7.1 Sodiumdodecylsulphate-Polyacrylamide Gel Electrophoresis (SDS-PAGE)

Sodiumdodecylsulphate-polyacrylamide gel electrophoresis (SDS-PAGE) was performed essentially according to Laemmli (Laemmli, 1970). SDS-PAGE gels were run in Minigel apparatures (Biometra) with 1 mm spacers.

2.7.2 Coomassie Blue Staining

After transfer onto PVDF-membranes, proteins were stained with a 0.1% Coomassie R-250 solution in 10% acetic acid and 25% isopropanol for 30-60 minutes. This was followed by destaining of the membrane in 10% acetic acid and 40% methanol.

2.7.3 Protein extracts from cultured cells

Extracts from adherent tissue culture cells were obtained as follows: first, the cells were washed with 1x PBS. For standard extracts, 4x reducing SDS-sample buffer was added directly to the cells (500 µl on a 10 cm-diameter dish), then scraped off the dish using a cell scraper, boiled at 95℃ for 5 minutes and stored at –20℃. For measuring the protein concentration in cell lysates, cells were lysed in ice cold IP-buffer (15mM KCl, 50mM NaCl, 8mM Tris base, 12mM Hepes, 5 mM $MgCl_2$, 1% Triton X -100 + 1 aliquot Roche complete Protease inhibitor per 10ml).

2.7.4 Pull-down Assays

To determine interactions between respective Rho-GTPases and FMNL2, B16-F1 cells growing in 10cm dishes were transfected with EGFP fusion constructs containing the GTPase-binding domain and the Armadillo repeats of FMNL2 (FMNL2-Arr) or a constitutively active FMNL2 construct lacking the DAD-domain (FMNL2ΔDAD). Cells were lysed with 500µl of ice cold IP-buffer (15mM KCl, 50mM NaCl, 8mM Tris base, 12mM Hepes, 5 mM $MgCl_2$, 1% Triton X - 100 + 1 aliquot Roche complete Protease inhibitor per 10ml). After centrifugation for 15 minutes at 15000 x g at 4℃, FMNL2-Arr and FMNL2ΔDAD, respectively, were precipitated from the cell lysate using 30µl gluthathione-sepharose beads coupled with dominant negative or constitutively active GST- or MBP-tagged recombinant Rho-GTPases for 1 hour at 4℃ on a rotary wheel. Beads were then washed three times with cold IP-buffer. Precipitates were resolved by SDS-PAGE and analysed by immunoblotting with the antibodies listed in Table 5 and Table 6.

2.7.5 Determination of protein concentration

Protein concentration was determined using the Precision Red Advance protein assay (Cytoskeleton) according to the manufacturer´s manual.

2.7.6 Pyrene assays and total-internal-reflection-microscopy (TIRFM)

Actin polymerization assays and TIRF microscopy assays were performed by Dennis Breitsprecher and Dr. Jan Faix (Hannover Medical School) as described in Schirenbeck *et al.* (2005), Breitsprecher *et al.* (2008) and Breitsprecher *et al.* (2009).

2.8 Immunobiological Methods

2.8.1 Primary Antibodies

Primary antibodies used in this study are listed in Table 5.

Description	Protein	Mc/Pc	Application	Provided by
101G4B2	GFP	Mc	WB	Barbara Behrendt, HZI, Braunschweig, Germany
270F3	GFP	Mc	IP, WB, IF	Synaptic Systems, Göttingen, Germany
Drf3	Drf3	Pc	WB	Jan Faix, MH Hannover, Germany
FMNL2	FMNL2	Mc	WB, IF	Abcam, Germany
323H3	ArpC5	Mc	IF	Millard *et al.*, 2002
W8.3	Abi	Mc	IF	Innocenti *et al.*, 2004
5500	VASP	Pc	IF	Andrea Jenzora, HZI, Braunschweig, Germany
55K2	Fascin	Mc	IF	Santa Cruz Biotechnology Inc, Santa Cruz,CA, USA
289H10	Cortactin	Mc	IF	Synaptic Systems, Göttingen, Germany
T4026	ß-Tubulin	ascites	WB	Sigma Aldrich, Germany

Table 5: Primary antibodies

2.8.2 Secondary Reagents

Secondary Reagents used in this study are listed in Table 6.

Description	Species Antibody	Species Antigen	Coupled to	Provided by
A4a	Goat	mouse	PO coupled	Dianova
B4C	Goat	rabbit	PO coupled	Dianova
B12C	Goat	Rabbit	Alexa Fluor 488	Invitrogen (molecular probes)
B13C	Goat	Rabbit	Alexa Fluor 594	Invitrogen (molecular probes)

A 12C	Goat	Mouse	Alexa Fluor 488	Invitrogen (molecular probes)
A13C	Goat	Mouse	Alexa Fluor 594	Invitrogen (molecular probes)
A16C	Goat	Mouse	Alexa Fluor 350	Invitrogen (molecular probes)
Ph12 Phalloidin			Alexa Fluor 488	Invitrogen (molecular probes)
Ph13 Phalloidin			Alexa Fluor 594	Invitrogen (molecular probes)
Ph16 Phalloidin			Alexa Fluor 350	Invitrogen (molecular probes)

Table 6: Secondary reagents

2.8.3 Western Blots

Western blots were performed as follows: after separation on SDS-PAGE gels, proteins were transferred onto PVDF-membrane (Immobilon P, Millipore) using a semidry blotting system (Pegasus, Phase, Germany) and a glycine methanol SDS blotting buffer [50mM Tris, 39 mM glycine, 0.037 (w/v) SDS, 20% (v/v) methanol] at a constant current of 2 mA per cm^2 of gel area for 60 minutes (for proteins of interest up to 60 kDa) up to 120 minutes (for proteins of interest up to 150 kDa). Transfer efficiency was monitored by staining of the membranes with Ponceau S solution [0.5% PonceauS (Sigma), 40% methanol, 15% acetic acid]. Membranes were blocked for 30 minutes at room temperature or at 4℃ overnight in blocking buffer [10% dry-milk in TBS-T buffer (20mM Tris-HCl pH 7.6; 137 mM NaCl; 0.1% Tween20)]. Afterwards, membranes were incubated overnight at room temperature or at 4℃ in 1% dry-milk in TBS-T buffer containing the primary antibody usually at a concentration of 1µg/ml. Membranes were washed three times in TBS-T buffer for 10 minutes and then incubated for 1 hour at room temperature with 1% dry-milk in TBS-T buffer containing the secondary antibody. Membranes were again washed three times with TBS-T buffer and then incubated for up to 4 minutes with the chemiluminescence substrate Lumilight (Roche) in the case of peroxidise-coupled secondary antibodies and exposed to Hyperfilm ECL (Amersham Biosciences).

2.9 Tissue culture, transfection and treatments

2.9.1 Media and solvents

Growth medium 1 :

DMEM (Dulbecco´s Modified Eagle Medium, Gibco)	
4,5g/l glucose	
FCS PAA EU (PAA)	10%
L-glutamine (Gibco)	2mM

Growth medium 2:

DMEM (Dulbecco´s Modified Eagle Medium, Gibco),	
4.5 g/l glucose	
FCS Lot: 047K3395 (Sigma)	10%
L-glutamine (Gibco)	2 mM
Non-essential amino acids (Gibco)	1 x
Sodium-pyruvate (Gibco)	1 mM

Growth medium 3:

DMEM (Dulbecco´s Modified Eagle Medium, Gibco)	
4,5 g/l glucose	
FCS PAA Clone (PAA)	10%
L-glutamine (Gibco)	2mM
Puromycin	1µg/ml

Microscopy Medium 1:

F12-HAM Medium Hepes Modification (Sigma)	
FCS PAA EU (PAA)	10%
L-glutamine (Gibco)	2mM
Penicillium (Gibco)	25000U
Streptomycin (Gibco)	25000µg

2.9.2 Used cell lines

Name	Organism	Type	Growth medium	Source
B16-F1	*Mus musculus*	Melanoma, skin	1	ATTC (CRL-6323)
3-9	*Mus musculus*	Cdc42 fl/- fibroblast	2	Cord Brakebusch, University of Copenhagen
3-9-7	*Mus musculus*	Cdc42 -/- fibroblast	2	Cord Brakebusch, University of Copenhagen
VA13 NS14-4	*Homo sapiens*	Pulmonary fibroblasts stably transfected with Nap1 RNAi (pSuper.retro.puro-Nap1 RNAi)	3	Annika Steffen, HZI
VA13 C33	*Homo sapiens*	Pulmonary fibroblasts stably transfected with mock RNAi (pSuper.retro.puro)	3	Annika Steffen, HZI
Hela S3	*Homo sapiens*	adenocarcinoma cerevix epithelial cells	2	ATTC (CCL-2.2)

Table 7: Cell lines employed in this work.

All cell lines were cultivated at 37°C and 7.6% (v/v) CO_2.

2.9.3 Culture of cells prior to microscopic analyses

For Live-cell imaging, cells transiently transfected with respective constructs were seeded subconfluently on 15mm acid–washed glass coverslips (15mm) coated with 25µg/ml Laminin (Roche) or 25µg/ml Fibronectin (Roche). Cells seeded on Laminin were allowed to spread for at least 3 hours, cells seeded on Fibronectin were allowed to spread for at least 3 hours or overnight.

Coverslips had been pretreated as follows: glass coverslips were incubated in a mixture of 60% ethanol and 40% concentrated HCl for 1 to 3 hours under agitation. Coverslips were then extensively washed in water that was repeatedly exchanged. Coverslips were allowed to dry separately on Whatman filterpaper overnight and autoclaved.

2.9.4 Transfections

Transfections were carried out using SuperFect (Qiagen, Germany, for B16-F1), FuGene HD (Roche, Germany, for HeLa S3) or with FuGene 6 [Roche, Germany, for Cdc42 (fl/-), Cdc42 (-/-) and B16-F1 cells used for FMNL2 knockdown experiments], according to manufacturer´s protocols.

In brief, 50 µl Optimem were mixed with 3 µl FuGene (6 or HD) and 1 µg DNA and incubated for 20 minutes at room temperature. The mixture was added to cells in a 3 cm diameter dish containing freshly replaced medium and incubated for 24 hours.

For B16-F1 transfections, 1 µg DNA was mixed with 300 µl DMEM high glucose and 6 µl SuperFect and incubated for 40 min at RT. 2 ml pre-warmed growth medium were added to the reaction mix and the complete solution was added to the cells (in a 3-cm diameter dish) after aspiring the old medium. Cells were cultivated with the transfection medium for 16 h. For transfections of cells in larger dishes, the mixture was scaled up accordingly.

2.9.5 Treatment of B16-F1 cell with Aluminium Fluoride

To induce lamellipodia in B16-F1 cells, cells were treated with aluminium fluoride (ALF_4-). As a phosphate analogue, aluminium fluoride binds with high affinity, but reversibly, to sites in proteins occupied by phosphate as e.g. in Rho-GTPases (Hahne *et al*, 2001). B16-F1 cells express high amounts of the Rho-GTPase Rac1, which is activated by aluminium treatment, resulting in the formation of lamellipodia.

50µM aluminium chloride and 30mM sodium fluoride were mixed in B16-F1 medium, added to the cells and incubated for 15-20 min immediately before fixation.

2.9.6 Knockdown of gene expression by transient RNA interference

Drf3 knockdown vectors were provided by Theresia Stradal and Petra Hagendorff (HZI, Braunschweig) and FMNL2 and FMNL3 knockdown vectors were purchased from Invivogen.

The time course of the run-down of Drf3, FMNL2 and FMNL3 was assessed by immunoblotting as a function of time after transfection of the knockdown plasmid.

For this purpose, cells were transfected with Drf3 knockdown or control vector (Table 8). 16-20 hours after transfection FACS-sorting was performed. For FMNL2 and FMNL2/3 knockdown, cells were co-transfected with the respective knockdown vector and the pPur vector mediating puromycin resistance. 16-20h after transfection, the growth medium was replaced by medium containing 2 µg/ml puromycin. Knockdown

cell populations from day 2 through day 6 after transfection were subjected to western blot analysis.

Target gene	Sequence 5´ to 3´	Specifity	Vector
Drf3 Hum 341	AAGCCACTGTCAGAGAATG	human	pSiren-ZsGreen
mDia2 Mus 1358	AACGGACCCTGACTTCACA	mouse	pSiren-ZsGreen
scrambled control	NNNNNNNNNNNNN		psiRNA-h7SK GFP:Zeo control
FMNL2-1	GGAAGTCTGCGGATGAGATAT	mouse	psiRNA-h7SK GFP:Zeo
FMNL2-2	GGAATTAAGAAGGCGACAAGT	mouse	psiRNA-h7SK GFP:Zeo
FMNL3	GAAACCTATCAAGACCAAGTT	mouse&human	psiRNA-h7SK GFP:Zeo
FMNL3	GGTGCAGATTCAAGCGTACCT	mouse	psiRNA-h7SK GFP:Zeo

Table 8: Knockdown vectors employed in this work

2.10 Immunofluorescence Microscopy and Live-Cell Imaging

2.10.1 Labelling of the Actin Cytoskeleton

Phalloidin, a component derived from the mushroom *Amanita phalloides*, specifically binds to actin filaments and stabilizes them against depolymerization (Cooper, 1987). Fluorescent derivatives Alexa Fluor™ 488 -coupled phalloidin and Alexa Fluor™ 594 -coupled phalloidin (Molecular Probes), 3 U/ml was dissolved in 1% BSA in PBS and used to stain actin filaments in permeabilized cells.

2.10.2 Fixation procedures, stainings and analysis

For phalloidin stainings, cells were fixed with 4% formaldehyde (PFA) in PBS for 20 minutes and extracted with a mixture of 0.1% Triton X-100 in PFA (4%) for 1 minute. For fascin stainings, cells were fixed in -20°C methanol for 10 minutes. Afterwards, cells were washed three times with PBS and blocked with 5% horse serum in 1%BSA for 1h at room temperature.

To stain for filamentous actin, fluorescently coupled phalloidin was added and the coverslips with cells were incubated on parafilm in a humid chamber at room temperature. For staining of other cytoskeletal proteins like Abi and Arp2/3-complex antibodies were diluted in 1% BSA and incubated for 1h at room temperature. After washing the coverslips extensively with PBS, the samples were incubated for 1h at room temperature with the appropriate secondary antibody that was either coupled with

Alexa Fluor™350, Alexa Fluor™ 488 or Alexa Fluor™ 594. The samples were mounted in 5 µl Mowiol 4-88 (Calbiochem) supplemented with n-propylgallate (2.5 µg/ml), dried and stored in the dark at 4℃ until analysis.

Preparations were analyzed on an inverted microscope (Axiovert 100TV, Zeiss, Jena, Germany) using a 63x/1.4 NA or a 100x/1.4 NA plan apochromatic objective. For triple stainings analysis was performed using a 63x/1.25 NA or a 100X/1.3 NA Plan-Neofluar objective. The microscope was equipped for epifluorescence with electronic shutters (i.e. Uniblitz Electronic 35mm shutter including driver Model VMMD-1, BFI Optilas) to allow for computer-controlled opening of the light paths, filterwheel (e.g. LUDL Electronic Products LTD, SN: 102691 and driver SN: 1029595) to enable two-colour epi-fluorescence in combination with appropriate dichroic beamsplitters and emission filters (Chroma Technology Corp., Rockingham, USA), tungsten lamp (Osram, HLX64625, FCR 12V, 100W) for phase contrast optics and mercury lamp (HBO 100W/2, Osram) for epifluorescence and immersion oil (refraction index of 1.518, Zeiss). Images were acquired with a back-illuminated, cooled charge-coupled-device (CCD) camera (TE-CCD 800PB, CoolSnap K4 or CoolSnap HQ_2, Princeton Scientific Instruments, Princeton, USA) driven by IPLab software (Scanalytics Inc., Fairfax, USA) or MetaMorph software (Molecular Devices, Sunnydale, USA). Data and images were processed using ImageJ and Adobe Photoshop 7.0 software.

2.10.3 Electron microscopy

Electron microscopy images were performed by Vic Small, Stefan Köstler and Edith Urban at the Austrian Academy of Science, Austria. For negative stain electron microscopy cells were grown on formvar films and processed essentially as described by Auinger & Small (2008).

2.10.4 Life cell Imaging and data analysis

Cells were observed in an open chamber (Warner Instruments, reading, UK) with a heater controller (model TC-324B, SN:1176) at 37℃. Ham's F12 HEPES buffered medium (Sigma) including complete supplements of the regular growth medium (see 2.9.1) was used for imaging B16-F1 cells. For Hela cells and Cdc42 fl/- and -/- fibroblast cells growth medium 2 + 25mM HEPES was used for live cell imaging. During these experiments, the imaging medium was exchanged roughly every 30 minutes.

Rates of filopodia initiation were assessed from randomly chosen cell peripheries with 30 µm in width and over a time period of ≈20 min. Twenty independent cells were analyzed for each experimental condition, i.e. control and Drf3 knockdown cells. Newly formed filopodia were marked manually at the time point of initiation and counted

subsequently. In total, 393 and 489 filopodia were marked and counted for control and Drf3 knockdown cells, respectively. Statistical analyses were carried out using SigmaPlot, version 11.0 (SPSS, Chicago, IL) and Microsoft Excel, 2003 (Redmond, WA).

Random cell migration assays (Pankov *et al.*, 2005; Kopecki *et al.*, 2007) were performed by using an AxioCam MRm camera (Carl Zeiss) on an Axiovert 200 automatic microscope equipped with closed heating and CO_2 perfusion devices. For random migration assays, cells were plated subconfluently in a 6 well petridish and recorded over 24h with a time intervall of 15min between frames. Migration analyses were carried out using the track objects function of Metamorph (Molecular Devices Corp.). Data were logged into Excel files and processed using Exel 2003 and Sigma Plot 10.0.

3 Results

Prominent protrusive structures generated by the polymerisation of actin filaments include filopodia and lamellipodia. The mechanism underlying the formation of these fundamental structures has been the subject of many studies over the last years. Meaningful data obtained from functional interference studies established that the formation of lamellipodia depends on the nucleating activity of the Arp2/3-complex (Nicholson-Dykstra and Higgs, 2008; Steffen *et al.*, 2006; Innocenti *et al.*, 2004). On the contrary, the way filopodia are nucleated still remains controversial. It has been proposed that filopodia are effectively and continuously initiated by the elongation of pre-existing lamellipodial filaments (Svitkina *et al.*, 2003; Korobova and Svitkina, 2008) but several studies failed to establish the requirement of lamellipodial filaments in filopodia formation (Gomez *et al.*, 2007; Steffen *et al.*, 2006). Therefore, another model has been put forward implicating distinct signalling pathways and separable core machineries driving the formation of filopodia and lamellipodia (reviewed in Faix *et al.*, 2009). This implies de novo nucleation of filopodia by a yet unknown actin nucleator. Diaphanous related formins (Drfs) appeared as promising targets to be analysed concerning this issue given that they nucleate linear, unbranched actin filaments as can be found e.g. in filopodia. This protein family has already been described to regulate a large variety of cellular and morphogenetic functions (reviewed in Faix and Grosse, 2006). More specifically they have already been implicated in the formation of stress fibres or actin cables in yeast (Watanabe *et al.*, 1997; Evangelista *et al.*, 2002), but if and how they contribute to filopodia and lamellipodia formation is still under discussion.

3.1 Subcellular localisation of Diaphanous related formin 3 (Drf3)

In *Dictyostelium* cells, the Drf dDia2 was shown to be critical for filopodia formation suggesting that nucleation and/or elongation of filopodial actin filaments by a formin regulate the assembly of these structures (Schirenbeck *et al.*, 2005). To obtain further insight into the functions of the mammalian homolog mDia2/Drf3, localisation studies were performed utilising genetically encodable fluorescent tags like e.g. EGFP. This allows to visualize precisely where in a given cell a protein accumulates and provides the opportunity to study the dynamic behaviour of a protein of interest in real time. Taking advantage of this tool, full length Drf3 was fused to EGFP and expressed in B16-F1 mouse melanoma cells. Western Blot analysis showed that the fusion protein could be detected in cell extracts running at the expected molecular weight (Figure 19). Similar to previous observations (Yang *et al.*, 2007), full length Drf3 was entirely

cytosolic and did not interfere with the motility of B16-F1 cells (Figure 7A, Supplementary movie 1). This was presumably due to autoinhibition of the full length formin as has been shown for instance for the Diaphanous related formins mDia1 and FRLα (Seth *et al.*, 2006). To obtain a Drf3 variant incapable of autoinhibition, and thus rendered active, a small C-terminal part of the protein encoding the DAD-domain (Figure 7B) was removed. Expression of this construct, called Drf3ΔDAD, in B16-F1 cells strongly induced the formation of filopodia, with the active formin localising to the tip of each filopodium (Figure 7C and Supplementary movie 2). The appearance of these filopodia correlated with the expression level of Drf3ΔDAD. B16-F1 cells expressing high levels of Drf3ΔDAD formed big, club-shaped filopodia, whereas filopodia in low expressing cells had a tapered shape, similar in morphology to constitutively formed filopodia (Figure 7D and E). In most cells, filopodia formation occurred at the expense of lamellipodia, suggesting a mutual antagonism between lamellipodia and filopodia formation in this cell type.

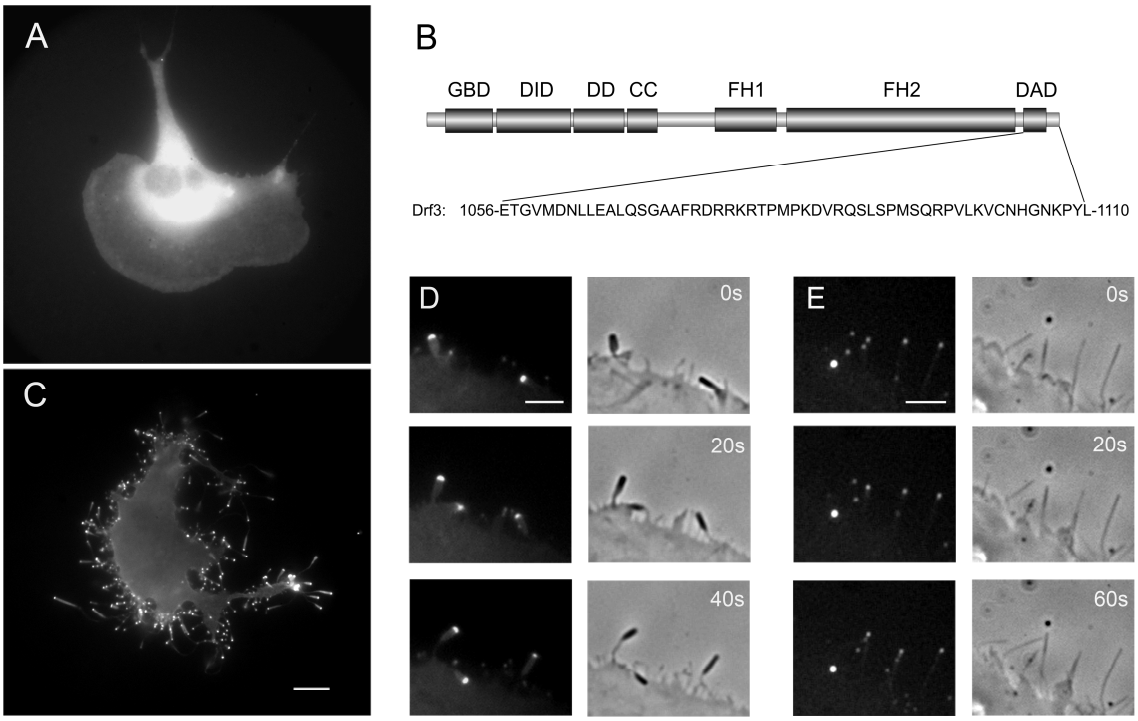

Figure 7: Expression of active Drf3ΔDAD induces the formation of filopodia

(A) EGFP-tagged full-length Drf3 is entirely cytoplasmic. (B) Schematic illustration of the used Drf3ΔDAD constructs lacking amino acid residues 1056–1110. GBD, GTPase-binding domain; DID, Diaphanous-inhibitory domain; DD, Dimerisation domain; CC, Coiled coil; FH, Formin-homology domain; DAD, Diaphanous-auto-inhibitory domain. (C) Drf3ΔDAD expressing cell displaying numerous filopodia. (D) and (E) Filopodial protrusions formed in high and low Drf3ΔDAD expressors, respectively. Scale bar in (C) is 10 µm and valid for (A) and (C). Scale bars in (D) and (E) are 5 µm.

3.2 Cdc42 and Rif induce filopodia via Drf3

One important feature of Diaphanous related formins is their ability to become activated upon interaction with Rho-GTPases in a nucleotide-dependent manner (Alberts, 2001; Watanabe *et al.*, 1997). Relieving the intramolecular interaction between the DID and the DAD-domain by binding of an activated Rho-GTPase is prerequisite for actin assembly and proper localisation within the cell (Seth *et al.*, 2006; Martin *et al.*, 2007). *In vitro* data showed that Drf3 binds Cdc42 in a nucleotide-dependent manner (Alberts *et al.*, 1998). Subsequently, FRET experiments indicated that active Cdc42 is able to interact with Drf3 at sites of actin remodeling (Peng *et al.*, 2003), but more striking results were observed upon co-transfection of Drf3 with constitutively active Rif, which induced filopodia tipped by the formin (Pellegrin and Mellor, 2005).

Assuming that co-expression of Cdc42 or Rif would release the autoinhibiton of Drf3 and subsequently cause proper subcellular localisation, B16-F1 cells transfected with EGFP-Drf3 full length were co-transfected with constitutively active Cdc42 (L61) or

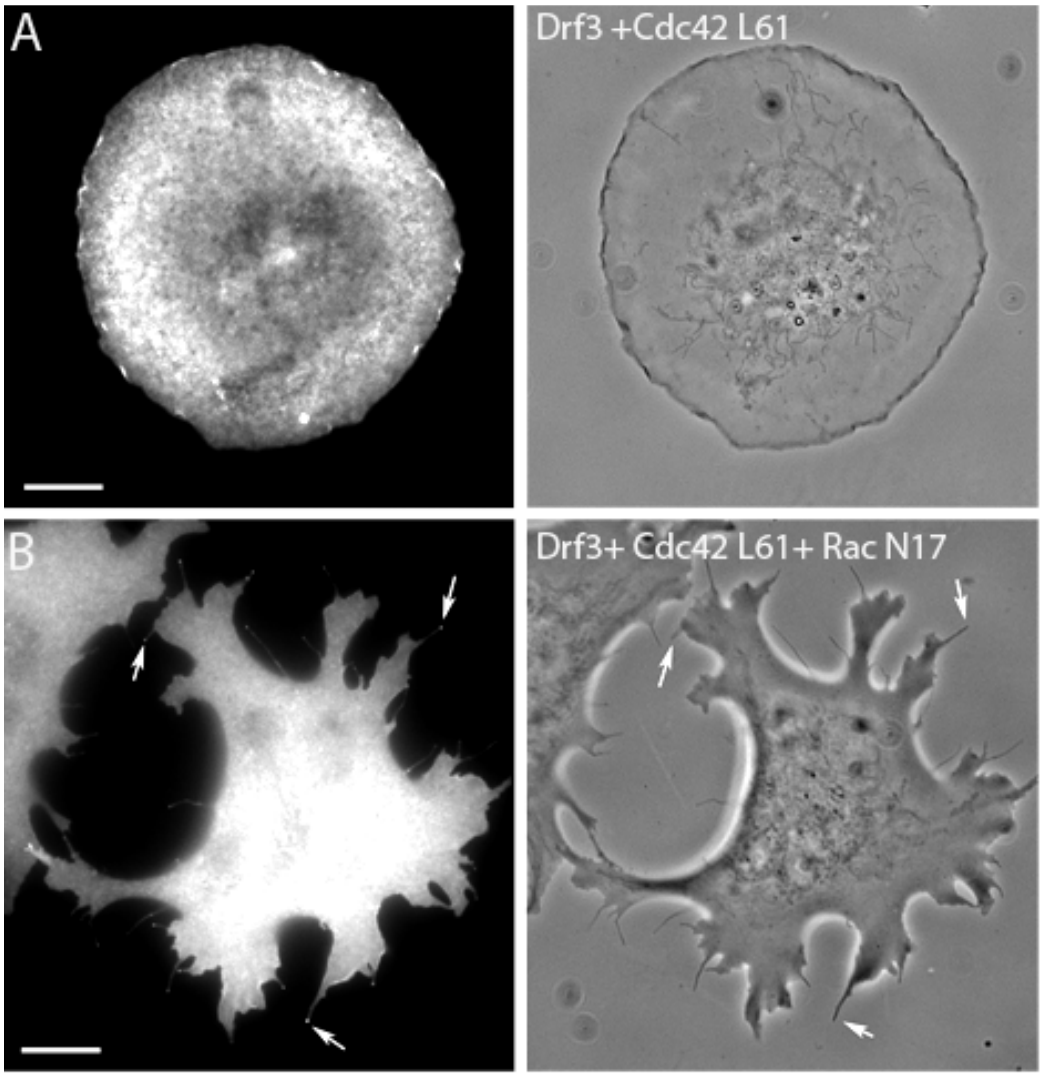

Figure 8: Cdc42-induced targeting of Drf3 to the plasma membrane and the tips of filopodia upon Rac inhibition.

A) Co-expression of full length Drf3 and active Cdc42 (L61) translocated Drf3 to the plasma membrane in B16-F1 cells. B) After suppression of Rac signalling by dominant negative approach, filopodia formation through active Cdc42 could be induced (arrows in B right panel), and Drf3 localised at tips of these filopodia (arrows in B left panel). Bars equal 10 µm

constitutively active Rif (L77). Surprisingly, co-expression of active Cdc42 was not sufficient to induce filopodia with Drf3 localising at the tips, but instead caused translocation of Drf3 to the whole plasma membrane (Figure 8A). This could be explained, at least in part, by strong activation of Rac via Cdc42, which would result in the formation of lamellipodia rather than filopodia (DerMardirossian *et al.* 2004; Nobes and Hall, 1995). This is supported by the fact that B16-F1 cells transfected with active

Cdc42 exhibit a pancake-like shape (Figure 8A), which can also be observed upon expression of active Rac GTPases. To overcome this, I exploited dominant negative mutants, which are a popular tool to suppress the activity of specific Rho-GTPases, because they can act as “dead ends” of specific signalling pathways (Feig, 1999). Thus, the activity of Rac has been suppressed via triple transfection of Drf3 full length, active Cdc42 (L61) and dominant negative Rac (N17). As expected, this induced the formation of filopodia without or with much less concomitant membrane ruffling, and Drf3 could be observed at the tips of filopodia (Figure 8B), although this phenotype was not as distinct as that caused by over-expression of Drf3ΔDAD alone.

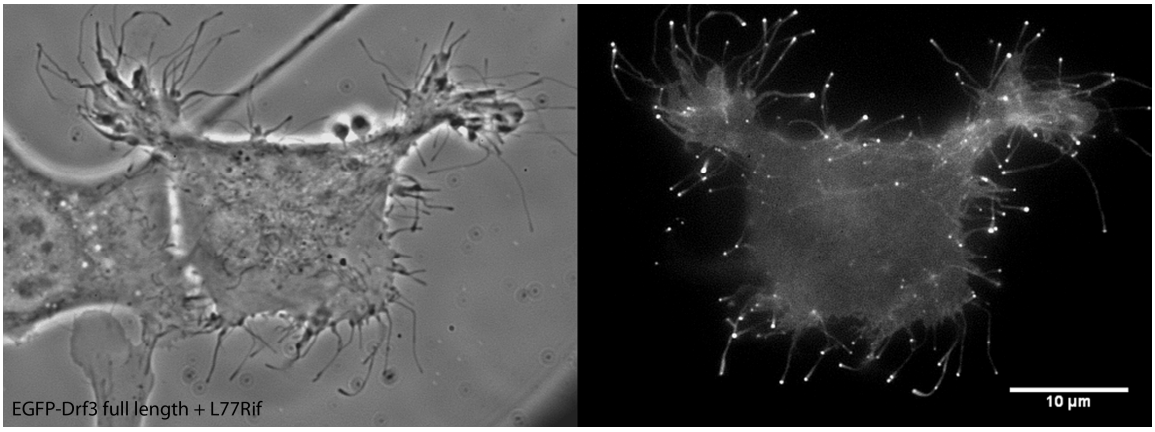

Figure 9: Co-transfection of Drf3 full length with constitutively active Rif induces filopodia.

Co-expression of constitutively active Rif (L77) induced the formation of filopodia (A) comparable to the phenotype observed with EGFP-Drf3ΔDAD and strongly targeted Drf3 to tips of filopodia (B). Bar equals 10 µm.

On the contrary, co-transfection of Drf3 with constitutively active Rif (L77) resulted in formation of dozens of Drf3 marked filopodia comparable to the phenotype observed upon transfection of B16-F1 cells with Drf3ΔDAD (Figure 9). This clearly demonstrates that Drf3 targeting to filopodia tips can be potently effected by Rif expression and may or may not involve Cdc42 signalling. In addition, this remarkable change in subcellular Drf3 localisation upon co-expression of active Rif proved the functionality of the Drf3 full length fusion protein.

3.3 Drf3-induced filopodia are initiated by de novo nucleation

To determine if filopodia are formed by convergent elongation of pre-existing lamellipodial filaments or if they are nucleated independently of lamellipodial filaments, the Drf3ΔDAD-induced filopodia were examined more closely. Following filopodia dynamics over time by live-microscopy revealed that frequently a thickening of filopodia after protruding beyond the lamellipodia edge could be observed (Figure 10).

Sometimes this thickening was accompanied by an increase in fluorescent intensitiy of EGFP-Drf3ΔDAD (data not shown). Additionally, fluorescent intensities of active Drf3 directly correlated with the intensitiy of phalloidin staining marking filamentous F-Actin (Figure 11), indicating that an increase in active Drf3 at filopodia tips results in an increase of actin filaments.

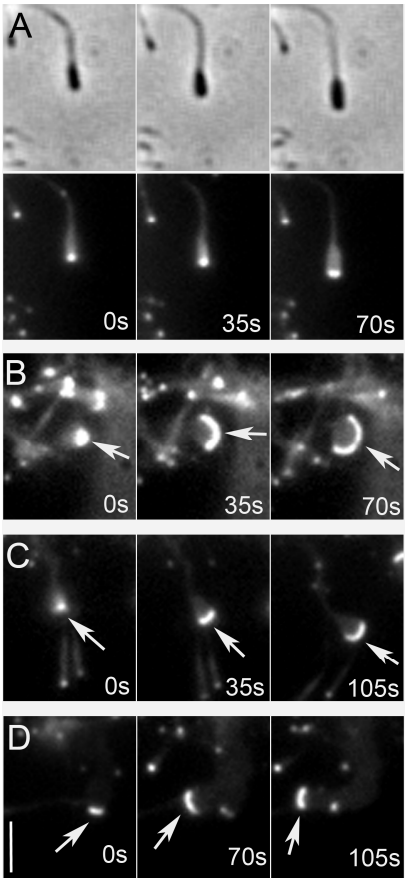

Figure 10: Spontaneous thickening of Drf3ΔDAD-induced filopodia.

Panels of time-lapse sequences of parts of Drf3ΔDAD-over-expressers showing filopodia after having separated from the cell periphery. Note thickening of filopodia tips and concomitant increase in intensity (A) or widening of the fluorescence signal (arrows in (B–D)). Bar in (D) is valid for all images and corresponds to 2 µm.

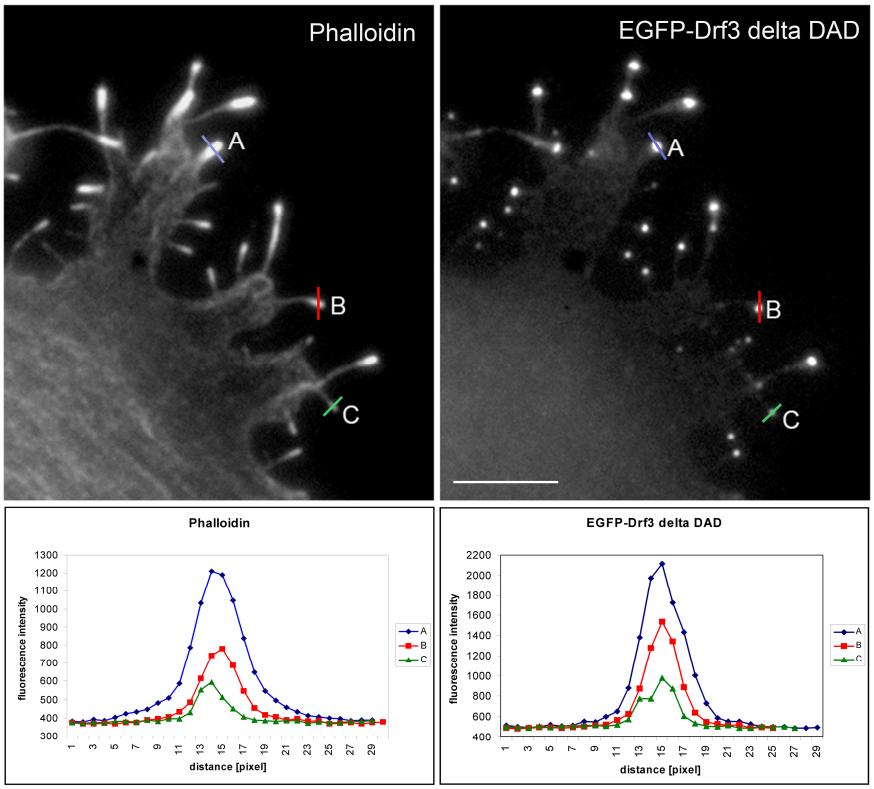

Figure 11: B16-F1 cell over-expressing EGFP-tagged Drf3ΔDAD and counterstained for phalloidin.

Line-scans show fluorescence intensities as measured for F-actin and Drf3ΔDAD in the tip regions of three distinct filopodia of variable prominence. Colour codes used in the curves at the bottom (curves A, B, C) highlight the different measurements as indicated in the images at the top. A robust correlation between Drf3ΔDAD and F-actin amounts is observed in these filopodia. Bar equals 3 µm.

To obtain more evidence in favour of or against the *de novo* nucleation of filopodia, the ultra-structure of actin filaments within the club-shaped filopodia was examined in more detail. Therefore, electron microscopy of whole mount specimen was performed in collaboration with Prof. J. Victor Small (IMBA, Vienna, Austria). An average filopodium has a uniform diameter of 0.1-0.2 µm and is composed of many densely packed filaments (Vignjevic *et al.*, 2006, Svitkina *et al.*, 2003), as shown in Figure 12A. The shafts of the Drf3-induced club-shaped filopodia consisted of a moderate number of long, parallel actin filaments. The tips however had a diameter up to 0.7 µm, with a higher number of filaments in the tips compared to the shafts of these structures (Figure 12B and C). Frequently, it could be observed that a newly formed filopodium is emanating from a pre-existing filopodium (Figure 12D), which can not be explained by convergent elongation of lamellipodial filaments.

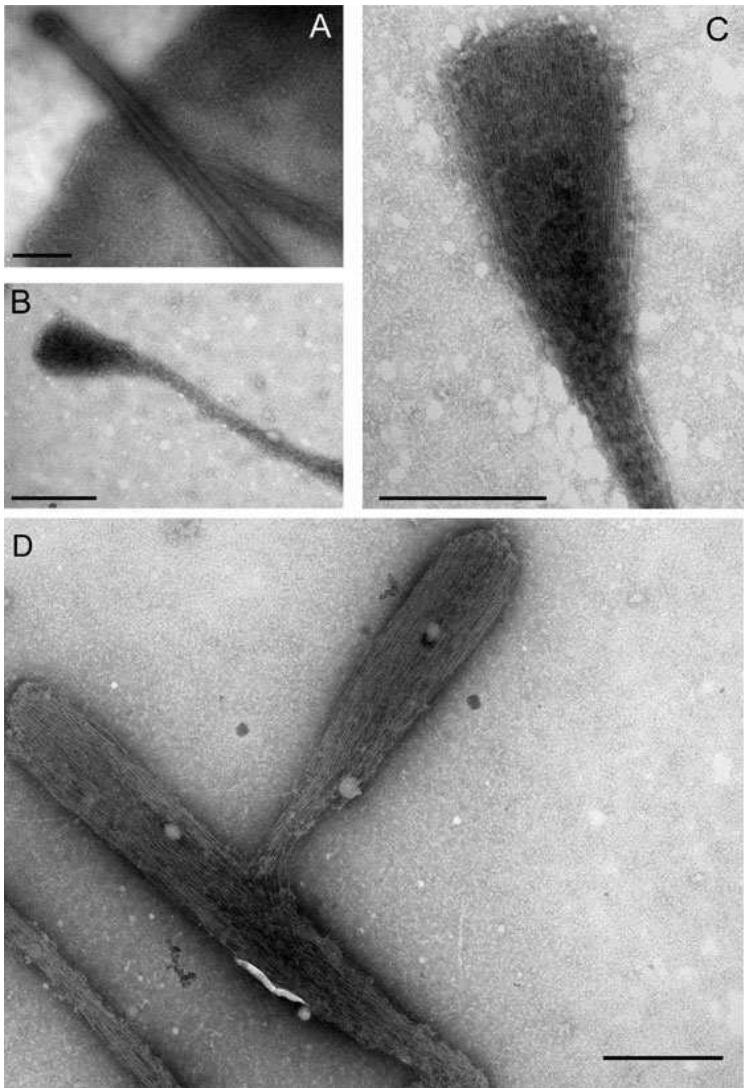

Figure 12: Filopodia ultra-structure in control and Drf3ΔDAD over-expressing cells.

Transmission electron micrographs of negatively-stained whole mount cytoskeletons of B16-F1 control cell (A) or Drf3ΔDAD over-expressors (B–D). (a) Typical control filopodium formed in non-transfected B16-F1 cell, not displaying filopodial thickening in the tips, frequently observed with Drf3ΔDAD-induced filopodia (B–D). Note prominent actin filament accumulation in filopodia clubs, and a low number of long, linear filaments along the shafts (B, C). (D) shows representative example of filopodial club, branching off another. Scale bars are 500 nm.

Counting of individual filaments in the tip and the shaft of Drf3-induced filopodia as indicated in Figure 13A revealed a linear correlation between filopodia width and filament number (Figure 13B), thus a constant packing density of actin filament within these structures (Figure 13C). All these data strongly indicate that it is very unlikely that filopodia are exclusively formed by convergent elongation as proposed by Svitkina *et al.*, but support *de novo* nucleation of Drf3-induced filopodia.

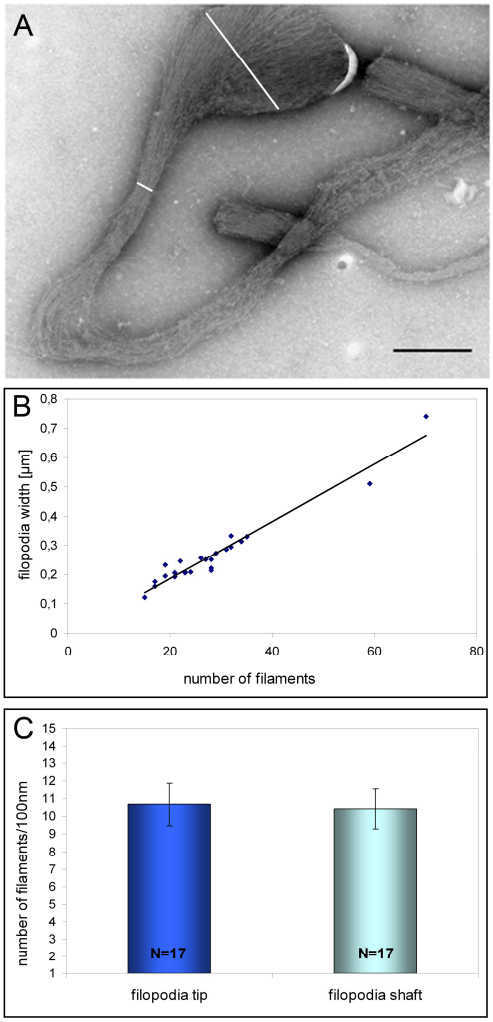

Figure 13: Analysis of filament numbers in Drf3ΔDAD-induced filopodia

B16-F1cells over-expressing EGFP-tagged Drf3ΔDAD were subjected to manual counting of filaments. Crossing white lines drawn across tip or shaft regions as indicated (A). Scale bar equals 500 nm. (B) Filament numbers as assessed from tips of filopodial clubs plotted versus tip widths (N =22). (C) Comparison of filament numbers in tips and shafts of Drf3ΔDAD-induced filopodia as indicated, which corresponded on average to 10.68 ± 1.19 and 10.42 ± 1.13 filaments per 100 nm, respectively.

3.4 Drf3-induced filopodia formation in the absence of functional WAVE-complex

Lamellipodia formation critically depends on WAVE-complex-mediated Arp2/3-complex activation leading to the nucleation of new lamellipodial filaments. Assuming that filopodia are exclusively formed by convergent elongation of lamellipodial filaments, cells expressing reduced levels of all WAVE-complex components by RNAi should be unable to form filopodia. Additionally, it was previously published that the WAVE-complex subunit Abi-1 interacts with Drf3 and is required for efficient induction of filopodia and targeting of the formin to the membrane (Beli *et al.*, 2008).

To test whether active Drf3ΔDAD required lamellipodial filaments for induction of filopodia and Abi for targeting to the membrane, I exploited stable Nap1 knockdown VA-13 fibroblast cells, previously established to lack lamellipodia and to display a strongly reduced level of all WAVE-complex components including Abi-1 (Steffen *et al.*, 2006). Stable control and Nap1 knockdown fibroblasts were transfected with EGFP-Drf3ΔDAD. As seen in Figure 14, active Drf3 was sufficient to induce filopodia in mock-treated fibroblasts tipped by the active formin as expected, although the response was not as pronounced as in B16-F1 cells (Supplementary movie 3). Remarkably, also Nap1 knockdown cells that lack lamellipodia were able to form numerous filopodia upon transfection with Drf3ΔDAD (Figure 15). Although these cells express reduced levels of Abi-1, which has been implicated for targeting Drf3 to the membrane, Drf3 still localized to the tips of filopodia to extents comparable to mock-treated cells (Figure 15 and Supplementary movie 4), strongly indicating that Abi is not required for Drf3 targeting to filopodial tips.

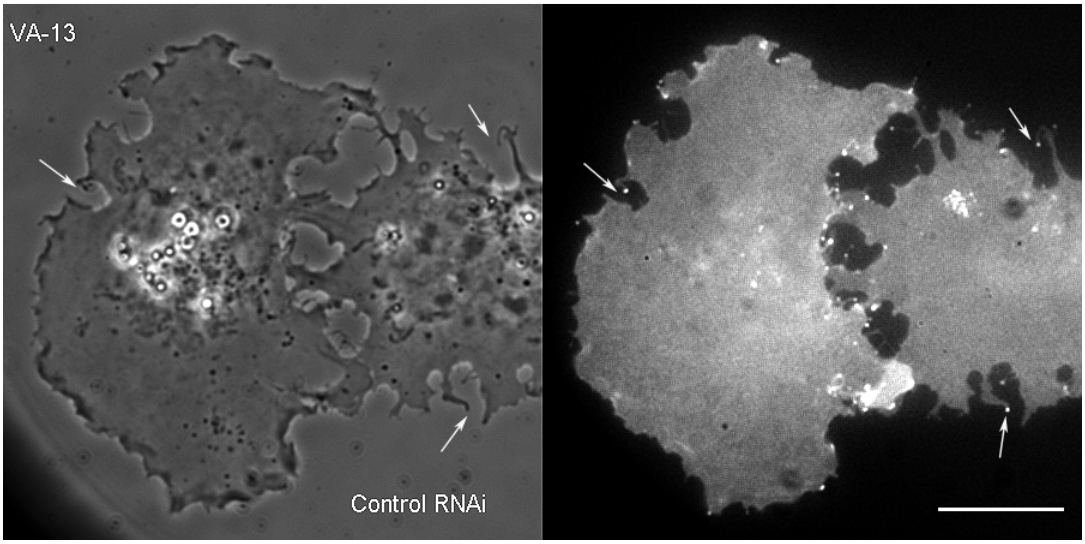

Figure 14: Control siRNA-treated (Control RNAi) VA-13 fibroblast cell (Steffen *et al.*, 2006) transiently transfected with Drf3ΔDAD.

Arrows mark filopodia tipped by the EGFP-tagged formin. Bar equals 10 µm.

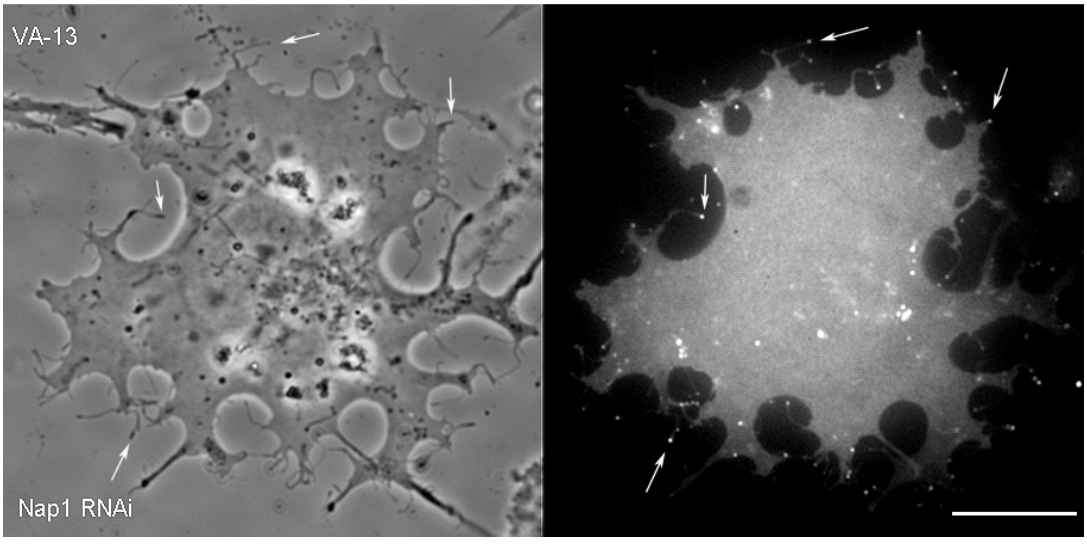

Figure 15: Nap1 knockdown VA-13 fibroblast (Nap1 RNAi) transiently expressing Drf3ΔDAD.

Note prominent formation of filopodia tipped by EGFP-tagged DRf3ΔDAD (arrows) in spite of WAVE-complex loss of function and coincident lack of lamellipodia (Steffen *et al.*, 2004) Bar equals 10 µm.

3.5 Drf3ΔDAD-induced filament networks contain lamellipodial marker proteins and fascin

As mentioned previously, filopodia formation in Drf3ΔDAD-expressing cells occurred at the expense of lamellipodia. However, in some cases Drf3ΔDAD could also be observed at the tips of protrusive sheet-like structures as seen in Figure 16 and Figure 17. Following the dynamics of Drf3ΔDAD in these lamellipodia-like-structures by live video microscopy, it became obvious that Drf3ΔDAD showed a lateral movement different from other components typically found in lamellipodia-like WAVE-complex components (Stradal *et al.*, 2001; Steffen *et al.*, 2004) and VASP (Rottner *et al.*, 1999) (see Supplementary movie 5). On top of that, the enrichment of Drf3ΔDAD was more variable than observed with other lamellipodia components. To further investigate the nature of these protrusive structures, immunofluorescence stainings were performed. Drf3ΔDAD expressing cells were stained with phalloidin (Figure 16A). Additionally, Drf3-enriched filament networks reminiscent of lamellipodia were counterstained for Arp2/3-complex and prominent nucleating promoting factors like the WAVE complex member Abi-1 and Cortactin. As seen in Figure 16B and Figure 17A and B, these

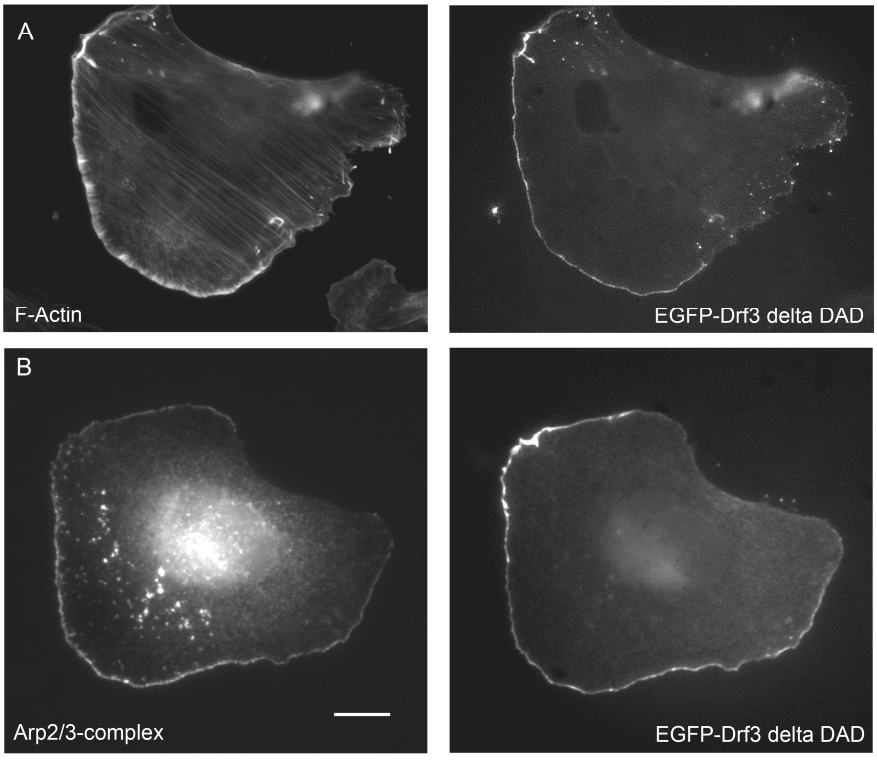

Figure 16: Drf3ΔDAD can target to the tip of a lamellipodium like structure.

EGFP-tagged Drf3ΔDAD accumulation at the tips of lamellipodial actin filament networks, as stained by phalloidin (A) and harbouring Arp2/3-complex (B) as indicated. Bars equal 10µm.

structures were prominently labelled by Arp2/3-complex, Abi-1 and Cortactin, indicating their structural relationship to lamellipodia. However, the same structures were also prominently enriched for the actin crosslinking protein fascin (Figure 17C, arrow). This protein is typically found in microspikes, as shown in Fig. 11C of a neighbouring untransfected cell (Figure 17C, asterisk), but also in filopodia (Nemethova *et al.*, 2008) and is well established to be required for microspike/filopodia formation (Vignjevic *et al.*, 2006). This unusual enrichment of fascin at Drf3ΔDAD-labelled lamellipodia-like-structures indicates that these protrusive structures do not represent canonical lamellipodia, but instead a hybride of lamellipodia and filopodia.

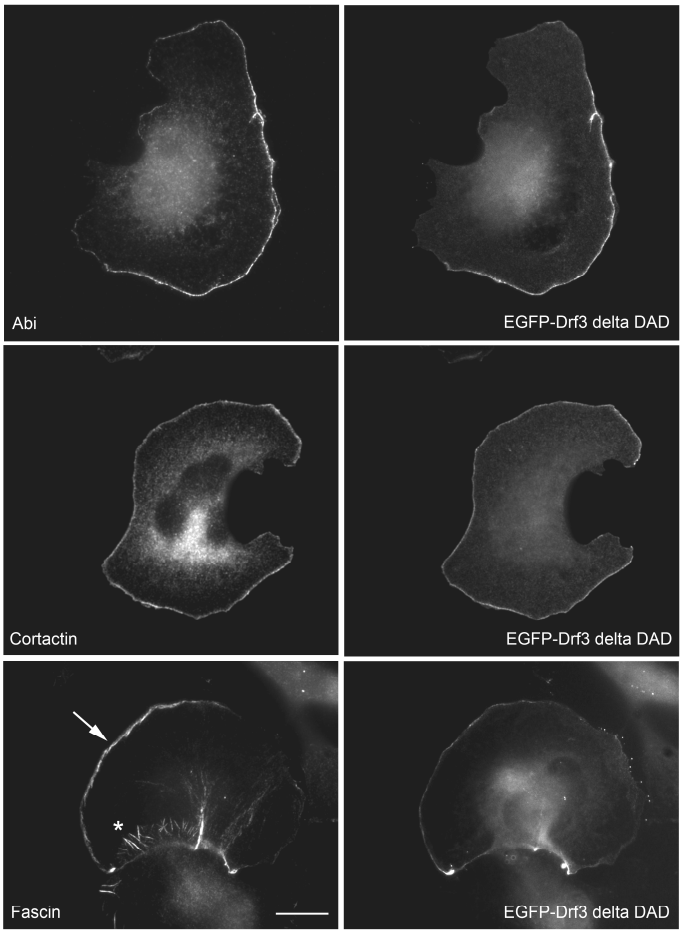

Figure 17: Drf3ΔDAD induced lamellipodia-like-structures contain Arp2/3 complex and fascin.

B16-F1cells expressing EGFP-tagged Drf3ΔDAD were counterstained for the WAVE-complex component Abi, cortactin and fascin as indicated. Note prominent co-accumulation of Drf3ΔDAD with the respective component. Asterisk in fascin image highlights typical label on micro-spikes (Vignjevic *et al.*, 2006) embedded into the lamellipodium of a neighbouring, non-transfected cell. Scale bar equals 10 µm.

3.6 Loss of Drf3 does not alter filopodia initiation in Hela S3 cells

Over the last years conflicting results on the influence of Drf3 on filopodia and lamellipodia formation have been published. In *Dicytostelium discoideum*, dDia2 is essential for the formation and maintenance of filopodia (Schirenbeck *et al.*, 2005). In the mammalian system, knockdown of mDia2 has been described to abrogate lamellipodia and filopodia formation on one hand (Yang *et al.* 2007), or to induce the formation of lamellipodia at the expense of filopodia on the other hand (Beli *et al.*,

2008). The latter results were obtained in Hela and the former in B16-F1 cells, although it is presently unclear if the observed differences are due to use of different cell types.

In any case an important prerequisite to study the influence of Drfs on cell migration is the information about their relative expression in different cell lines. Thus expression profiles of Drf1- 3 in different murine and human cells lines were acquired using Genechip technology (cooperation with Drs. Robert Geffers and Theresia Stradal, HZI, Braunschweig) (Figure 18).

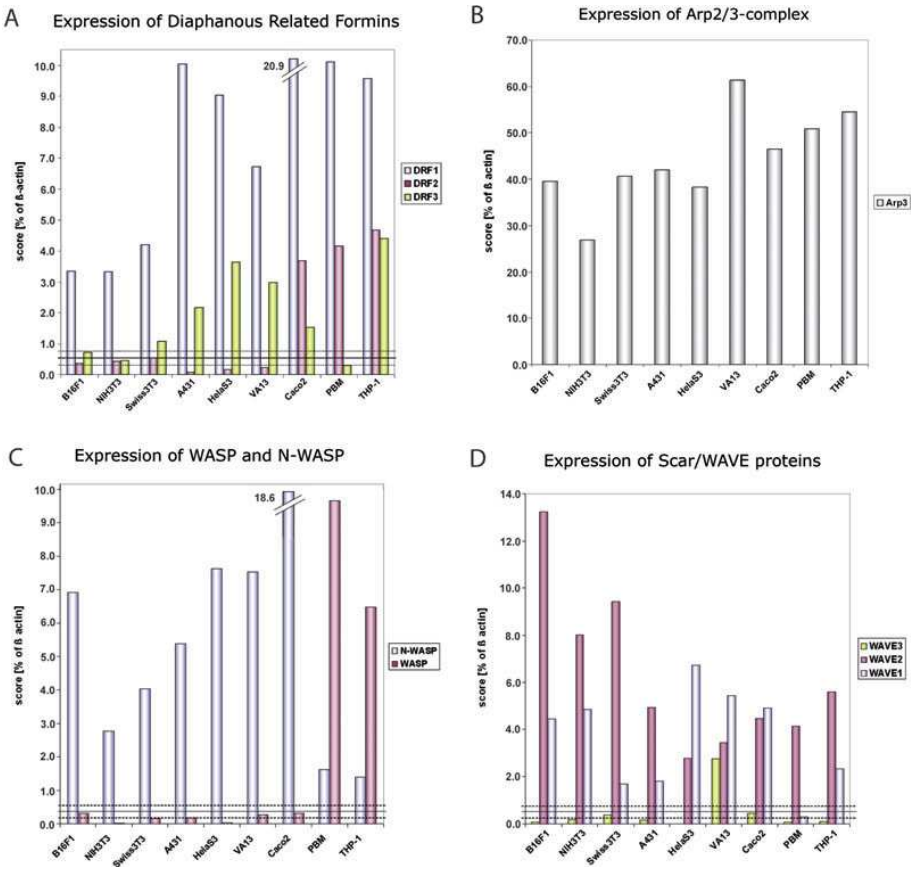

Figure 18: Microarray analyses of cell lines as indicated.

(A) Expression levels of Drf1-3 normalized to ß-actin. Note most prominent Drf3 expression in Hela S3, VA-13 and THP-1. (B) Arp3, (C) N-WASP/WASP and (D) WAVE isoform expression as normalized to *β*-actin. Black solid and dashed lines in (A), (C) and (D) indicate average background levels ± standard deviation from all Gene Chips.

It turned out that Drf1 (mDia1) was expressed in all tested cell lines, whereas Drf2 (mDia3) and Drf3 (mDia2) were much less abundant. Specifically, Drf3 was of low abundance in the murine cell lines tested here, including B16-F1 cells, that have been used by Yang *et al.*, as well as in NIH 3T3 cells as reported previously (Tominaga *et al.*, 2000; Peng *et al.*, 2003). In contrast high expression of Drf3 could be detected in

VA-13 fibroblasts and the epithelial cell lines Hela S3 and CaCo2. These results were confirmed by western blot analyses of murine and human cell lines commonly used in our lab using a polyclonal anti-Drf3 antibody (Figure 19), originally raised against an N-terminal fragments (residues 1-565) of human Drf3.

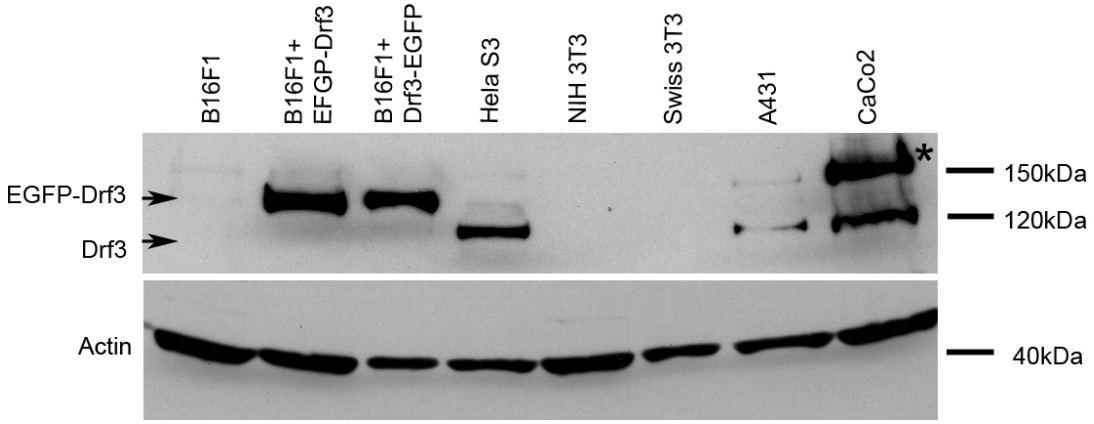

Figure 19: Expression of Drf3 in different murine and human cell lines

Different murine and human cell lysates subjected to western blot analysis using a polyclonal α-Drf3 antibody. Please note expression of Drf3 in Hela S3, A431 and CaCo2 cells and the correct molecular weight (150 kDa) of N- and C-terminal EGFP-Drf3 fusion proteins. Antibody against actin was used as loading control. Asterisk marks non-specific crossreaction in CaCo2 cells.

In line with the microarray data, no expression of Drf3 could be detected in B16-F1, NIH 3T3 and Swiss 3T3 cells, whereas most prominent Drf3 expression was observed in Hela S3 and CaCo2 cells. We conclude this was not due to a lack of reactivity of the antibody with murine mDia2/Drf3, since the murine N-terminus tagged with EGFP was readily detected (data not shown).

As mentioned above, the function of Drf3 in lamellipodia and filopodia formation is still controversial. To reconcile these differences and in order to get more insight into the mechanism of filopodia formation, loss of function studies using Hela S3, which express a high amount of Drf3, have been performed. To do this expression of Drf3 in Hela S3 cells was transiently knocked-down by RNAi. These cells have been subjected to video microscopy to study their ability to form filopodia and to analyse their dynamics in the absence of Drf3 (Figure 20A). Surprisingly, counting the number of newly formed filopodia in a 30µm-wide cell periphery over a period of 20min showed that interference with Drf3 protein levels in Hela S3 cells did not impair filopodia formation, which is in contrast to previously published results (Figure 20B). In fact, the average rate of filopodia initiation was increased rather then decreased in Drf3 knockdown compared

to mock-treated cells, although the reasons for this remained unclear. These data do not support the idea of Drf3 being the main nucleator of actin filaments in filopodia formed by Hela cells.

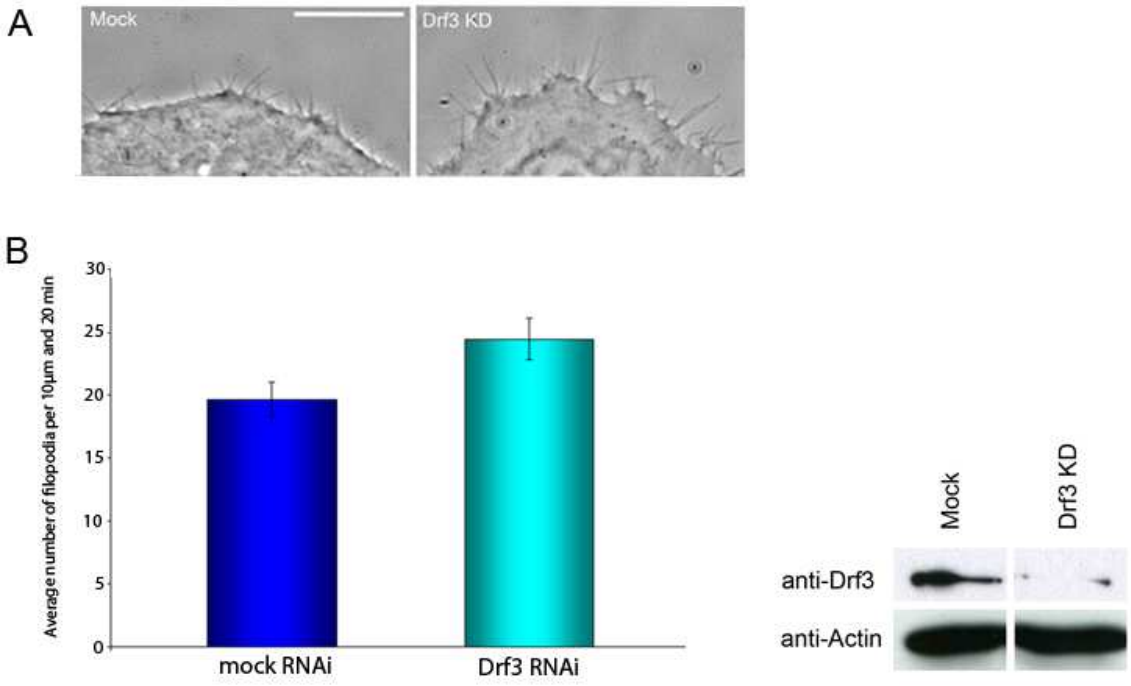

Figure 20: Filopodia formation does not require Drf3 in Hela cells.

(A) Hela S3 cells transiently knocked down for Drf3 were still able to form filopodia. Bar equals 10µm. (B) Quantification of newly formed filopodia in mock and Drf3 knockdown cells derived from four independent experiment. Hela S3 cells expressing reduced levels of Drf3 can initiate filopodia. Mock treated cells formed 19,65 ± 1,4 and Drf3 knockdown cells 24,45± 1,7 filopodia per 30µm cell periphery and a time period of 20min. Data represent filopodia analysed from 20 cells for each condition, in total 393 filopodia for control and 489 filopodia for Drf3 knockdown cells were counted. Efficient knockdown of Drf3 was confirmed by Western Blotting (right panel). Actin was used as a loading control.

As mentioned above, Drf3ΔDAD was occasionally observed to accumulate at the tips of lamellipodia-like structures that were interpreted to constitute canonical lamellipodia previously (Yang *et al.*, 2007). To test if Drf3 might indeed have a role in lamellipodia formation, mock-treated and Drf3 knockdown Hela S3 cells were co-transfected with myc-tagged constitutively active Rac (L61), which is well known to elicit the formation of lamellipodia (Ridley *et al.*, 1992). Expression of active Rac was confirmed by α-myc staining. Control cells and Hela cells with reduced Drf3 levels exhibited a pancake-like shape, which is typical for expression of active Rac (Figure 21). Both cell populations where capable of lamellipodia formation as shown in Figure 21A, D and G. Together these data indicate that Drf3 is dispensable for the formation of both filopodia and lamellipodia, at least in Hela S3 cells.

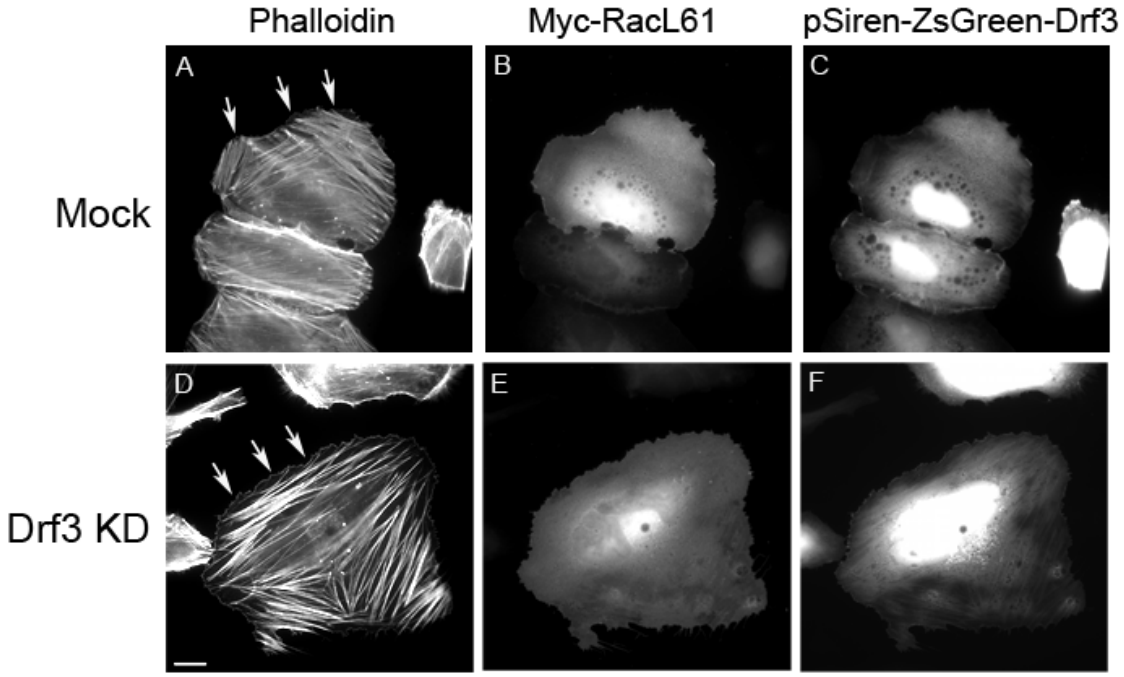

Figure 21: Drf3 is not required for Rac-induced lamellipodia formation.

Mock (A-C) and Drf3 knockdown (D-F) Hela S3 cells expressing the pSiren-ZsGreen Drf3 silencing vector, visible by a green fluorescence (ZsGreen). (B and E) Cells have been co-transfected with myc-tagged-constitutively active Rac (L61) stained by α-myc antibody, to induce the formation of lamellipodia. (A and D) Phalloidin staining revealed that Mock and Drf3 knockdown cells are able to form lamellipodia upon expression of active Rac. Bar in G is valid for all images and equals 10µm.

3.7 Formin expression profiles

Filopodia are an evolutionary conserved structure found in many different cell types. Although they can clearly occur downstream of multiple signalling pathways it is conceivable that a core machinery of filopodial actin assembly and a common molecular mechanism exists in all cell types able to form these protrusive structures (Ladwein and Rottner, 2008; Faix *et al.*, 2009). In contrast to published results the data accumulated so far indicate that Drf3 is not required for filopodia formation in Hela S3 cells. This conclusion is supported by the fact that cell lines like Swiss or NIH 3T3 and B16-F1 cells are able to form filopodia in a robust fashion, although they express

	B16	NIH	Swiss	A431	Hela S3	VA-13
Drf1	+++	+++	+++	++++	++++	++++
Drf2	-	-	-	-	-	-
Drf3	+	(+)	+(+)	+++	+++	+++
DAAM1	+++	+++	++	++++	++	+++
DAAM2	+(+)	-	-	-	-	-
Delphilin	-	-	-	-	-	-
FMN1	(+)	(+)	-	-	-	-
FMN2	-	-	-	-	+++	+++
FMNL1	-	-	-	-	+	-
FMNL2	+++	+++	+++	+++	+++	+++
FMNL3	++	+++	+++	(+)	-	-
FHOD1	-	(+)	(+)	(+)	+(+)	+(+)
FHOD3/FHOS2	-	-	-	+++	-	(+)

Figure 22: Expression profile of formins in different murine and human cell lines.

Microarray analyses showed abundant expression of Drf1, DAAM1 and FMNL2 in all tested cell lines (marked yellow), some formins like FMNL3 where only expressed in significant amounts in murine cell lines, others like Drf3 only in human cell lines. ++++ represents values >500; +++ >250; ++ >150; +(+) >100; + =app. 100; (+) >50; - <50; only values above 100 are considered significant.

minute amounts of Drf3, pointing towards significant redundancy in the system, mediated perhaps by other formins.

To narrow down further candidates of mammalian formins potentially capable of effecting filopodia formation in addition to mDia2/Drf3, the expression of thirteen members of the formin family in various tissue culture cell lines was analysed by array analysis (collaboration with Drs. Robert Geffers and Theresia Stradal, HZI, Braunschweig). Given that filopodia formation can occur in multiple cell types such as fibroblasts, epithelial or neuronal cells, widely expressed formins were considered most interesting for further analysis. As shown in Figure 22, Drf1, DAAM1 (Dishevelled-associated activator of morphogenesis-1) and FMNL2 (Formin related gene in leukocytes 2) are the only formins that are expressed in high levels in all tested cell lines.

Since mDia1 binds to Rho rather than Cdc42 (Faix and Grosse, 2006), and its genetic removal in fibroblasts enhances filopodia formation rather than compromising it (Peng *et al.*, 2003), mDia1 was unlikely to be crucial for filopodia formation and was therefore not studied in more detail.

Work in *Xenopus leavis* oocytes implicated a role for DAAM1 to relay signalling from the Wnt:Frizzled ligand receptor system, via dishevelled, to regulate cell polarity during gastrulation (Habas *et al.*, 2001). A recent publication concerning dDAAM1 in *Drosophila* reported a critical role for this formin in filopodia formation of axonal growth cones (Matusek *et al.*, 2008). In addition, DAAM1 has been described as downstream effector of RhoA and Cdc42 (Aspenström *et al.*, 2006), making it an interesting candidate to study its function in Cdc42-induced filopodia formation. I therefore explored the subcellular localisation of the diaphanous related formin DAAM1. DAAM1 cDNA was amplified from a RZPD Clone (see 2.6.3) and fused to the enhanced green fluorescent protein (EGFP), expressed in B16-F1 cells and subjected to live-cell microscopy. However, neither full length DAAM1 nor an active variant lacking the DAD-domain associated to any protrusive structures such as lamellipodia or filopodia in these cells (data not shown).

I then turned to the next ubiquitously expressed formin FMNL2 (Figure 22). To date, FMNL2 is poorly characterized and not many data concerning its function in the mammalian system are available. It has been reported that FMNL2 is upregulated in colorectal cancer tumors and metastatic lymph nodes that harbour a high invasive ability (Zhu *et al.*, 2008). Recently, different active variants of FMNL2 (and -3) or hybrids of them have been shown capable of targeting to the cell periphery (Vaillant *et*

al., 2008). Altogether these data pointed towards a potential role of FMNL2 in migration and in the protrusion of lamellipodia or filopodia.

3.8 Generation of fluorescently-labelled FMNL2

To have a closer look at the subcellular localisation of FMNL2 it was necessary to generate a fluorescently-labelled fusion protein. Amplification of FMNL2 cDNA by PCR and subsequent cloning was challenging, since FMNL2 contains approximately 300bp with a very high GC-content (above 80%) encoding the proline-rich region in the FH1-domain. Therefore, EGFP-FMNL2 fusion protein was engineered by fusion of a cDNA clone harbouring a truncated sequence (RZPD Clone IRALp962K1959Q2) with PCR-derived Hela S3 FMNL2 cDNA sequences and codon-optimised, synthesised fragments (GenScript) (see 2.6.3).

The C-terminal part of FMNL2 amplified from Hela S3 cDNA contained a FMNL2 splice variant referred to below as FMNL2C, according to the NCBI reference sequence NM_001004422.1 that has been temporarily suppressed because of insufficient data supporting this transcript. In addition to the FMNL2C variant, two other well described splice variants FMNL2A and FMNL2B (Katoh and Katoh, 2003; Vaillant *et al.* 2009) with C-terminal divergence due to alternative splicing of exon 26 (Figure 23) were of major interest to the project. Thus, FMNL2A and FMNL2B C-terminal regions where synthesised by GenScript and exchanged with the C-terminal part of FMNL2C.

FMNL2 belongs to the family of diaphanous related formins and possesses a conserved domain organisation with a GTPases binding domain (GBD), a FH1- and FH2-domain, a Diaphanous-inhibitory- (DID) and a diaphanous-autoinhibitory-domain (DAD) as shown in Figure 23. Based on my experience with other formins like Drf3 and DAAM1, I first designed a potentially active variant of FMNL2 lacking the DAD-domain. To do this the core DAD-domain containing the GAIEDIIT-motif (Higgs and Peterson, 2005 and see Figure 23) was deleted, resulting in a construct lacking the C-terminal 56 aminoacids; this construct was termed FMNL2ΔDAD.

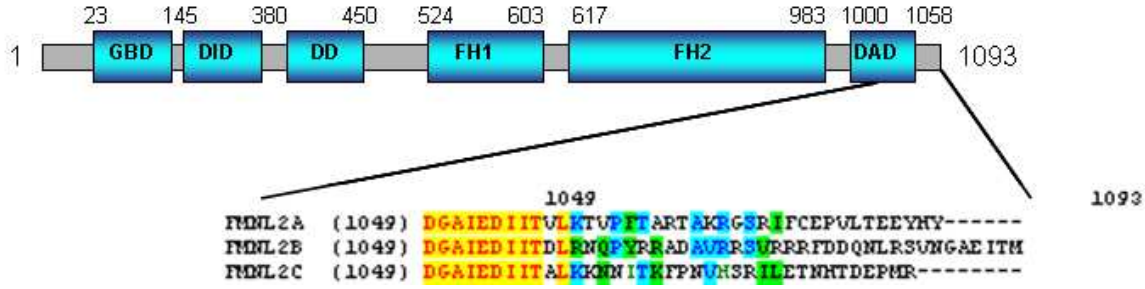

Figure 23: Domain organisation of FMNL2 and splice variants

Overview of domain organization of FMNL2, showing the longest isoform described so far (FMNL2B). Numbers correspond to amino acid residues. FMNL2 possesses an GTPase binding domain (GBD), a Diaphanous-inhibitory-domain (DID) and dimerisation-domain (DD), a formin homology 1 (FH1) and 2 (FH2) and a diaphanous-autoinhibitory-domain (DAD). The bottom provides a sequence comparison of isoforms derived from alternatively-spliced transcript variants.

3.9 Subcellular localisation of FMNL2 splice variants

Based on published data and the abundant expression of FMNL2 in all tested cell lines, FMNL2 appeared as promising target to be analysed concerning its potential function in protrusions such as filopodia and lamellipodia. Therefore, I explored the subcelluar localisation of three FMNL2 splice variants A, B and C by transiently transfecting B16-F1 cells with the respective EGFP-tagged full length FMNL2 constructs. The transfected cells were subjected to video microscopy. As control for non-specific targeting to cytoskeletal structures, B16-F1 cells were transfected with a vector expressing EGFP alone (EGFP-C1, Clontech) and treated in the same way (Figure 24A).

In line with the conclusion that FMNL2 is an autoinhibited formin, full length EGFP-FMNL2A and EGFP-FMNL2B did not accumulate in any specific way at protrusive structures like lamellipodia and filopodia. A strong signal of both splice variants could be observed in the perinuclear region simply due to high thickness in this area. The much thinner peripheral regions of the cells were almost entirely devoid of detectable fluorescence (Figure 24B and C, white arrows), although they contained an actively protruding lamellipodium (Figure 24B and C and Supplementary movie 6 and 7). On the contrary, EGFP-tagged full length FMNL2C weakly associated with the lamellipodium, but did not affect the motility or the morphology of B16-F1 cells (Figure 24D and Supplementary movie 8). This accumulation in the leading edge was clearly more distinct than the unspecific localisation of EGFP alone (Figure 24A), and was therefore considered to be of potential functional relevance.

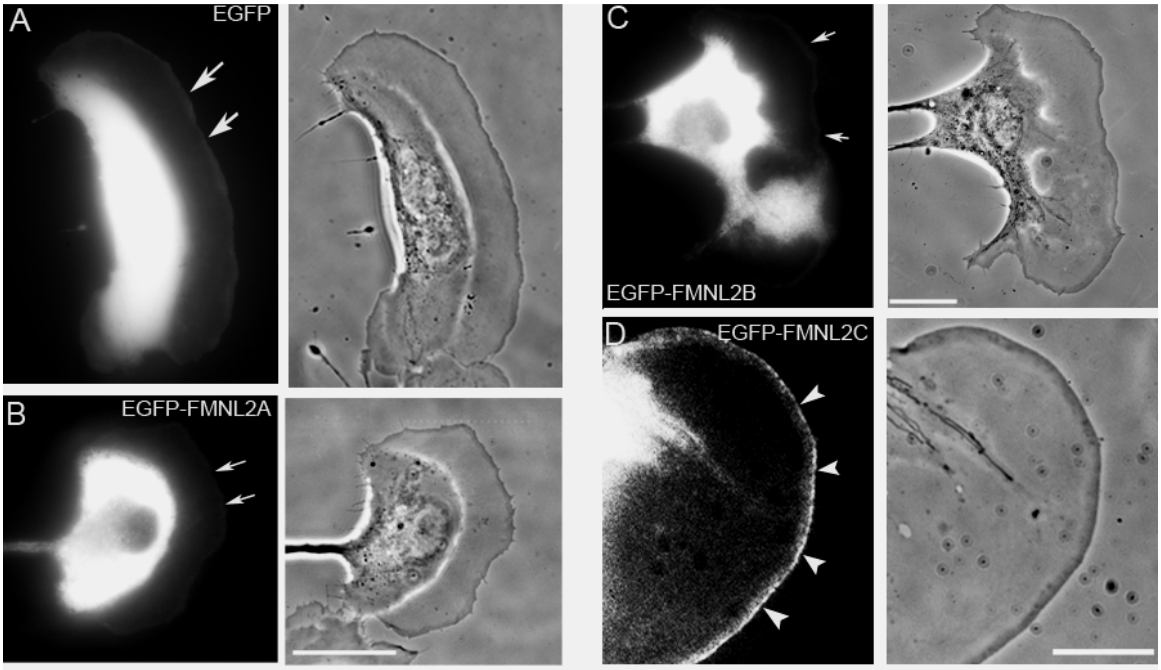

Figure 24: FMNL2A and FMNL2B are entirely cytosolic whereas FMNL2C localises to the leading edge of B16 mouse melanoma cells.

As a control, B16-F1 mouse melanoma cells were transiently transfected with EGFP alone and subjected to video microscopy using fluorescence and phase contrast optics (A). Please note a weak accumulation of EGFP to the lamellipodium (arrows). Expression of EGFP-FMNL2A (B) and FMNL2B (C) in B16-F1 cells did not interfere with lamellipodia formation. Both splice variants lacked any accumulation at the leading edge of the cell (arrows in B and C). In contrast to FMNL2A and -B, full length EGFP-FMNL2C accumulated at the lamellipodium tip in B16-F1 cells (arrowheads in D). Scale bars equal 10µm.

The lack of localisation of full length FMNL2A and B was considered to be due to autoinhibition of the protein. To overcome this, the C-terminal diaphanous autoinhibitory domain (DAD) was removed leading to a presumably active FMNL2 variant. Interestingly, FMNL2ΔDAD strongly accumulated at the tips of protruding filopodia (Figure 25 and Supplementary movie 9), similar to what was previously observed with mDia2 (Block *et al.*, 2008, Yang *et al.*, 2007). In contrast to mDia2, FMNL2ΔDAD did not interfere with lamellipodia formation as frequently observed for mDia2, and did localize to the tips of protruding lamellipodia as was observed above for full length FMNLC. This suggests that FMNL2C may not be fully autoinhibited, as has previously been described for the close relative FRL2 (FMNL3) (Vaillant & Copeland, 2008) and a splice variant of FMNL1 (Han *et al.*, 2009). The authors of both studies proposed that the C-termini of this FRL/FMNL subfamiliy formins do not comprise functional DAD-domains. Our data would fit this hypothesis in case of the C-variant of FMNL2 but not in case of FMNL2A and B.

The previously shown localisation of mDia2ΔDAD to structures reminiscent of but not identical to lamellipodia (Figure 17) was accompanied by an unusual accumulation of the actin bundling protein fascin, normally found in microspikes. To ensure that the

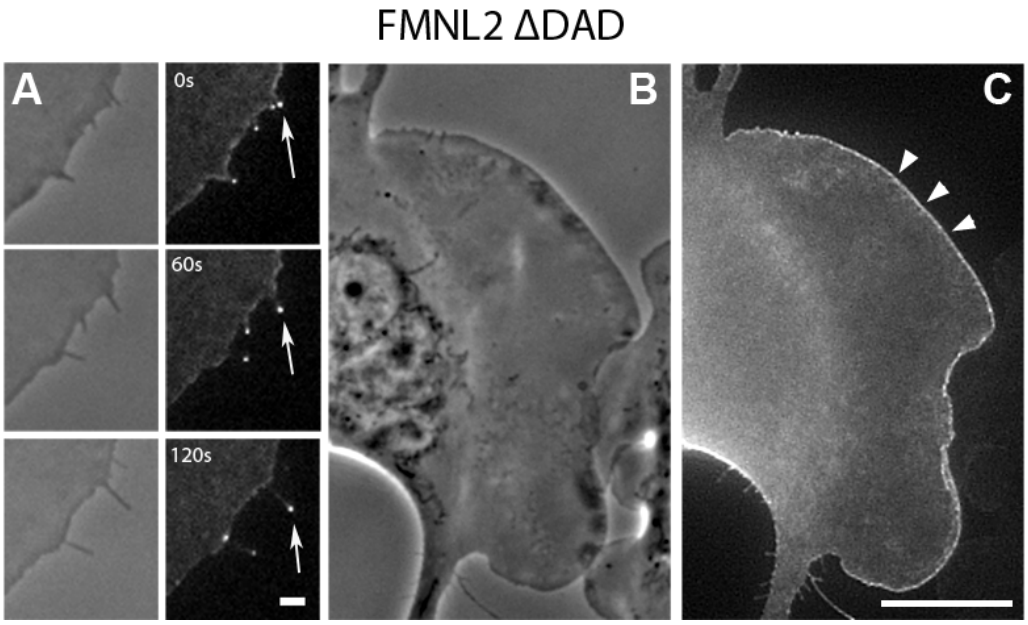

Figure 25: FMNL2ΔDAD at the tips of protruding filopodia and lamellipodia.

B16-F1cells were transiently transfected with EGFP-tagged FMNL2ΔDAD, and subjected to video microscopy using phase contrast and widefield fluorescence imaging essentially as described previously (Block *et al.*, 2008). (A) Examples of protruding filopodia; note the accumulation of the active formin at the tips of centrifugally growing filopodia (arrow). (B) Phase contrast and (C) fluorescence image of the same cell forming a prominent lamellipodium as characteristic for these cells moving on laminin (Rottner *et al.*, 1999). Arrowheads in (C) highlight the specific accumulation of active FMNL2 at the tip of the protruding lamellipodium. Bar in (A) and (C) corresponds to 1µm and 10µm, respectively.

localisation of FMNL2 to lamellipodia tips was not an artefact derived from overactivation of the formin, cells were stained for lamellipodial marker proteins and fascin. Phalloidin staining of FMNL2ΔDAD expressing B16-F1 cells confirmed the formation of lamellipodia, as expected (Figure 26A). Any other lamellipodia marker protein like Arp2/3-complex (Figure 26B), Abi-1 (Figure 26C), Cortactin (Figure 26D) and VASP (Figure 26E) nicely co-localised with FMNL2ΔDAD lamellipodia. In addition, fascin displayed a normal subcellular positioning, strongly associating with microspikes within the lamellipodium, but absent form the very leading edge of the cell (Figure 26F). This was in marked contrast to the fascin localisation of mDia2ΔDAD overexpressors, which appeared to force fascin to the leading edge (Figure 17). Thus, we conclude that FMNL2ΔDAD-labelled structures at the cell periphery constitute *bona fide* lamellipodia. To prove that the localisation of FMNL2 to lamellipodia was of physiological relevance

and no over-expression or overactivation artefact, B16-F1 cells were stained for endogenous FMNL2 using a commercially available monoclonal α-FMNL2 antibody.

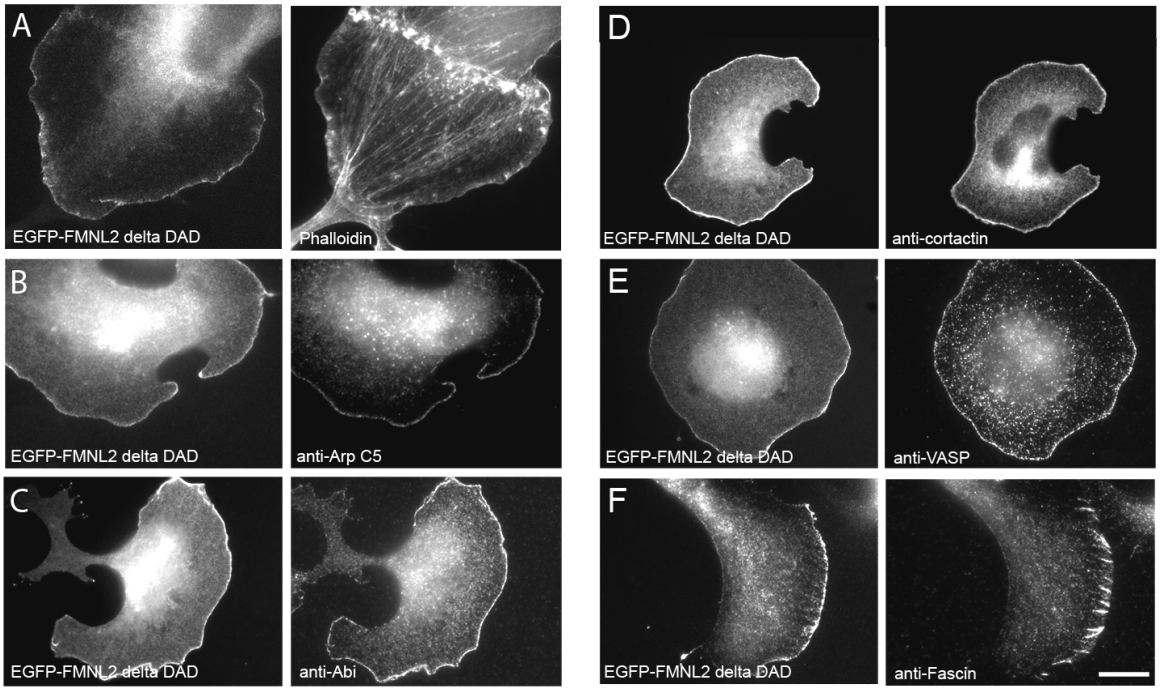

Figure 26: FMNL2ΔDAD-stained lamellipodia contain Arp2/3-complex and Arp2/3-complex activators but no fascin.

B16-F1 cells were transiently transfected with EGFP-FMNL2ΔDAD, fixed with paraformaldehyde and counterstained for Arp2/3-complex (B), the WAVE-complex subunit Abi-1(C), the Arp2/3-complex activator Cortactin (D) and VASP (E). Note prominent co-accumulation of EGFP-FMNL2ΔDAD with the respective component. In (F), EGFP-FMNL2ΔDAD transfected cells were counterstained for the actin bundling protein fascin. Note prominent accumulation of fascin at microspikes, as expected, but no targeting to the leading edge. Scale bar is valid for all images and equals 10µm.

As shown in Figure 27, endogenous FMNL2 is enriched at the leading edge of B16-F1 cells showing for the first time convincingly the endogenous localisation of a diaphanous-related-formin to the lamellipodium. Together, the enrichment of endogenous FMNL2 and EGFP-FMNL2ΔDAD in these protrusive structures point towards a functional role for FMNL2 in lamellipodial protrusion and organisation.

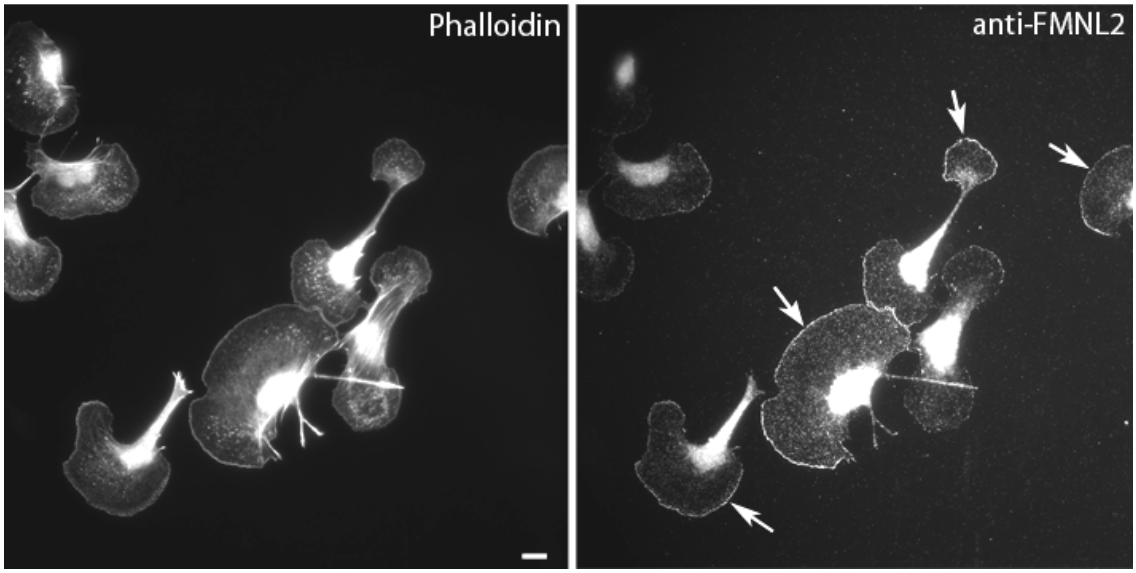

Figure 27: Endogenous FMNL2 localizes to the lamellipodium of B16F1 cells.

B16-F1 melanoma cells were immunolabelled for FMNL2 and counterstained for the actin cytoskeleton by fluorescent phalloidin. Cells were treated with aluminium fluoride to induce lamellipodia. Note specific accumulation of FMNL2 at the leading edge (white arrows). Scale bar equals 10µm.

3.10 FMNL2 interacts with Cdc42 and Rac1 in a nucleotide dependent manner

Rho-GTPase are widely established to stimulate actin polymerisation by activating WASP/WAVE-family proteins and diaphanous-related formins. The latter exist in an autoinhibited state via intramolecular interaction of the DAD and the DID domain. Upon binding of a GTP-bound Rho-GTPase to the GTPase-binding domain (GBD) of the formin, this autoinhibition is released (Nezami *et al.*, 2006; Wallar *et al.*, 2006), which is thought to be a prerequisite for proper subcellular localisation of the activated formin. In general, each Drf is activated by a distinct subset of Rho-GTPase (Ridely, 2006).The formation of the active, GTP-bound state of the GTPase is accompanied by a conformational change in two regions (known as switch I and II), which provide a platform for the selective interaction with downstream effectors such as formins (Dvorsky and Ahmadian, 2004). Over the last years, binding of the Rho-GTPases RhoA and Cdc42 to the N-terminus of the Drf mDia1 has been extensively studied (Lammers *et al*, 2008; Otomo *et al.*, 2005; Lammers *et al.*, 2005). RhoA binds mDia1 via interaction of the Switch I region to the GBD of mDia1, and interaction of Switch II with

the GBD and the Armadillo repeat subdomain (Rose *et al.*, 2005b), which is located within the Diaphanous inhibitory domain (DID, see Figure 23) of the formin.

To further characterise the contribution of FMNL2 to cell migration and lamellipodia formation, it was essential to determine which Rho-GTPases signal to FMNL2. Assuming that the structural requirements of Rho-GTPase-binding to the N-terminus of FMNL2 would be similar to the ones previously described for RhoA and mDia1, I generated a construct harbouring the GBD and the Armadillo repeat subdomain of FMNL2 (AA 1-428), called FMNL2-Arr.

To assess whether the N-terminus of FMNL2 can interact with certain Rho-GTPases, pull-down assays using EGFP-FMNL2-Arr or EGFP-FMNL2ΔDAD and beads coupled to respective GTPases were performed.

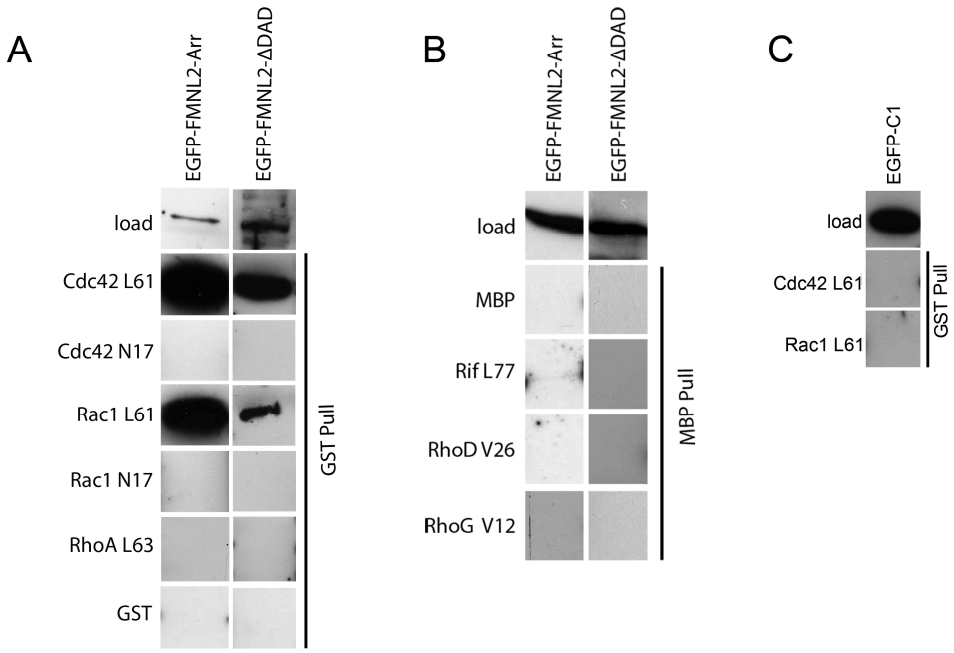

Figure 28: FMNL2 interacts with constitutively active Cdc42 and Rac1.

B16-F1 cells transfected with EGFP-tagged FMNL2-Arr or FMNL2ΔDAD as indicated, were subjected to pull-downs using beads coupled to active and inactive variants of Rho-GTPases. Rho-GTPases were fused to GST (A) or MBP (B) and coupled to Gluthatione-sepharose and amylose beads, respectively. Note binding of FMNL2-Arr and FMNL2ΔDAD to active Cdc42 (L61) and active Rac1 (L61), but not to their dominant negative counterparts or any other GTPase tested. No binding of EGFP to active Cdc42 and active Rac could be detected (C).

Interestingly, pull-downs indicate strong, perhaps direct interactions between FMNL2 and active, mostly GTP loaded, Cdc42 (L61) and Rac1 (L61) (Figure 28A). FNML2-Arr

was not able to pull down dominant negative, so mostly GDP-bound, Cdc42 (N17) and Rac1 (N17), suggesting a nucleotide-dependent binding of FMNL2 to Cdc42 and Rac1, as has been reported previously for other Drfs (Alberts, 2001, Watanbabe *et al.*, 1997). FMNL2-Arr did not bind to active Rho A (L63), RhoG (V12), RhoD (V26), Rif (L77) and GST or MBP alone (Figure 28). To exclude non-specific binding of the EGFP-tag to active Cdc42 or active Rac1, pull-down assays using EGFP alone were performed as control (Figure 28C). Together, these data suggest that FMNL2 acts as novel *bona fide* effector of Cdc42 and Rac1.

To directly test the *in vivo* relevance of the interaction between FMNL2 and Cdc42 or Rac1, EGFP-tagged, full length FMNL2A and FMNL2B constructs have been co-expressed with the respective Rho-GTPase in B16-F1 cells. The FMNL2C variant was not explored in this assay, since it targeted to the cell periphery without co-expression of ectopic GTPase, and might thus be already sufficiently activated by endogenous Rho-GTPases.

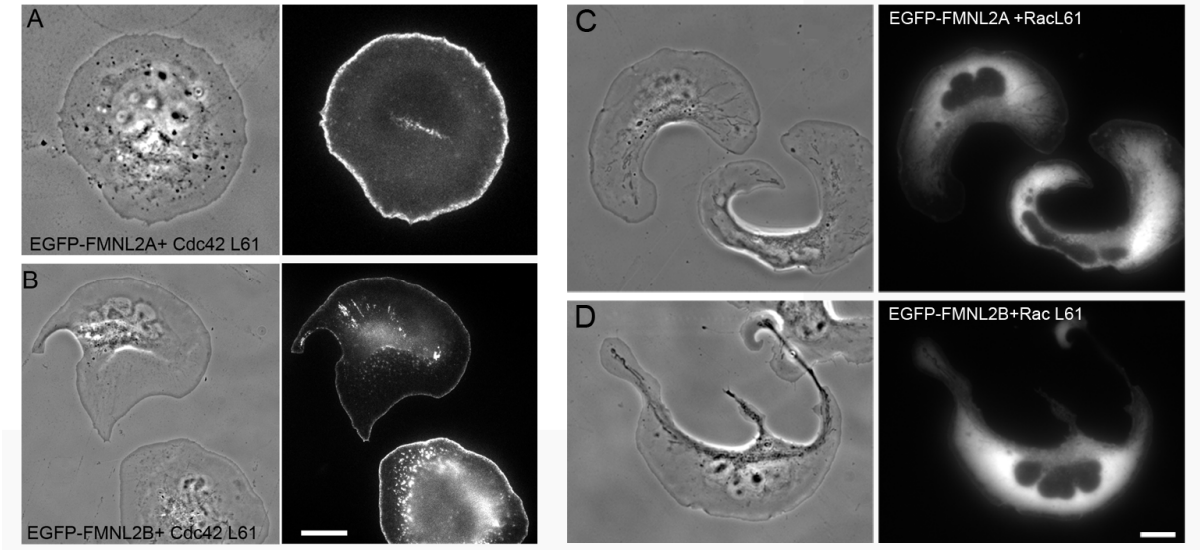

Figure 29: Cdc42 (but not Rac) induced targeting of FMNL2 to the cell periphery

B16-F1 cells transiently co-expressing EGFP-FMNL2A and myc-tagged Cdc42(L61) (A), EGFP-FMNL2B and myc-tagged Cdc42 (B), EGFP-FMNL2A and myc tagged Rac(L61) (C) and EGFP-FMNL2B and myc tagged Rac (L61) (D). Note prominent accumulation of FMNL2A and FMNL2B at the cell periphery upon co-expression of active Cdc42 (A and B) but not active Rac (C and D). Scale bars equal 10µm.

A direct confirmation of the physiological relevance of the interaction between FMNL2 and Cdc42 is presented in Figure 29. In contrast to full length FMNL2A and B that

remained entirely cytosolic (see Figure 24), co-expression of L61-Cdc42 caused strong accumulation of FMNL2A and FMNL2B at the cell periphery (Figure 29A and B) at sites coincident with lamellipodia formation. Surprisingly co-expression of constitutively active Rac (L61) failed to drive FMNL2A and -B targeting to the cell periphery (Figure 29C and D). Thus, the physiological relevance of Rac1 binding to FMNL2 observed *in vitro* remains elusive at this stage.

As mentioned previously and in contrast to FMNL2A and FMNL2B, the splice variant FMNL2C accumulates at the cell periphery in B16-F1 cells. Considering all available data so far, this could be interpreted as this variant either to be constitutively active or to be sufficiently activated by endogenous levels of Cdc42 in B16-F1 cells. To distinguish between this possibilities, EGFP-FMNL2C was expressed in Cdc42 fl/- and Cdc42 -/- cells kindly provided by Prof. Cord Brakebusch (Copenhagen, Denmark). As expected, EGFP-FMNL2C localised to the leading edge in Cdc42 fl/- cells (white arrows in Figure 30A) but failed to do so in Cdc42-deficient cells (arrowhead in Figure 30B), although these cells were still able to form lamellipodia. To test directly if the lack of EGFP-FMNL2C localisation in Cdc42-deficient cells was indeed due to the lack of Cdc42 expression, I re-expressed ectopic constitutively active Cdc42 in cdc42-/- cells.

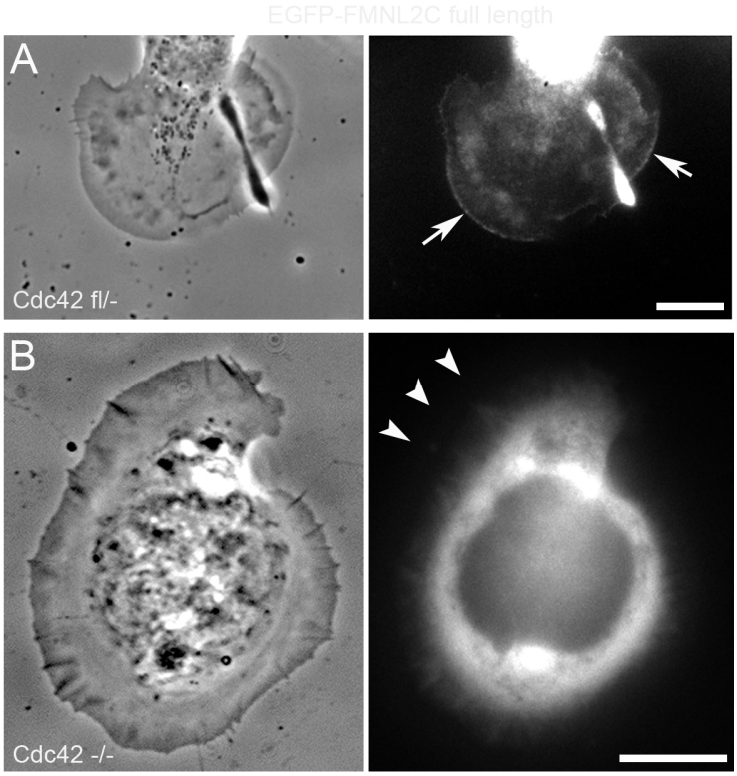

Figure 30: Expression of FMNL2C splice variant in cdc42 fl/- and cdc42 -/- cells

EGFP-FMNL2C full length accumulates at the cell periphery in cdc42 fl/- (white arrow in A). Note lack of accumulation of FMNL2C full length in cdc42-/- cells (arrowheads in B). Bars equal 10µm.

As can be seen in Figure 31A, re-expression of active Cdc42 was sufficient to drive targeting of EGFP-FMNL2C to the cell periphery. This was not the case upon co-expression of active Rac (L61) with FMNL2C in these cells (Figure 31B) consistent with the inability of Rac to drive FMNL2A and –B recruitment to the cell periphery in B16-F1 cells (Figure 29). These data suggest that basal Cdc42 levels in B16-F1 and Cdc42 WT cells are sufficient to cause activation and subsequent localisation of FMNL2C but not FMNL2A and B to the lamellipodium. Note that the only sequence difference between splice variants lies within the extreme C-terminus encoding the DAD-domain. Thus. The different behaviour of FMNL2C must be due to inefficient autoinhibition or, in other words, efficient release from autoinhibition affected by Cdc42, since this splice variant harbours the shortest C-terminus.

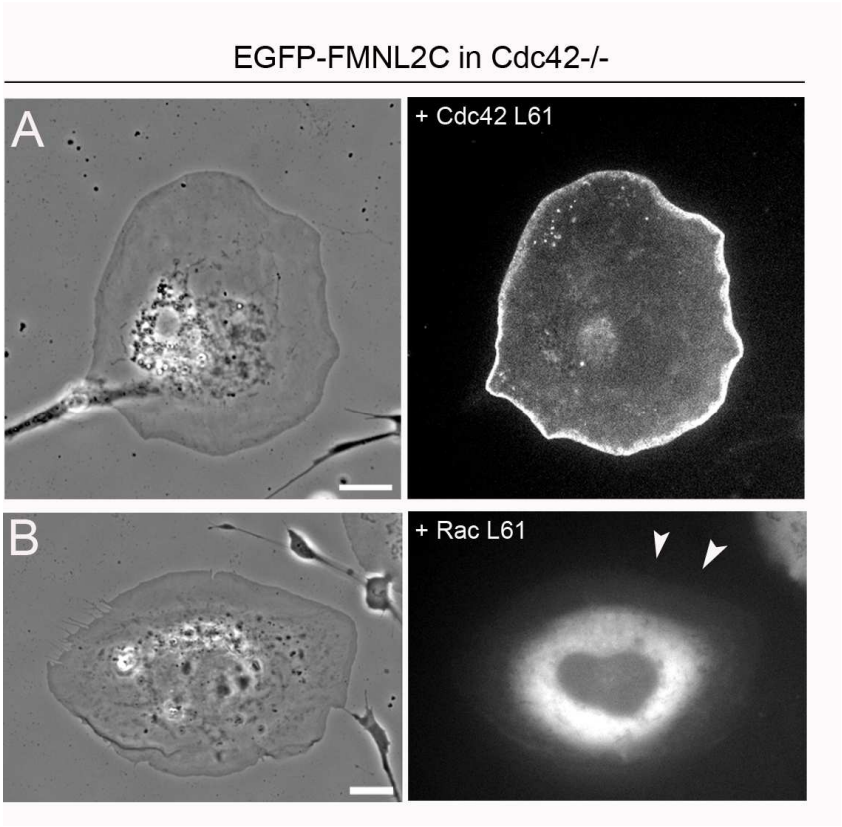

Figure 31: Co-expression of FMNL2C and Cdc42 (but not Rac) drives targeting in Cdc42-/- cells

Cdc42-/- fibroblast cells transiently transfected with EGFP-FMNL2C and myc-tagged Cdc42 (L61) and myc-tagged Rac (L61), respectively. (A) Note prominent localisation of FMNL2C at the cell periphery at sides coincident with lamellipodia formation. (B) Cotransfection of EGFP-FMNL2C with myc-tagged Rac (L61) was not sufficient to target FMNL2C to cytoskeletal structures such as lamellipodia (arrowheads). Bars equal 10µm.

3.11 Potential N-terminal myristoylation of FMNL2 influences subcellular localisation, but is not required for Cdc42-induced accumulation at the cell periphery

Co- and posttranslational modifications occur on a wide variety of cellular proteins, one important modification being the covalent attachment of fatty acids. The two most common forms of protein fatty acylation are modifications with myristate, a 14-carbon saturated fatty acid, and palmitate, a 16-carbon saturated fatty acid (Resh MD, 1999). Using an online tool to search for sequences prone to posttranslational modifications (Maurer-Stroh *et al.*, 2002), FMNL2 was established to belong to roughly 0.5% of all eukaryotic proteins harbouring the consensus sequence MGXXXS/T, which identifies FMNL2 as a N-terminal myristoylated protein (collaboration with Dr. Matthias Geyer, Max-Planck-Institute for Molecular Physiology, Dortmund). Although not following this consensus, FMNL1 was also reported recently to be N-myristoylated (Han *et al.*, 2009). The function of protein myristoylation has been linked to membrane binding and protein stabilisation. The myristate moiety can adopt an exposed conformation able to promote membrane binding or lie hidden inside a hydrophobic binding pocket within the myristoylated protein. The transition between these two conformations is regulated by a myristoyl switch that can be induced by ligand binding or phosphorylation (Resh, 2006).
The predicted myristoylation of FMNL2 could have relevant implications for autoregulation and membrane targeting of this protein, and was therefore examined more closely. Myristoylation is a cotranslational lipid modification, where the N-myristoyltransferase (NMT) covalently attaches a C14-fatty acid to the C-terminus of the protein. Since the NMT requires the myristoylation consensus sequence (MGxxxS) to be the first aminoacids of the protein, an N-terminal tag could disrupt the signal for the incorporation of the lipid anchor. (Keller *et al.*, 2005; Tang and Teng, 2004; Neumann-Gießen *et al.*, 2004). Thus, to preserve the lipid modification of the N-terminus, it is important to use constructs that will produce C-terminally EGFP-tagged formin variants. These constructs have been expressed in B16-F1 cells and analysed concerning their subcellular dynamics.
Fusing the EGFP-moiety to the C-terminus of the respective splice variants had a drastic effect on the subcellular localisation of the formin. As shown in Figure 32, FMNL2A and -B constructs which are presumed to become myristoylated, accumulates at the cell periphery, in contrast to constructs harbouring the EGFP-moiety at the N-terminus of the formin, remaining entirely cytosolic (compare with Figure 24B and C).

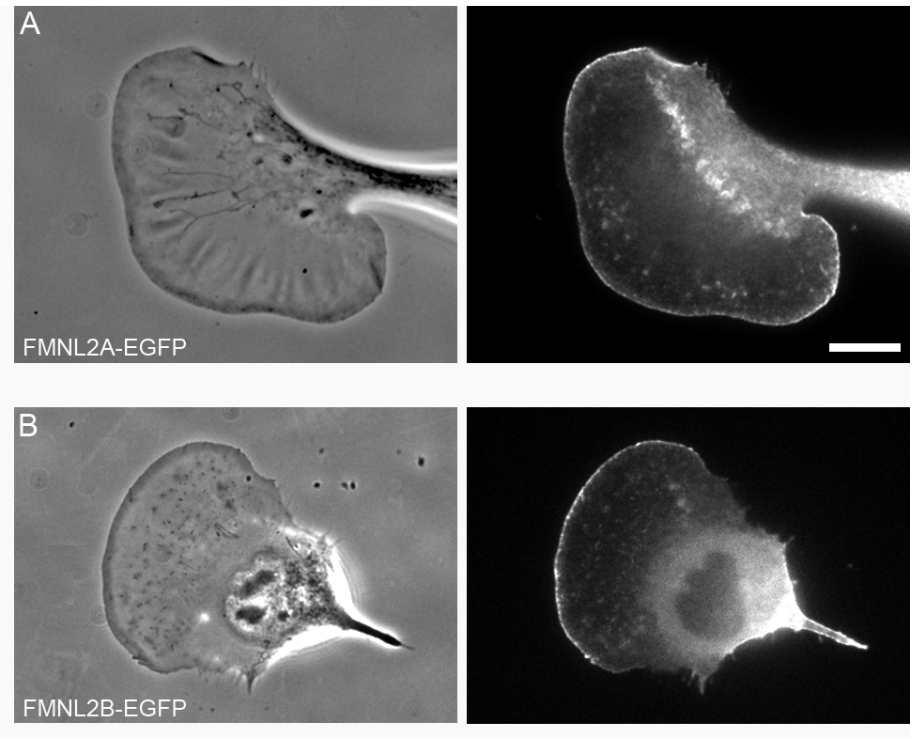

Figure 32: C-terminally tagged FMNL2A and –B accumulate at the leading edge of B16 cells.

B16-F1 cells transiently expressing FMNL2A-EGFP and FMNL2-EGFP, respectively. To preserve potential lipid modification, the EGFP moiety was fused to the C-terminus of FMNL2A and B. Note prominent accumulation at the cell periphery in contrast to C-terminal fusions that remained largely cytosolic. Bar equals 10µm.

To further characterise how the myristate modification influences the subcellular behaviour of FMNL2, non-myristoylatable FMNL2 variants were generated by mutating the N-terminal Glycin, which is essential for covalent linking of the fatty acid, to Alanin (G2A) (Perez *et al.*, 2004). Biochemical experiments have recently demonstrated that this mutation does indeed abolish myristoylation of FMNL2 (Mathias Geyer, MPI Dortmund, Germany, unpublished observations). In order to exclude any influence of endogenous Cdc42 on the cellular localisation pattern or the autoinhibition of FMNL2, experiments were performed in Cdc42-deficient cells.

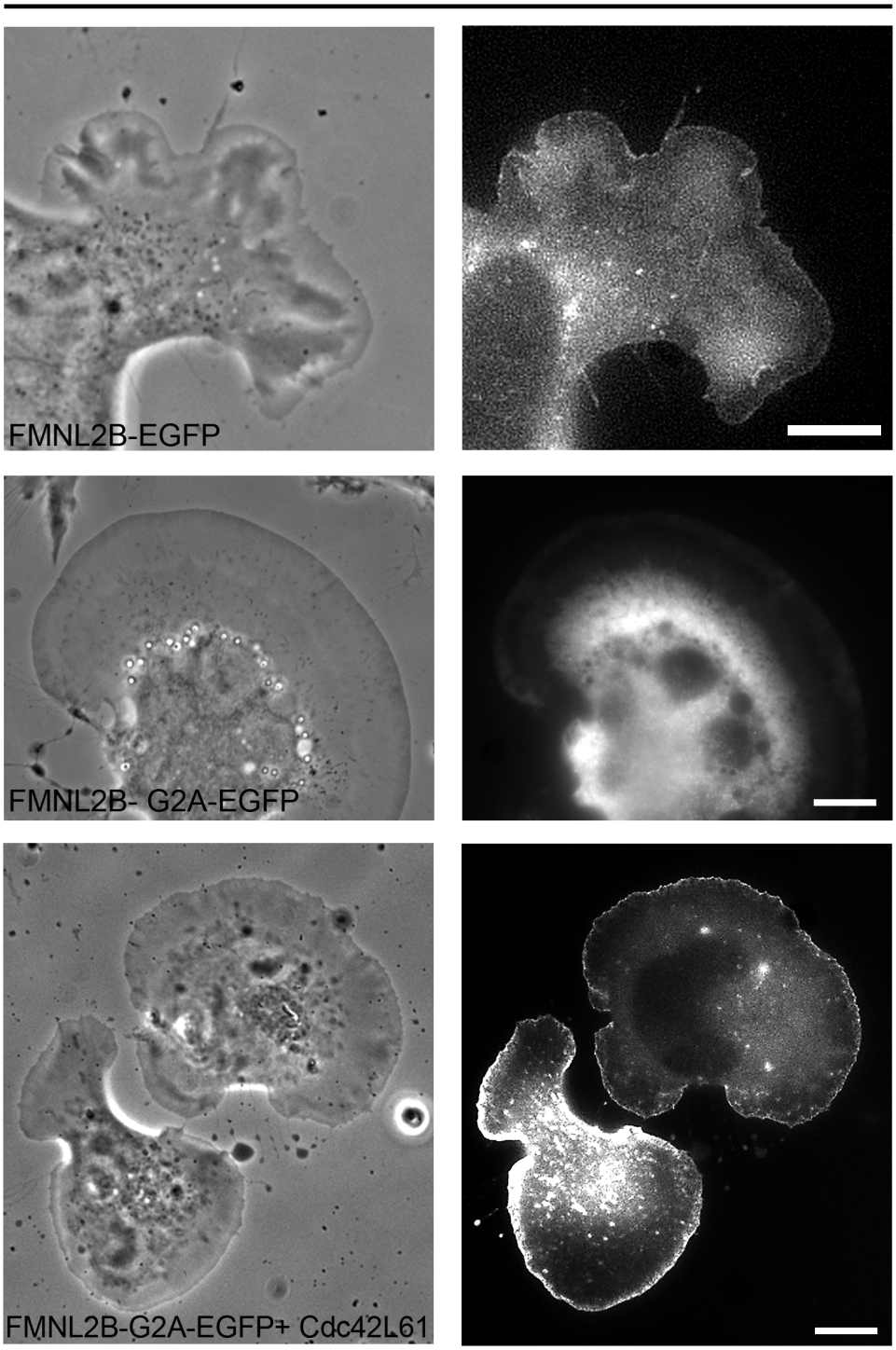

Figure 33: Myristoylation can contribute to, but is not essential for subcellular positioning of FMNL2.

A) Cdc42 deficient cells transiently transfected with presumably myristoylated FMNL2B-EGFP. Note weak association of wildtype FMNL2B to the leading edge. (B) Mutation of Glycin at position 2 to Alanin (G2A) abrogates membrane accumulation of FMNL2B in Cdc42-/- cells. (C)The non-myristoylatable FMNL2B mutant is capable of targeting to the cell periphery upon co-transfection of active Cdc42. Images are shown for FMNL2B, but are representative for the two other splice variants as well (data not shown). Bars equal 10µm.

A weak association to the leading edge of the cells could be observed for all three splice variants (Figure 33A). To ascertain that this Cdc42-independent accumulation at the cell periphery was not caused by interfering with the autoinhibition of the formin by fusing the EGFP-tag in close proximity to the regulatory DAD-domain, the subcellular localisation of the myristoylation-deficient mutant was analysed. This mutant showed no specific accumulation to cytoskeletal structures such as lamellipodia but remained cytosolic (Figure 33B). The same localisation pattern was previously observed for N-terminally-tagged FMNL2A and –B full length and interpreted to be indicative of autoinhibition. Even more importantly the behaviour of the myristoylatable FMNL2-constructs compared to the myristoylation-deficient mutants indicates that N-terminal myristoylation of FMNL2 contributes to FMNL2 accumulation at the cell periphery in the absence of Cdc42. This could be explained either by interference of the myristate moiety with autoinhibiton of the formin splice variants or targeting activity to the cell periphery by the lipid modification itself.

In any case, myristoylation would also have additional effects, e.g. it could be a prerequisite of proper interaction with Cdc42. To test this the myristoylation-deficient mutant was co-expressed with constitutively active Cdc42 in Cdc42-/- cells. As shown in Figure 33C, this treatment caused strong accumulation of non myristoylatable FMNL2 at the cell periphery. Thus, the N-terminal myristoylation is dispensable for binding and activation of the formin by Cdc42.

3.12 Cdc42 is not essential for FMNL2 targeting to the leading edge

Considering published results in context of other diaphanous-related formins, we assume that co-expression of active Cdc42 is able to release the autoinhibited state of FMNL2 resulting in an accumulation of the formin at the cell periphery. However, it was still unclear whether Cdc42 can directly mediate targeting of FMNL2 to the leading edge. Previous data concerning the influence of Rho-GTPases on formin localisation have led to conflicting statements. The membrane localisation activity of mDia1 and FRLα was concluded to derive, in part, from the interactions with Rho-GTPases, however, an additional membrane associated factor seems to be involved in membrane binding at least for these Drfs (Seth *et al.*, 2006). Other studies utilised mDia1 and mDia2 variants lacking their GTPase binding domains. Over-expression of these constructs showed that the interaction with the respective GTPase does not determine intracellular localisation (Tominaga *et al.*, 2000, Gazman *et al.*, 2003, Yang *et al.*, 2007). To evaluate whether FMNL2 requires Cdc42 for proper targeting to the leading edge, I expressed constitutively active FMNL2 variants lacking the DAD-

domain in Cdc42-/- cells. Taking into account the possible influence of myristoylation on membrane targeting, constructs harbouring the EGFP moiety at the C-terminus of FMNL2 and thereby preserving the lipid modification and a myristoylation-deficient mutant were used.

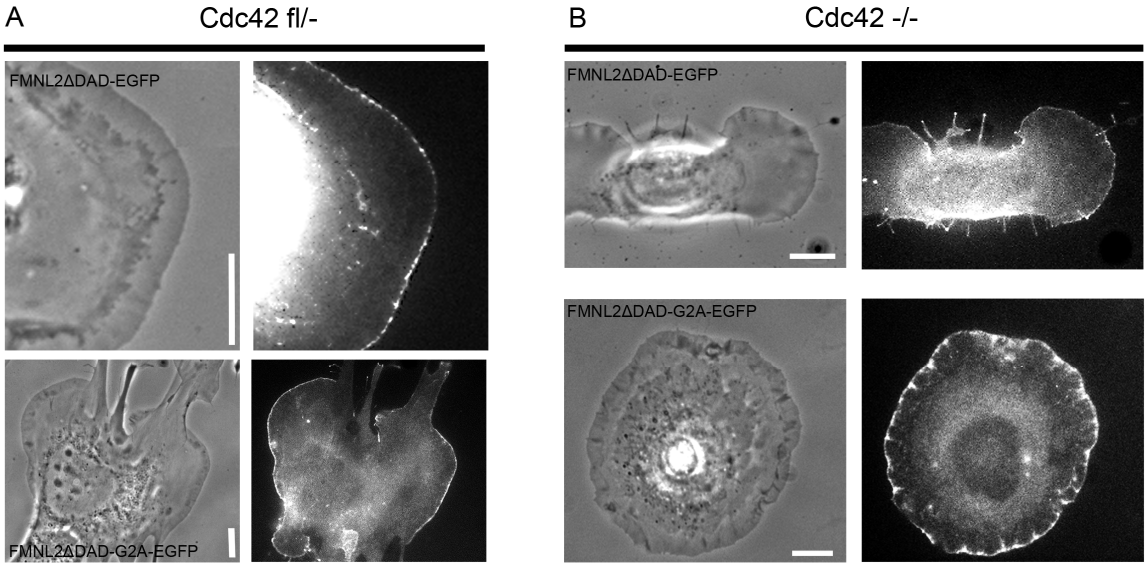

Figure 34: Cdc42 is not required for targeting of FMNL2ΔDAD to the cell periphery

(A) FMNL2ΔDAD-EGFP and FMNL2-G2A-EGFP expressed in Cdc42fl/- cells. Note localisation of both FMNL2 constructs to the cell periphery. (B) FMNL2ΔDAD-EGFP and FMNL2-G2A-ΔDAD-EGFP expressed in Cdc42 deficient cells. Active FMNL2 is capable of accumulating at the leading edge in the absence of both Cdc42 and the N-terminal lipid modification. Bars equal 10µm.

As expected, FMNL2ΔDAD-EGFP and the myristoylation-deficient mutant (FMNL2ΔDAD-G2A-EGFP) accumulated at the cell periphery of Cdc42 control cells without affecting the cell morphology of fibroblast cells (Figure 34A).

However, Figure 34B shows that FMNL2-ΔDAD-EGFP was also strongly enriched in the leading edge of Cdc42-deficient cells, indicating that Cdc42 is not required for subcellular targeting of FMNL2, and suggesting that Cdc42 operates solely in relieving autoinhibition of FMNL2. This is consistent with the view that myc-tagged Cdc42 does not specifically accumulate at the tips of protrusions, but the entire plasma membrane (data not shown). To examine whether the N-terminal myristoylation could at least contribute to the accumulation to protrusive structures in the absence of Cdc42, a myristoylation-deficient construct (FMNL2ΔDAD-G2A-EGFP) was analysed in the absence of Cdc42. However, the non-myristoylatable ΔDAD-FMNL2 accumulated at

the cell periphery equally well as the myristoylatable construct (Figure 34B), thus subcellular targeting does not require either signal, Cdc42 and myristoylation. We conclude that in FMNL2 full length, all splice variants of which are autoinhibited in the absence of the myristate moiety and Cdc42, these signals can both contribute to activation, but both are dispensable for localisation, which must be mediated by other means.

3.13 FMNL2 elongates but does not nucleate actin filaments in vitro

Recent studies by Vaillant *et al.* (2008) explored the induction of actin assembly of isolated FH2-domains of FMNL2 and -3 and proposed that FMNL2 and -3 can nucleate and bundle actin filaments *in vitro*. However, the actin nucleation activity reported in this study was comparably modest (e.g. relative to mDia1) (Seth *et al.,* 2001). Since it is well established today that actin nucleation mediated by formins is significantly enhanced by the profilin-binding activity of the FH1-domain (Kovar *et al.*, 2003; Kovar and Pollard, 2004; Romero *et al.*, 2004; Kovar *et al.*, 2006), we aimed at studying the effects of FMNL2-FH1-FH2-mediated actin assembly *in vitro*. The FH1-domain in FMNL2 contains a stretch of 8 prolines and a second stretch of 21 consecutive proline residues with the potential to bind profilactin (complex of profilin and actin). Spectroscopic and calorimetric studies (Petrella *et al.*, 1996) and crystal structures (Mahoney *et al.*, 1997; 1999) show that eight prolines span the full binding site of profilin. To aid expression and purification in bacteria, we engineered expression constructs with 8 out of 21 proline residues [FMNL2-FH1(8P)-FH2] and a second one with the complete second stretch of 21 proline residues [FMNL2-FH1(21P)-FH2]. Both constructs lacked the first stretch of 8 proline residues. The biochemical characterisation of FMNL2 including protein purification and construct design has been carried out in collaboration by Dr. Jan Faix and Dennis Breitsprecher (Hannover Medical School), who kindly provided the data presented in this chapter.

First, pyrene-actin polymerisation (Cooper *et al.*, 1983) were performed. In this assay, unlabelled actin and 10% pyrene-labelled actin were mixed in the presence of FMNL2-FH1(8P)-FH2. Subsequently, the fluorescence intensity, which is much higher after polymerisation of pyrene-actin, was measured. In Figure 35A, the polymerisation time course for actin alone (black line) or with increasing concentrations of FMNL2-FH1(8P)-FH2 is displayed. Apparently, the FMNL2 variant inhibited spontaneous actin assembly, which was confirmed by plotting the polymerisation rate against the molar ratio of FMNL2/actin (Figure 35B).

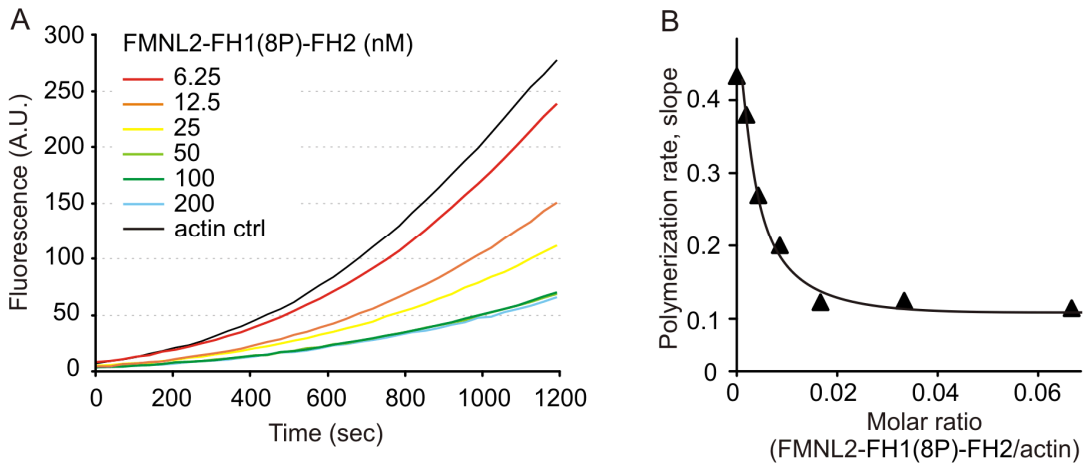

Figure 35: Biochemical analysis of FMNL2-mediated actin assembly

(A) FMNL2 inhibits actin polymerization. 3 µM G-actin (10% pyrene-labelled) were polymerised in 1x pyrene buffer in the presence of FMNL2 8P at concentrations as indicated. (B) Plot of the dependence of the polymerization rate (slope) on the concentration of FMNL2 8P.

A disadvantage of pyrene-actin-polymerisation assays is the inability to distinguish between filament nucleation and elongation. To directly visualise individual actin filaments in real time, total internal reflection microscopy (TIRF) was employed, which allows elongation rates of individual actin filaments to be measured directly, in a manner uncoupled from nucleation (Amman and Pollard, 2001; Harris and Higgs, 2006).

A direct confirmation of FMNL2-mediated actin assembly is presented in Figure 36A. FMNL2 (21P) incubated with actin alone did not significantly promote processive actin assembly. Just in the presence of profilin and actin filament barbed ends captured by FMNL2(8P) or FMNL2 (21P) grew substantially faster and appeared dimmer than free barbed ends (Figure 36A). This behaviour can be explained by the notion that FH1-bound profilin-actin is highly favoured for addition to barbed ends over bulk-phase actin, and that profilin has a higher affinity to unlabelled actin. It is well established that profilin bound to actin does not elongate actin filaments (Pollard and Cooper, 1984; Kaiser *et al.*, 1999) but promotes actin elongation in the presence of formins (Kovar *et al.*, 2003; Romero *et al.*, 2004). In addition, filament buckling, which occurs when both ends of the filament are attached to the glass slide and the formin continuously elongates the filament, can be observed for both constructs, and can be taken as evidence for actin filament assembly mediated by the formin fragment.

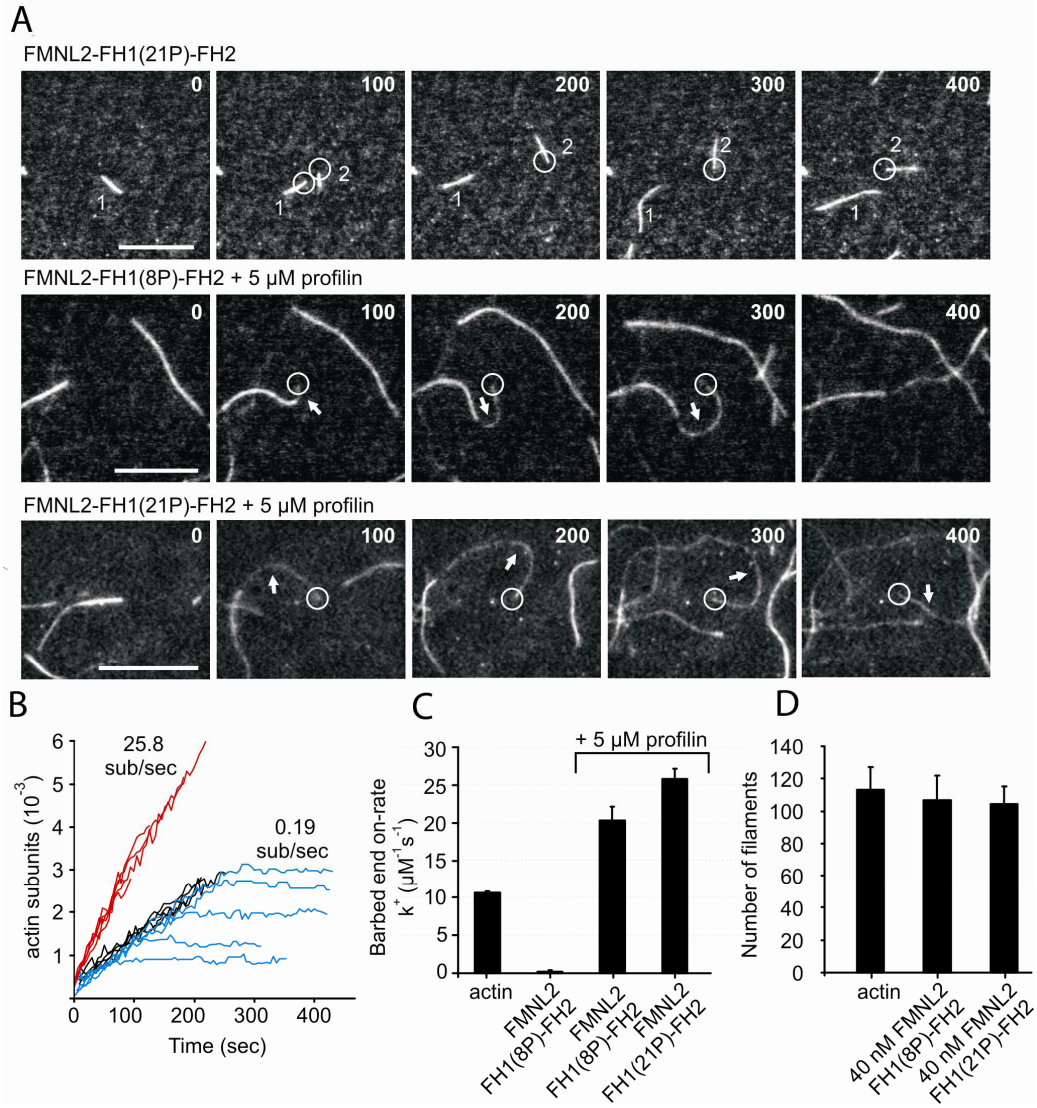

Figure 36: TIRF analyses of FMNL2 mediated actin assembly.

(A) FMNL2 processively assembles actin filaments. Spontaneous assembly of 1.5 µM actin (30% Alexa-488 labelled) in the presence of 20 nM of FMNL2 8P (top) or FMNL2 21P (bottom) and 5 µM profilin monitored by TIRF microscopy. Formin-captured barbed ends are encircled; arrows indicate dim, buckling filaments. Time is indicated in seconds. Scale bar 10 µm. (B) Single filament analysis of FMNL2-FH1(21P)-FH2 elongated actin filaments. Blue lines represent actin subunits added on filaments in the presence of FMNL2 alone, red lines correspond to actin filaments elongated in the presence of FMNL2 and 5µM profilin (C) FMNL2 enhances filament elongation in the presence of profilin. Barbed end on-rates are determined by TIRF microscopy. For actin alone and FMNL2-FH1(8P)-FH2 45 and 21 actin filaments were measured, respectively. For FMNL2-FH1(8P)-FH2 and FMNL2 FH1(21P)-FH2 13 and 8 actin filaments were analysed, respectively. Error bars represent standard deviation (STD). (D) FMNL2 does not nucleate actin filaments. Barbed ends in an area of 100 x 140 µm in the presence and absence of FMNL2 8P and 21P over a time period of 15min were quantified. Error bars represent STD. All data derive from three independent measurements.

Actin subunits on-rates of individual filaments (Figure 36B and C) with or without profilin were significantly enhanced in the presence of FMNL2 and profilin. For single filaments 25.8 subunits per second were added by FMNL2 in the presence of profilin

whereas only 0.19 subunits per second were added without profilin. These data demonstrate that FMNL2 elongates actin filaments in a processive fashion.

The prevailing view that formins per se nucleate actin filaments has been challenged again in Figure 36D. Counting filament numbers in the absence and presence of FMNL2(8P) or FMNL2(21P) revealed that FMNL2 does not alter the number of filaments. These data taken together with results obtained from pyrene polymerisation assays performed in the absence of profilin implicate that FMNL2 does not nucleate but elongate actin filaments *in vitro*.

3.14 FMNL3 interacts with Cdc42 and accumulates at the cell periphery upon co-expression with active Cdc42

The FMNL or FRL subfamily of diaphanous related formins consists of 3 members, FMNL1 (FRL1), FMNL2 (FRL3) and FMNL3 (FRL2). FMNL2- and -3 are not identical in sequence (roughly 70% identity), but slightly more homologous to each other than each one of them to FMNL1 (Katoh and Katoh, 2003). As shown in the gene array analysis, FMNL3 is mainly expressed in the tested murine cell lines (Table 7), where it might be interesting to look for potential redundant functions of FMNL2 and -3. Interestingly, the FMNL3 gene harbours sequence deletions as compared to FMNL2 slightly N-terminal to and within the FH1-domain. This might have interesting consequences for effects on actin assembly.

To determine possible FMNL3 interactions with Rho-GTPases, I cloned the FMNL3 N-terminus according to FMNL2-Arr and performed pull-down assays. I transfected B16-F1 cells with EGFP-FMNL3-Arr and pulled this construct by using constitutively-active and dominant negative Rho-GTPases coupled to sepharose-beads.

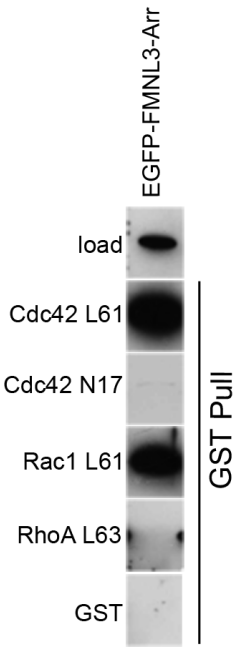

Figure 37: FMNL3 interacts with constitutively active Cdc42 and Rac1.

B16-F1 cells transfected with EGFP-tagged FMNL3-Arr were subjected to pull-downs using beads coupled to active and inactive variants of Rho-GTPases. Rho-GTPase were fused to GST and coupled to glutathione-sepharose.
Note binding of FMNL3-Arr to active Cdc42 (L61) and active Rac1 (L61), but not dominant negative Cdc42 (N17) or active RhoA (L63) or GST.

The N-terminus of FMNL3 showed strong, presumably direct interactions with active, so mostly GTP-bound Cdc42 (L61) and Rac1 (L61) (Figure 37), comparable to the results obtained in FMNL2 pull-down experiments. FMNL3-Arr was not able to pull-down dominant negative, mostly GDP bound Cdc42 (N17 (Figure 37), supporting a nucleotide dependent binding to Cdc42. No interactions could be observed between FMNL3 and active RhoA (L63) and GST (Figure 37).

To further characterise potential redundant functions of FMNL2 and -3, it was essential to have a closer look at the subcellular localisation of FMNL3. At first, I generated an EGFP-FMNL3 full length construct and expressed this in B16-F1 cells.

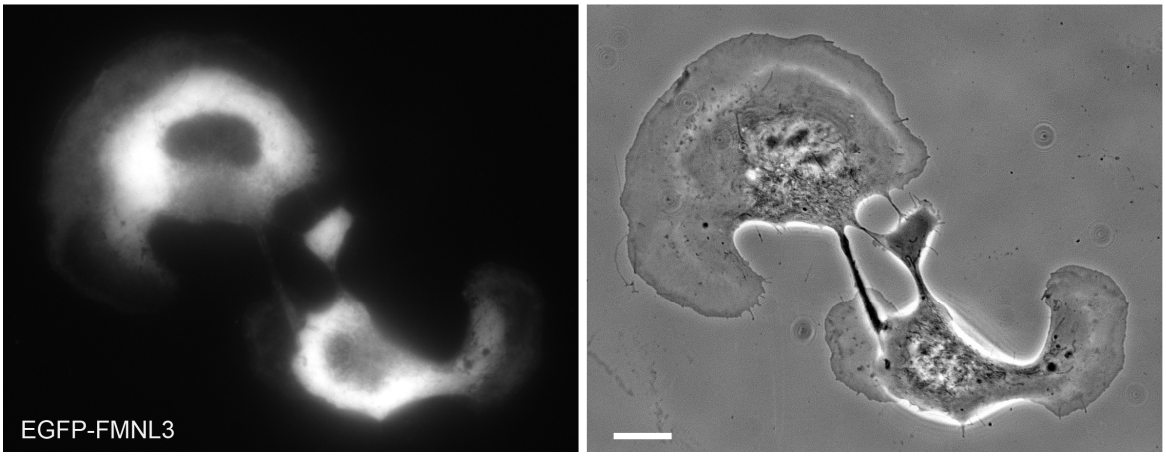

Figure 38: EGFP-FMNL3 full length is cytosolic in B16 cells

B16-F1 mouse melanoma cells transfected with EGFP-FMNL3 and subjected to live microscopy. Cells show an actively protruding lamellipodium but lack an accumulation of FMNL3 to the cell periphery. Bar equals 10µm.

Although the cells exhibit an actively protruding lamellipodium no specific accumulation at peripheral regions could be observed (Figure 38). Instead, FMNL3 accumulated in the perinuclear region, which can be explained simply by high thickness in this region. To explore a potential physiological relevance of the interactions of FMNL3 with Cdc42 and Rac1 *in vitro*, EGFP-FMNL3 was co-expressed with either Rho-GTPases.

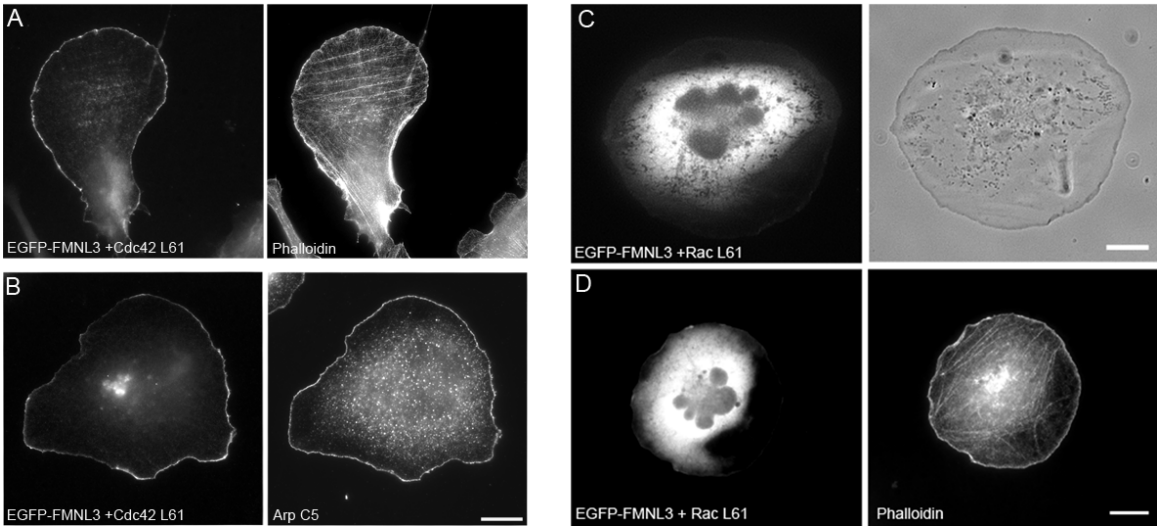

Figure 39: Co-expression of active Cdc42 but not active Rac leads to an accumulation of FMNL3 at the leading edge

(A) B16-F1 cells transiently co-expressing EGFP-FMNL3 and myc-tagged Cdc42 (L61). The actin cytoskeleton has been visualised by Phalloidin staining. Note prominent localisation of EGFP-FMNL3 at the cell periphery. (B) Counterstaining of FMNL3 and Cdc42 expressing cells for Arp2/3-complex revealed prominent co-accumulation of Arp-complex at the leading edge. (C) and (D) Co-expression of myc-tagged active Rac (L61) is not sufficient to target FMNL3 to the cell periphery. Bar in B is valid for (A) and (B). Bars equal 10 µm.

Interestingly Cdc42 co-expression resulted in a prominent localisation of FMNL3 at the cell periphery at sites coincident with lamellipodia formation (Figure 39A and B). Fluorescence microscopy of FMNL3- and Cdc42- co-expressing cells stained with Phalloidin indicated FMNL3 targeting to coincide with formation of lamellipodia. This was confirmed by counterstaining of FMNL3-containing structures with Arp2/3-complex. FMNL3 and Arp2/3-complex showed virtually identical localisation at the cell periphery (Figure 39B).

As opposed to Cdc42, co-expression of active Rac was not sufficient to target FMNL3 to the leading edge which has been shown both by live-cell microscopy (Figure 39C) and counterstaining with phalloidin (Figure 39D). Similar results were obtained previously for co-expression of active Rac with FMNL2. Thus, both FMNL2 and FMNL3 can be induced to target to the leading edge by active Cdc42 but not Rac1.

3.15 FMNL2 and FMNL3 regulate the migration speed of B16 cells

So far the data showed that both FMNL2 and FMNL3 can localise to the cell periphery, implicating functional importance of the endogenous protein for the formation and/or maintenance of these protrusions. Although Rac is best established to drive the formation of lamellipodia (Ridley *et al.*, 1992), I failed to establish a physiological connection between Rac/FMNL interactions in pull-down experiments and accumulation of FMNL2 and -3 at the cell periphery. Cdc42 was initially shown to be capable of inducing lamellipodia and filopodia although activation of the former was concluded to be driven indirectly through Cdc42-mediated activation of Rac (Nobes *et al.*, 1995). The direct Cdc42-interactor and promising effector N-WASP, linking Cdc42 activity and actin assembly, lacks an accumulation in the lamellipodium and was additionally shown to be dispensable for lamellipodia and filopodia formation (Lommel *et al.*, 2001; Snapper *et al.*, 2001). Another prominent Cdc42 effector, mDia2, was occasionally observed to accumulate at the leading edge (Block *et al.*, 2008; *Yang et al*., 2007), but this has been interpreted as an artefact derived from mDia2 over-activation (see chapter 3.5).

As a first step to shedding more light on the function of FMNL2 and -3 in the formation of cellular protrusions, and thereby potentially gaining additional information about the contribution of Cdc42 to lamellipodia formation, I examined the effect of FMNL2 and FMNL3 knockdown by RNA interference in B16-F1 cells. A prerequisite for this technique however is the availability of antibodies, which are sensitive enough to reliably assess protein rundown -at least in Western Blotting- in response to RNAi.

Therefore, a commercially available monoclonal antibody raised against FMNL2 was characterised in detail. Surprisingly, this antibody detected two different bands with molecular weights at ~ 120kDa and ~150kDa when used on cell lysates of different murine and human cell lines (Figure 40B). Taking into consideration a sequence identity of roughly 70% between FMNL2 and -3 I hypothesized that the antibody may be able to detect both FMNL subfamily formins. Expecting that FMNL3 would run at a lower molecular weight due to the absence of sequence stretches N-terminal of the FH2 and within the FH1-domain, I figured that the 120kDa band might correspond to FMNL3 and the 150 kDa band represents FMNL2. Comparison of the gene array data (Figure 18) and the Western Blot results supported this theory. In line with the expression profile obtained from gene array analyses, the upper band was present in all cell lines tested. According to the microarray analyses, FMNL3 is restricted mainly to murine cell lines. Western blot analyses revealed that the 120 kDa band can be detected in the murine cell lines B16-F1, Swiss 3T3 and NIH 3T3 but not in the human lines Hela S3 and A431. The only discrepancy arises in VA-13 cells, where no FMNL3 message could be detected but a strong signal occurs in western blot analyses. The reason for this inconsistency is presently not clear. In any case, additional experiments revealed reactivity of the FMNL2 antibody with ectopically-expressed EGFP-FMNL2 and EGFP-FMNL3 in western blot analysis (Figure 40A). To precisely determine the specificity of the antibodies, FMNL2- and FMNL3-specific RNAi experiments were performed, and reduced expression levels of respective bands were evaluated (Figure 40B and C). Importantly, FMNL2- and FMNL3-specific knockdown reduced the top and bottom band recognised by the FMNL2 antibody, respectively. Thus, all these data clearly indicate that the 150kDa band corresponds to FMNL2 and the 120 kDa band represents FMNL3 migrating at a lower molecular weight due to the absence of sequences N-terminal of the FH2-domain.

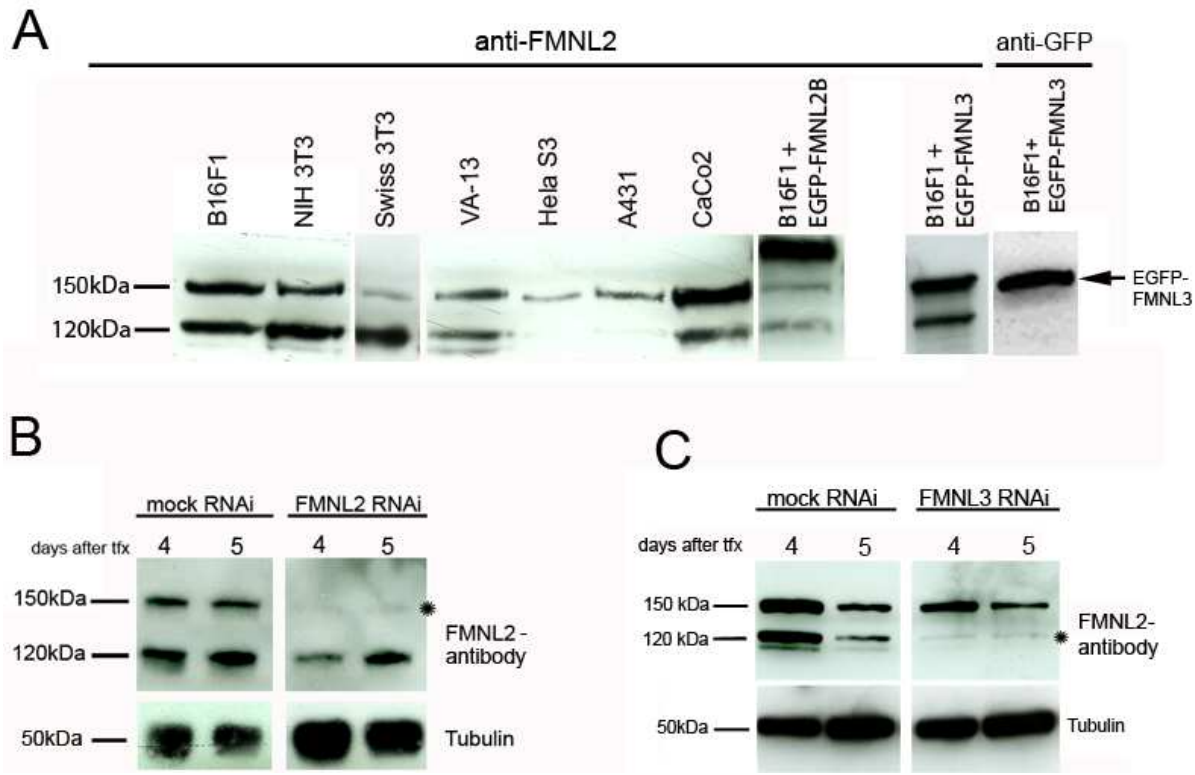

Figure 40: Expression analyses of FMNL2 and -3 and FMNL2 antibody characterisation

(A) Western Blotting of cell extracts as indicated using a commercial anti-FMNL2 antibody, which detects a protein with a molecular weight of roughly 150kDa (as expected) and another protein with a molecular weight of 120kDa in various cell lines, and EGFP-tagged FMNL2 as well as EGFP-tagged FMNL3 ectopically expressed in B16-F1 mouse melanoma cells. Note that EGFP-FMNL3 migrates at the same molecular weight as endogenous FMNL2; the correct size of EGFP-FMNL3 was additionally confirmed by detection with α-GFP antibody. (B and B) Determination of band specificity by using FMNL2- and FMNL3-specific RNAi constructs in B16-F1 cells. Note reduced expression level of the protein with a molecular weight of 150 kDa in the FMNL2-specific RNAi approach (B, asterisk) and reduced expression level of the protein with a molecular weight of 120 kDa in the FMNL3-specific RNAi approach (C, asterisk).

To analyse the precise function of FMNL2 and -3 in the formation of cellular protrusions, I downregulated their expression by RNA interference. First, I studied the involvement of FMNL2 and -3 in lamellipodia formation by knocking down either FMNL2 alone or in combination with FMNL3. To examine morphological changes upon reduced protein expression, transient FMNL2, FMNL2/FMNL3 knockdown and mock-treated cells were seeded on laminin-coated coverslips and treated with aluminium fluoride, which was demonstrated earlier to strongly induce lamellipodia formation in these cells (Hahne *et al.,* 2001).

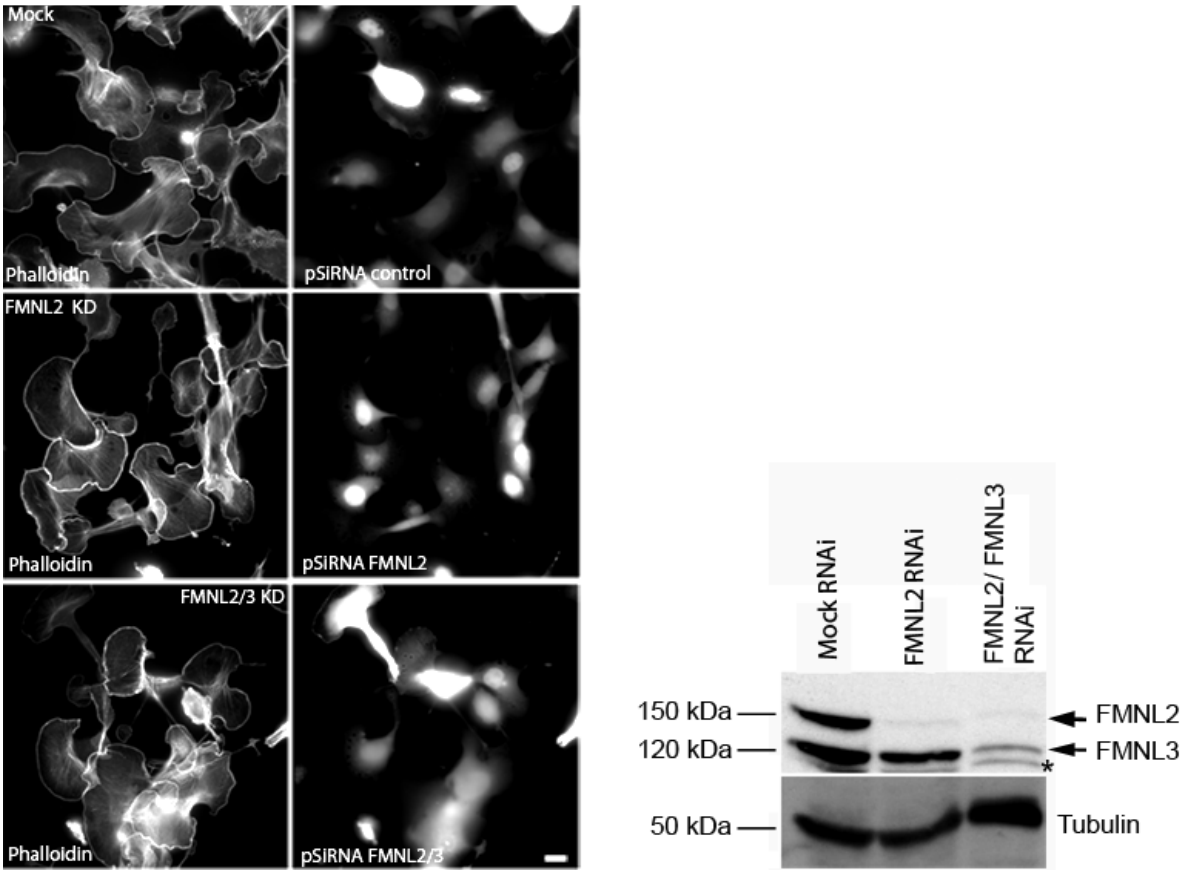

Figure 41: Lamellipodia formation in B16 cells is largely unaffected by FMNL2 or FMNL2 and -3 knockdown

Architecture of the actin cytoskeleton in Mock, FMNL2 and FMNL2/3 RNAi-treated B16-F1 cells after ALF_4-stimulation. Transfection with RNAi vectors is documented by expression of a EGFP variant encoded by the pSIRNA vectors. Bar equals 10µm. Efficient knockdown is verified by Western blotting using FMNL2- and -3-reactive antibody and tubulin as a loading control. Asterisk marks crossreaction of the antibody in these cells.

Examining the morphology of both mock treated and FMNL2 or FMNL2 and -3 knockdown cell populations revealed that all cell populations formed prominent lamellipodia after ALF_4-stimulation (Figure 41). Lamellipodia formation triggered by this treatment was reported to be strongly abrogated for instance in cells interfered for WAVE-complex components (Steffen *et al.*, 2004) and Arp2/3-complex (Steffen *et al*., 2006). These data suggest that lamellipodia formation does not require the Cd42 effectors FMNL2 and -3 as essential components of the core actin nucleation machinery.

Assuming that FMNL2 and -3 affect actin reorganisation events downstream of Cdc42, I explored potential functions of these formins in cell migration. For this purpose, cells were seeded subconfluently and tracks of individually migrating cells were followed using low magnification phase contrast and epifluorescence optics. Knockdown efficiency was analysed by Western Blotting using FMNL2- and FMNL3-reactive

antibody (Figure 42B). Interestingly, the speed of randomly migrating cells was reduced in the absence of FMNL2. Average velocity (arithmetic mean as calculated from the average distance over time) was 0,45µm/min (±0,02, n= 92) and 0,38µm/min (±0,01; n= 107) for mock-treated and FMNL2 knockdown cell populations, respectively (p =0,001) (Figure 42A). However, reduction in migration speed was more severe if cells were simultaneously reduced for expression of both FMNL2 and -3. In this case, the velocity averages 0,3µm/min (±0,02, n= 98) for FMNL2 and -3 double knockdown cells in comparison to 0,45µm/min in mock treated cells ($p < 0,001$) (Figure 42A). Tracks of individually migrating cells are displayed in a so called polar plot, the FMNL2/FMNL3 double knockdown population appears much more concentrated around the centre than the FMNL2 knockdown or control population (Figure 42C).

The data obtained so far documented that FMNL2 and -3 are new *bona fide* effectors of Cdc42. In contrast to the prevailing view that formins are per se actin nucleators, FMNL2 exhibits no nucleation activity but processively elongates actin filaments in the presence of profilin. To finally understand the function of FMNL2 and -3 in cell migration, which is impaired upon knockdown of both formins, additional data are required to analyse whether FMNL2 and -3 directly influence protrusion of the lamellipodium or if the reduced migration speed is connected to other processes accompanying cell motility.

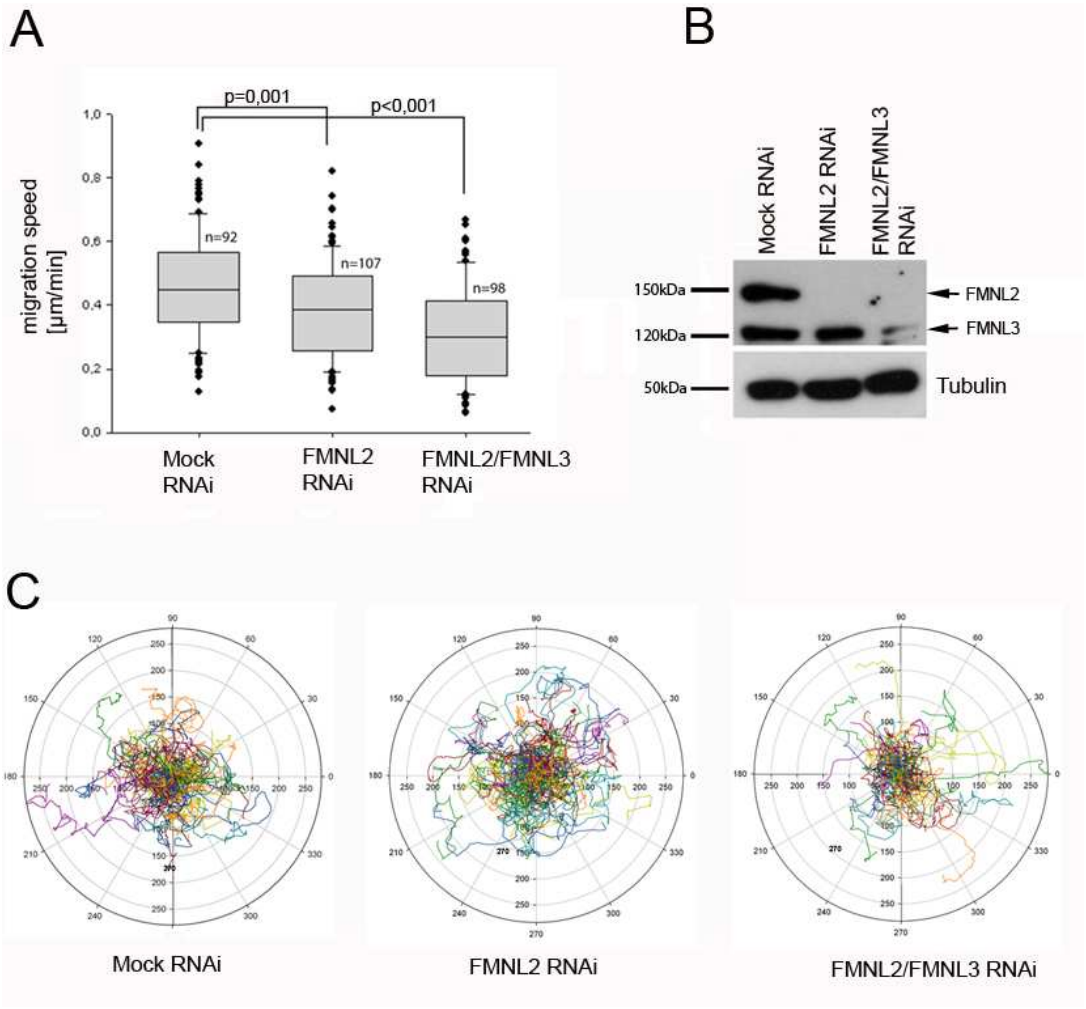

Figure 42: FMNL2 and FMNL2 and -3 knockdown reduces migration speed in B16 cells

(A) Box plot diagrams showing migration speed in FMNL2, FMNL2 and -3 and mock-treated RNAi cells in subconfluent cultures. The line within the box indicates median, the box boundaries contain 50% (25–75%) and the whiskers 80% (10–90%) of all measurements, whereas outlying points are shown as dots. The reduced migration speed in FMNL2 knockdown and FMNL2 and -3 double knockdown cells was statistically significant at p=0,001 and p<0,001 (Mann-Whitney rank sum test). (B) Efficient knockdown proved by western blotting. Tubulin was used as loading control. (C) Polar plots of mock treated, FMNL2 and FMNL2 and -3 knockdown cells in random migration assay. The position of each cell at time zero was centered at the origin of the grid and the tracks correspond to the movement of individual cells over time. The total duration of the movies was 24h. Tracks of FMNL2 and -3 double knockdown cells do not spread far away from the center compared to mock treated cells. All data derive from three independent experiments.

4 Discussion/Outlook

Diaphanous related formins emerged as key regulators of many actin-based processes including endocytosis, mitosis and cell motility. Although the knowledge about cellular functions of diaphanous related formins drastically increased over the last years, their contribution to lamellipodia and filopodia formation remains poorly defined. So the aims of this thesis were to investigate how the Drfs Drf3 and FMNL2 influence the formation of these protrusive structures.

4.1 Drf3-induced filopodia formation

To characterise diaphanous related formins such as Drf3 and FMNL2 in more detail it was essential to determine the subcellular positioning of these proteins. A widely used tool to study the localisation of proteins of interest in mammalian and other systems is the fusion to a fluorescent tag such as EGFP. Although it could be argued that fusing an EGFP-tag to a Drf could interfere with proper autoinhibiton or subcellular positioning, it has been shown that many EGFP-tagged proteins retain their biological activity and display the same trafficking pattern as the native proteins (Bialkowska *et al.*, 2005; Jarvik *et al.*, 2002; Tarasova *et al.* 1997; Carter and Sorkin, 1998). Using fluorescent tags allows to directly visualise not only the protein distribution within the cell but also provides information about the dynamic behaviour of the targeted protein which can not be obtained by immunofluorescence staining of endogenous proteins. In addition, visualisation of EGFP-tagged proteins eliminates the risk of introducing artefacts into protein distribution due to fixation procedures (Brock, Hamelers *et al.* 1999).

Many full length Drfs labelled with EGFP or other tags were reported to be mainly cytoplasmic, which was explained by an inactive conformation of the formin preventing specific subcellular localisation (Homem and Pfeifer, 2009; Pellegrin and Mellor, 2005; Wallar *et al.*, 2006; Han *et al.*, 2009; Vaillant *et al.*, 2008). This seems to apply as well to full length EGFP-tagged Drf3, which was enriched in the cytoplasm and did not target to any cytoskeletal structures (Figure 7). To gain insight into the subcellular localisation and dynamics of the formin, it was essential therefore to maintain Drf3 in an active conformation enabling specific targeting to cytoskeletal structures. Thus, I used a Drf3 construct rendered active through removal of the C-terminal DAD-domain permitting accumulation at sites of activity. Expression of active Drf3 in B16-F1 and other cell lines induced the formation of dozens of filopodia tipped by the active formin (Figure 7 and Figure 14). These findings confirmed other studies reporting the recruitment of Drf3 or its homologs to filopodia tips and its ability to induce these

structures in various cell types (Homen and Pfeifer, 2009; Beli *et al.*, 2007; Yang *et al.*, 2007; Schirenbeck *et al.*, 2006).

4.1.1 Convergent elongation or de novo nucleation of filopodia

To unravel the precise machinery generating these finger-like protrusions major efforts have been made over the last years leading to two contradictory models, the convergent elongation and the *de novo* nucleation model (reviewed in Faix *et al.*, 2009 and see 1.2.2). A recent study observing similar club shaped filopodia upon expression of an N-terminally deleted mDia2/Drf3 proposed that mDia2/Drf3-induced filopodia are formed by convergent elongation of lamellipodial filaments (Yang *et al.*, 2007). However, the club shaped nature of mDia2/Drf3-induced filopodia is apparently difficult to reconcile with filopodia originating from a limited number of filaments within the lamellipodium as proposed in the convergent elongation model. The authors explained the club-like shape of mDia2/Drf3-induced filopodia by fast depolymerisation of mDia2/Drf3-nucleated filaments from unprotected pointed ends and proposed that these aberrant filopodia are caused by an imbalance between mDia2/Drf3 and Arp2/3-complex activities. Consistent with the latter hypothesis, the data presented here demonstrate that the formation of club shaped filopodia strongly depends on the expression level of the formin (Figure 7). Since cells expressing low levels of Drf3 formed normally tapered filopodia, it is not very likely (although it can not be excluded) that over-expression of the active formin interferes with the machinery in general. However, I agree with Yang and colleagues in so far as the club like phenotype suggests that the protrusion of these filopodia results from imbalanced activities between the active formin at the tip and other factors required for filopodia formation. Furthermore it has to be considered that the deleted DAD-domain might fulfil additional functions besides the interaction with the DID domain. Recent publications claimed e.g. that some DAD-domains might comprise an additional actin binding WH2-domain (Vaillant *et al.*, 2008; Chhabra and Higgs, 2006).

Nevertheless, the active Drf3 construct was used as a tool to determine whether filopodia are exclusively formed by convergent elongation or whether formin-mediated nucleation at the filopodium tip generates these structures. Convergent elongation of lamellipodial filaments postulates that only a limited number of filaments are available for filopodia formation. As a consequence, the clubbed shape of Drf3-induced filopodia would have to arise either from splaying of a constant number of filaments at the tip or increased depolymerisation in the shaft. The results obtained in this work argue against both possibilities. The observed thickening of filopodia after protruding beyond the cellular network in coincidence with an increase in fluorescence intensity of formin at

the filopodium tip (Figure 10) could admittedly be explained by splaying apart of a constant number of filaments in the tip or increased depolymerisation in the shaft. However, the direct correlation between active Drf3 and filament mass (Figure 11) demonstrates that the active formin causes the formation of new actin filaments. In addition, Drf3-induced filopodia display a constant packing density and a linear correlation between filopodium width (e.g. tip *versus* shaft) and filament number (Figure 13), proving that filaments within the club-shaped filopodium tip do not splay apart during growth as proposed by Yang *et al.* (2007). Furthermore filopodia were even found to emanate from the sides of existing filopodia, without any apparent involvement of lamellipodial filaments (Figure 12). Finally, active Drf3 induced filopodia in the absence of functional WAVE-complex (Figure 15), which is essential for Arp2/3-complex mediated nucleation of lamellipodial filaments. Due to the fact that these cells lack lamellipodia (Steffen *et al.*, 2006), Drf3-induced filopodia can not employ lamellipodial filaments for their generation, indicating that the filaments formed within the filopodium are newly nucleated. Taken together, these data can only be explained by *de novo* nucleation of actin filaments in the filopodium tip presumably mediated by the active formin in these conditions, although I can not exclude that convergent elongation of lamellipodial filaments might be at play to allow the generation of specific types or subsets of filopodia. In any case unlike previous dogma my data unequivocally demonstrate that convergent elongation is certainly not an essential, and presumably not even the predominant mechanism of filopodia initiation.

4.1.2 Drf3 targeting to filopodia tips

A critical role for Abi1 in recruiting mDia2 to the leading edge has been proposed by Yang *et al.*, who could detect direct binding of mDia2 to Abi but not to any other member of the WAVE-complex. These data suggest that mDia2 and Abi1 form a distinct macromolar signalling unit with respect to the WAVE-complex (Yang *et al.*, 2007). A later study reported conflicting data proposing that WAVE (and indirectly the Arp2/3-complex) but not Abi1 interact with mDia2 (Beli *et al.*, 2008). The authors suggested that mDia2 forms a complex with Wave and Arp2/3-complex jointly inhibiting the formation of filopodia. The reasons for this discrepancy are unclear and since no interaction studies with Drf3 have been performed in this work, I can not shed light on this issue. However, since Drf3 is concentrated at the tips of filopodia elicited in Nap1 knockdown VA-13 cells (Figure 15), which have been shown to express reduced amounts of all other WAVE-complex components including Abi1 (Steffen *et al.*, 2006), a crucial role for Abi1 in Drf3 targeting could not be confirmed. It is worth noting however, that protein knockdown efficiency by RNAi is never complete, especially in this case

where downregulation of Abi1 is an indirect effect of Nap1 RNAi, and remaining levels of Abi1 might be sufficient to target Drf3 to the tips of filopodia. Future experiments should aim at verifying the dispensability of Abi proteins in mDia2/Drf3 targeting and at identifying missing candidates of interaction mediating mDia2/Drf3 recruitment.

4.1.3 Drf3 is involved but not essential for filopodia formation in Hela S3 cells

Since my data excluded the convergent elongation model as the exclusive mechanism of filopodia formation, but instead argued for *de novo* nucleation of filopodial filaments by a formin, I aimed at defining the contribution of mDia2 to filopodia formation. Even though active mDia2 strongly induced filopodia and accumulated at their tips, cell lines like Swiss 3T3 and NIH 3T3 expressing only minute amounts of Drf3 (Figure 18; Tominaga *et al.*, 2000) are well established to form these finger-like structures. This points towards significant redundancy with other formins in the system. In *Dictyostelium* the mDia2 homolog dDia2 is critical for the formation of these finger-like projections (Schirenbeck *et al.*, 2006), and knockdown of mDia2 in mammalian cells has been reported to abrogate filopodia (Beli *et al.*, 2007; Yang *et al.*, 2007). However, data presented in this work could not corroborate a crucial role of mDia2 in filopodia formation in Hela S3 cells (Figure 20). The reason for this discrepancy remains unclear, especially as Beli *et al.* (2007) observed loss of filopodia upon mDia2 knockdown in exactly the same cell type. However, it has to be mentioned that Beli *et al.* counted filopodia in Hela S3 cells after fixation and phalloidin stainings. Filopodia are highly dynamic structures and in particular Hela S3 cells display many kinds of membrane projections and retractions, which, especially in fixed samples, can easily be mistaken for filopodia. Filopodia are characterised by their protrusive nature, thus the only way to reliably count them is by live-video microscopy, as has been done here. It is worth mentioning that Yang *et al.* employed B16-F1, cells which only express minute amounts of Drf3 (Figure 18). It is difficult to envisage how knockdown of a marginally expressed protein can cause such strong phenotypical effects. I refrained from knockdowns in this cell type, since it would have been impossible to document the knockdown in Western Blotting.

In my experimental setup, Hela S3 cells expressing reduced levels of Drf3 were even slightly enhanced in their ability to generate filopodia. This is in contrast to published studies and might at first glance appear inconsistent with my afore mentioned results that were suggestive of Drf3 nucleation activity in filopodia. However, it is difficult to exclude that Drf3 performs additional yet unknown functions explaining the enhanced filopodia phenotype upon Drf3 knockdown. In addition, the knockdown of Drf3 could

affect expression levels of other formins which might enhance the generation of filopodia. This hypothesis is supported by the fact that mDia1 (Copeland *et al.*, 2007; Higashida *et al.*, 2004; Sarmiento *et al.*, 2008) and FMNL2 (Figure 25) concentrate at the tips of filopodia in various cell lines, potentially sharing similar functions with mDia2. Redundancy between formins is a frequently observed phenomenon, found e.g. in yeast where neither one of the two yeast formins Bni1p and Bnr1p is essential, but both are required for viability (Vallen *et al.*, 2000; Ozaki-Kuroda *et al.*, 2001; Sagot *et al.*, 2002b; Pruyne *et al.*, 2004). Partial redundancy has also been observed in mammalian cells, in which invadopodia formation and invasion of breast cancer cells depends not on one specific but on all three Dia isoforms (Lizárraga *et al.*, 2009), indicating that at least mDia1, 2 and 3 can fulfil overlapping functions in certain cellular processes. In order to clarify which formins contribute to the formation of filopodia, it will be essential to determine the precise signalling pathways leading to the generation of these structures. It becomes evident that the signalling pathways driving filopodia formation are divergent, as these structures can be formed downstream of several different Rho-GTPases e.g. Cdc42 and Rif. Due to the fact that structural constraints exclude an interaction of mDia1 with the well-established filopodia effector Cdc42 (Lammers *et al.*, 2008), future experiments will have to aim at identifying Rho-GTPase(s) activating mDia1 and resulting in subsequent filopodia targeting. Potential candidates are Rho GTPases influencing filopodia such as Rif, TC10 and Wrch1 (Aspenström *et al.*, 2009; Burridge and Wennerberg, 2004; Ellis and Mellor, 2000), but whether they are capable of interacting with and activating mDia1 and how that might affect filopodia formation is currently unknown.

4.1.4 Drf3 and lamellipodia formation

In addition to its function in filopodia formation, contradictory results have recently been published concerning the impact of mDia2/Drf3 on the generation of lamellipodia. Interestingly, Yang *et al.* observed the loss of filopodia and lamellipodia upon mDia2 knockdown, whereas in a conflicting work, mDia2 was instead suppressed by the Arp2/3/WAVE-complex pathway driving lamellipodia formation (Beli *et al.*, 2008). In an attempt to shed light on this controversy, I explored the impact of Drf3 on lamellipodia formation in more detail. First of all, the atypical accumulation of fascin in Drf3ΔDAD-stained lamellipodia (Figure 17), which is consistent with published data by Yang *et al.* (2007) strongly indicate that Drf3ΔDAD stained lamellipodia differ from canonical lamellipodia lacking fascin at their tips. In addition knockdown of Drf3 in Hela S3 cells did not alter the formation of Rac-induced lamellipodia (Figure 21). Although I can not fully exclude that Drf3 contributes to filament formation or elongation within the

lamellipodium, these data suggest that lamellipodia-like structures containing active Drf3 might reflect unnatural protrusive entities. The accumulation of constitutively active Drf3 at the cell periphery apparently drives the formation of hybrids of filopodia and lamellipodia marked by the filopodial marker protein fascin. The development of functional antibodies to confirm the absence of endogenous Drf3 within the lamellipodium will be crucial to verify this hypothesis.

4.2 Functional characterisation of FMNL2

The data presented here demonstrate so far that mDia2/Drf3 is involved but not essential for filopodia formation. Other formins might be able to substitute mDia2/Drf3 function in its absence. To narrow down other formins capable of effecting or modulating lamellipodia and filopodia formation in mammals, I explored the expression of different formins in various tissue culture cell lines. FMNL2, also referred to as FRL3, is widely expressed and abundant in all cell lines tested (Figure 18; Katoh *et al.*, 2003). Therefore, it was a promising candidate to be analysed concerning its contribution to the formation of actin dependent protrusive structures. The expression profile of two FMNL2 splice variants, A and B, have been analysed previously in detail by a bioinformatic approach (Katoh *et al.*, 2003). Surprisingly, amplification of FMNL2 from Hela S3 cDNA revealed a third splice variant FMNL2C, the existence of which had already been proposed previously (NCBI reference sequence: NM_001004422.1), but experimental data confirming its expression were so far not available. Data presented in this work suggests FMNL2C to be expressed in Hela S3 cells, but additional experiments should explore the expression profiles of different FMNL2 splice variants in various cell types, which will allow more insights into the physiological functions of all these variants.

4.2.1 FMNL2 localises to the lamellipodium and filopodium tip

Similar to many other full length formins FMNL2A and B are entirely cytosolic (Figure 24), at least when expressed by itself and when fused to EGFP on its N-terminus. For reasons having become clear at later stages of my work, FMNL2 A and B variants fused to EGFP at their C-terminus did show distinct subcellular localisation (see below) In contrast to EGFP-FMNL2A and B, EGFP-FMNL2C was not cytoplasmic but accumulated at the leading edge and at tips of filopodia in B16 cells (Figure 24) similar to an active FMNL2 construct lacking the DAD-domain (Figure 25), suggesting that autoinhibition in this splice variant is less efficient. Similar observations have already been made for other full length Drfs such as FRL2 (also referred to as FMNL3) and FMNL1γ, which were observed not to be cytosolic but to accumulate at membranes

(Vaillant *et al.*, 2008; Han *et al.*, 2009). The authors of both studies concluded that these specific Drf family members are constitutively active, thus do not comprise functional DAD-domains. Due to the fact that EGFP-FMNL2C localisation was abrogated in Cdc42-deficient cells (Figure 30) the absence of autoinhibition seems unlikely. FMNL2A and B are dramatically translocated to the leading edge upon co-expression of active Cdc42 (see below), indicating that the localisation of FMNL2C, which only differs in its sequence to –A and –B at its extreme C-terminus, is also mediated by Cdc42. If endogenous Cdc42 activity in B16-F1 cells was indeed sufficient to release the autoinhibiton of FMNL2C, this could be explained by weaker interactions between the DAD and the DID domain, resulting in more efficient release of the autoinhibition upon Cdc42 binding compared to the FMNL2A and B splice variants. However, this hypothesis needs to be experimentally verified e.g. by structural data and *in vitro* assays analysing DID-DAD binding in these variants. It would be interesting to investigate the expression profiles of these specific formin splice variants in appropriate cell lines and tissues, and combine this with the knowledge of expression levels of interacting Rho-GTPases. One possibility would be that Drf splice variants that feature weaker DID-DAD interactions are restricted to tissues and cell lines expressing reduced amounts of the relevant Rho-GTPase, thereby facilitating activation of the Drf.

Interestingly EGFP-FMNL2 is the first formin variant convincingly localising to the lamellipodium front without inducing atypical lamellipodial behaviour or unusual accumulation of fascin (Figure 26), as has previously been observed for active Drf3. In addition, such a localisation to the leading edge could also be confirmed by immunofluorescence stainings using an antibody raised against FMNL2 (Figure 27). However, since the antibody used for immunofluorescence stainings detected FMNL3 in addition to FMNL2 on western blots, stainings might reflect localisation of both endogenous FMNL2 and -3. This is not entirely unlikely, since EGFP-tagged FMNL3 was also found to target to the leading edge in a fashion indistinguishable to FMNL2 (see below). Whatever the case, the data strongly indicate that FMNL proteins can accumulate in principle to the tips of lamellipodia, pointing at potential functions for these proteins in the protrusion of these structures, so far considered to exclusively depend on Arp2/3-complex function.

4.2.2 Regulation and targeting of FMNL2 to the leading edge

Although pull-down assays revealed strong, perhaps direct, interactions with Cdc42 and the well established lamellipodia effector Rac (Figure 28), I failed to link Rac binding to the accumulation of FMNL2 at the lamellipodium tip (Figure 29). Surprisingly, targeting of FMNL2 to the lamellipodium occurs downstream of Cdc42 (Figure 29). This

small Rho-GTPase is thought to be involved in filopodia formation rather than in the generation of lamellipodia, although numerous studies reported that active Cdc42 is capable of triggering the formation of lamellipodia (Aspenström *et al.*, 2004; Hall, 1998; Nobes and Hall, 1995). Since Cdc42-induced lamellipodia formation could be blocked by dominant negative Rac (Nobes and Hall, 1995), this phenotype was interpreted to derive from Cdc42-mediated Rac activation. In spite of this view, a recent study indicated Cdc42 functions in migration on top of, and not just upstream of Rac-GTPases (Monypenny *et al*., 2009). However, it remains to be demonstrated that Cdc42 can indeed induce the formation of lamellipodia or lamellipodia-like structures in the absence of Rac-GTPases. Irrespective of the question whether Cdc42 can trigger the protrusion of a lamellipodium in the absence of Rac, I was able to identify a new Cdc42 effector convincingly accumulating at the leading edge and presumably playing a role in the formation of these protrusive structures.

I was surprised to find that the interaction between FMNL2 and Rac1 *in vitro* is not sufficient to cause membrane targeting of the formin *in vivo*. The reasons for this are currently unclear. While characterising FMNL2 in this thesis, an N-terminal myristoylation site was identified (see below). Since the interaction studies were performed with non-myristoylatable constructs (due to an N-terminal EGFP-tag), I can not exclude at present that myristoylation contributes to the specificity of interaction of the FMNL2 N-terminus with different Rho-GTPases. Besides its well established ability to mediate membrane targeting, the myristate moiety has in the past been implicated in influencing protein-protein interactions (Resh, 2006; 1999). To clarify whether the myristate moiety could have an impact on the specificity of interactions with different Rho-GTPases, additional pull-down assays utilising potentially myristoylatable constructs compared with the myristoylation-deficient mutants are required (collaboration with Dr. Mathias Geyer, MPI Dortmund). Another explanation for the observed binding of FMNL2 to Rac1 could be that Rac1 is not upstream but downstream of FMNL2 implicating that the formin is affecting Rac1 activity. This has already been proposed for other Drfs such as mDia1 and DAAM1, both of which seem to be capable of activating RhoA by interacting with a Rho GEF (Habas *et al.*, 2001; Kitzing *et al.*, 2007). It can not be excluded at this stage that FMNL2 interacted indirectly with Rac in pull-down experiments through a Rac interacting protein such as a GEF or GAP. It would be interesting to compare activation levels of Rac in FMNL2-expressing and FMNL2-knockdown cells, e.g. by pull-downs with PAK-CRIB beads that bind exclusively to activated Rac and Cdc42.

4.2.3 Regulation by myristoylation

A recent publication discovered a myristoylation consensus in the hematopoietic family member FMNL1. The authors described that the membrane localisation of FMNL1 and the induction of blebbing critically depends on the myristate moiety, since a myristoylation deficient mutant failed to induce membrane blebs and did not target to the cell membrane (Han *et al.*, 2009). Importantly, the myristoylation characterised here was discovered based on a sequence consensus lacking in FMNL1 (Maurer-Stroh *et al.*, 2002; collaboration with Mathias Geyer, MPI Dortmund). To gain further insight into the function of this cotranslational modification, I generated constructs preserving the lipid modification by fusing the EGFP-tag to the C-terminus of the protein and a myristoylation-deficient mutant by changing the second Glycin of FMNL2, which is essential for addition of the myristate moiety, to Alanin. Surprisingly, presumably myristoylatable full length constructs accumulated at the leading edge in B16-F1 cells in a fashion comparable to active FMNL2ΔDAD or full length FMNL2 co-expressed with active Cdc42 (Figure 32). To explore whether this targeting in B16-F1 cells is achieved by release of autoinhibition of FMNL2 by endogenous Cdc42, I analysed the localisation of the myristoylatable FMNL2 variants in a Cdc42-deficient cell line. Since the myristoylatable FMNL2 constructs also concentrated weakly at the leading edge in the absence of Cdc42, whereas the non-myristoylatable mutant did not (Figure 33), the myristate moiety in theory could either mediate targeting to the leading edge on its own or interfere with proper autoinhibition. However, as opposed to published results (Han *et al.*, 2009), I found the myristoylation to be required neither for release of autoinhibition nor for targeting, since the myristoylation-deficient FMNL2 mutant is enriched at the cell periphery upon co-expression of active Cdc42 in Cdc42 -/- cells (Figure 33) and a comparable mutant rendered active through removal of its DAD-domain was capable of accumulating at the leading edge even in the absence of Cdc42 (Figure 34). In conclusion, these data not only demonstrate that both myristoylation and Cdc42 can aid intracellular targeting presumably by counteracting autoinhibition, but also that neither signal constitutes an essential localisation determinant once the formin is activated.

4.2.4 Potential regulation by formin binding proteins

The data described above suggest that other yet unknown factors mediate subcellular positioning of the formin. Although the myristate moiety has been implicated in membrane targeting (Han et al., 2009) many studies indicated that this modification alone is not sufficient to mediate localisation to cell membranes (Swierczynski *et al.*, 1996; Zhou *et al.*, 1994). Usually membrane targeting by such lipid modifications is

achieved by myristate plus additional basic aminoacid residues, an additional palmitoylation of the protein or a domain that interacts with other membrane-bound components (Resh *et al.*, 2006; 1999), indicating that there has to be an additional yet unidentified signal causing membrane targeting of FMNL2. Although Rho-GTPases have been implicated in recruiting formins to specific sites (Martin *et al.*, 2007; Seth *et al.*, 2006), my data suggest that at least Cdc42 is not required for determination of membrane localisation, since constitutively active FMNL2 is enriched at the leading edge even in Cdc42-deficient cells in a fashion comparable to Cdc42-expressing control cells (Figure 34). I would like to argue that Cdc42 is only responsible for releasing autoinhibition as a prerequisite for membrane targeting, the latter of which is mediated by other FMNL2-interacting proteins, lipid modification or both. Furthermore, the fact that co-expression of active Cdc42 with full length Drf3 and full length FMNL2 does not cause similar subcellular localisation patterns implies that Cdc42 is indeed not capable of mediating subcellular positioning. More specifically, co-expression of Drf3 with active Cdc42 resulted in the concentration of Drf3 at the entire plasma membrane (Figure 8) whereas the same treatment caused FMNL2 targeting to the lamellipodium (Figure 29). Thus, this data suggest that subcellular targeting can not solely be achieved by interactions with Cdc42 or any other GTPases such as Rac, since none of the GTPases have been found to convincingly accumulate at the tips of lamellipodia (data not shown).

In addition to Rho-GTPases many other formin binding proteins have been identified, some of them influencing the subcellular localisation of formins (Aspenström, 2009). For instance Src family kinases are prominent modulators of formin function. These non receptor tyrosine kinases can bind formins directly and Src has been reported to relocate Formin-1 from the nucleus to the plasma membrane (Uetz *et al.*, 1996). Interestingly the FH3-domain, which comprises the DID and the dimerisation domain, has been shown to determine subcellular localisation (Petersen *et al.*, 1998; Katoh *et al.*, 2001; Ozaki-Kuroda *et al.*, 2001; Sharpless and Harris, 2002). This is supported by a recent study showing that IQGAP1 interacts with the FH3-domain of mDia1 and is required for the localisation of mDia1 without activating or inhibiting the formin (Brandt el al., 2007). It will be instrumental in future experiments to determine how localisation of FMNL2 at the leading edge is achieved.

4.3 FMNL2 does not nucleate actin filaments *in vitro*

The majority of previously analysed formins have been demonstrated to nucleate actin filaments. FMNL1, the hematopoietic homolog of FMNL2, bundles actin filaments, competes with capping protein for barbed end binding, severs actin filaments and

accelerates polymerisation from actin monomers (Harris *et al.*, 2004; 2006). Previous work utilising the FH2-domains of FMNL2 and -3 demonstrated that these formins are also capable of filament bundling *in vitro* (Vaillant *et al.*, 2008). In addition, the FH2-domains of both FMNL2 and -3 appeared to induce actin polymerisation, even though the effect observed in pyrene–actin polymerisation assays was comparably modest. Although the FH2-domain in formins is necessary and sufficient to induce actin polymerisation, it is well established that the profilin-binding activity of the FH1-domain critically contributes to formin-mediated actin assembly (Kovar *et al.*, 2003; Kovar and Pollard, 2004; Romero *et al.*, 2004; Kovar *et al.*, 2006). Since the biochemical properties of FMNL2 and -3 were previously analysed by using isolated FH2-domains, it seemed important to extend this analysis to the FH1-FH2-domains of FMNL2. Surprisingly, using this experimental setup FMNL2 was not capable of nucleating actin filaments from actin monomers neither in pyrene-actin polymerisation nor TIRF assays (Figure 35 and Figure 36). This discrepancy to published results could arise from using a construct comprised of the FH1- and FH2-domains instead of isolated FH2-domains used in previous *in vitro* assays. So far the only other described formin not capable of nucleating actin filaments *in vitro* is FHOD3 (Taniguchi *et al.*, 2009). Together with the data presented in this thesis, one could assume that actin nucleation is not a necessarily feature applying to all formins. However, I can not exclude that additional factors not present in the *in vitro* system influence FMNL2 activity and facilitate FMNL2 mediated actin nucleation *in vivo.*

Due to the prominent accumulation of FMNL2 in the lamellipodium, it can be assumed that it fulfils certain functions such as regulating elongation or nucleation in this cellular compartment. Although the Arp2/3-complex is well established to be responsible for filament nucleation within the lamellipodium, formins such as FMNL2 and -3 might contribute to filament formation in these protrusive structures. However, functions mediated by FMNL2 and -3 must be different from Arp2/3-complex, since B16-F1 cells expressing reduced levels of FMNL2 and -3 did form lamellipodia (Figure 41), which is in contrast to Arp2/3-knockdown cells largely lacking these structures (Steffen *et al.*, 2006; Gomez *et al.*, 2007; Nicholson-Dykstra and Higgs, 2007). Whatever the case, the precise role of FMNL2 accumulation in the lamellipodium remains uncertain at present.

4.3.1 FMNL2 elongates actin filaments *in vitro* and regulates cell motility *in vivo*

Although FMNL2-FH1-FH2 does not nucleate actin filaments, it binds to barbed ends of actin filaments and promotes processive barbed end elongation in the presence of

profilin *in vitro* (Figure 36). Since profilinactin is the predominant species of actin monomers available for polymerisation within the cell (Pollard *et al.*, 2000; Kaiser *et al.*, 1999), this biochemical behaviour might be quite close to the situation within living organisms. In conjunction with its localisation at the leading edge and reduced migration speed in B16-F1 melanoma cells upon FMNL2 knockdown (Figure 42), this suggests that FMNL2 positively regulates motility in B16 F1 cells. This is consistent with upregulation of FMNL2 in colorectal cancer cells, which could be directly correlated with higher invasiveness and enhanced metastasis (Zhu *et al.*, 2008). FMNL2 might regulate elongation of actin filaments nucleated by the Arp2/3-complex within the lamellipodium, thereby enhancing cell motility, although this remains to be directly demonstrated. As the double knockdown of FMNL2 and -3 causes an even more severe reduction in migration speed, these two formins might work closely together and fulfil similar functions. This could be consistent with the observations that FMNL3 also interacts with active Cdc42 and active Rac1 in pull-down experiments (Figure 37), and is enriched at the leading edge upon co-expression of active Cdc42, supporting potential redundant functions of the two formins. In addition, FMNL2 and -3 were reported to be capable of forming heterodimers via their DID-, DAD-, their dimerisation- and FH2-domains, possibly regulating the activity of both proteins (Vaillant *et al.*, 2008). Whether the sequence stretches lacking N-terminal to and within the FH1-domain of FMNL3 compared to FMNL2 are relevant for its ability to interact with actin filaments remains to be investigated in the future, but this might have interesting consequences for FMNL3 functions within the lamellipodium and in cell motility.

FMNL2, and maybe also FMNL3, might act as a filament elongation factors within the lamellipodium similar to VASP, another actin binding protein promoting filament assembly at the tip of the lamellipodium. However, in contrast to the reduced migration speed in FMNL2 and -3 knockdown cells, genetic removal of the Ena/VASP family members Mena and VASP in fibroblast cells results in increased other than decreased cell motility (Bear *et al.*, 2000). This seems paradoxical given that lamellipodial protrusion rate positively correlates with the intensity of GFP-VASP at the leading edge, and Ena/VASP proteins were shown to enhance actin-based motility of *Listeria monocytogenes* (Rottner *et al.*, 1999a; Laurent *et al.*, 1999; Loisel *et al.*, 1999). However, the protrusion rates of lamellipodia do not necessarily correlate with global migration rate observed in these cells. Mena/VASP-deficient lamellipodia appeared to protrude slower but more persistently, resulting in increased cell translocation rates, indicating that an optimal balance between lamellipodia extension, adhesion, translocation and cell polarisation controls productive locomotion (Bear *et al*., 2002;

Krause *et al.*, 2003). It will be a very interesting task to explore how lamellipodial protrusion rates correlate with EGFP-FMNL2 intensity at the leading edge, or with RNAi-mediated knockdown of FMNL2 and -3. It also might be attractive to compare FMNL2 and -3 with VASP functions in the lamellipodium. Of note, immunofluorescence stainings showed normal accumulation of VASP in the lamellipodia of cells over-expressing active FMNL2 (Figure 26), indicating that both proteins can localise simultaneously in these protrusive structures.

4.3.2 FMNL2 and FMNL3 have potentially redundant functions

In this work, I additionally characterised FMNL3, another member of the diaphanous related formins sharing roughly 70% sequence identity with FMNL2. As previously observed for FMNL2, the N-terminus of FMNL3 is capable of binding active Cdc42 and Rac1 (Figure 37). Co-expression of active Cdc42 but not active Rac is sufficient to cause accumulation of FMNL3 full length in the leading edge in B16 cells. As mentioned for FMNL2 earlier, the physiological relevance of Rac binding to FMNL3 remains elusive at this stage. In addition, FMNL3 also contains a myristoylation consensus sequence (Han *et al.*, 2009) making it reasonable to assume that this lipid modification will regulate the protein´s activity in a fashion comparable to FMNL2. Remarkably, FMNL3 has been proposed to be constitutively active, although its DID is able to bind its DAD both *in vivo* and *in vitro* (Vaillant *et al.*, 2008). Vaillant *et al.* employed a reporter gene assay, which records activation of the actin/MAL/SRF pathway in response to depletion of the cellular G-actin pool, as observed e.g. in case of formin-mediated actin polymerisation. Since all experiments in this study concerning the autoregulation of FMNL3 were performed in NIH3T3 cells, so in the presence of endogenous Cdc42, it is possible that the endogenous GTPase interfered with proper autoinhibition *in vivo* as observed in our case for EGFP-FMNL2C (see above). In my experimental setup, I could not obtain any indication that FMNL3 is constitutively active, as the full length protein did not accumulate to any protrusive cytoskeletal structures. Future experiments employing SRF reporter assays should benefit from carefully choosing cell lines, devoid perhaps of high activity of the respective interacting Rho-GTPase.

4.4 Concluding remarks

This work has provided new insights into the formation of filopodia mediated by formins. A constitutively active variant of Drf3 lacking the C-terminal DAD-domain strongly induced filopodia and localised to the tips of these protrusive structures. The data presented here strongly suggest that filopodia are generated by *de novo* filament

nucleation and not by convergent elongation of lamellipodial actin filaments. In contrast to the prevailing view that mDia2/Drf3 is required for the formation of filopodia, my experiments also showed that Drf3 is dispensable for filopodia formation in Hela S3 cells. Future experiments will have to evaluate how other diaphanous related formins such as mDia1 influence the formation of filopodia and whether they share redundant functions. We still have to wait for an individual factor the removal of which will abolish filopodia formation.

In a second project, I examined the molecular regulation and cellular function of the yet poorly characterised formin FMNL2, and the related protein FMNL3. Both formins are activated by the small Rho-GTPase Cdc42 to localise to the leading edge of the cell. An N-terminal myristoylation of FMNL2 contribute to the regulation of autoinhibition, but is not essential for subcellular positioning per se, as proposed previously (Han *et al.*, 2009). Biochemical evidence suggests that FMNL2 does not nucleate but instead elongates actin filaments, promising exciting effects on the modulation of the actin filament network in the lamellipodium. Finally, FMNL2 and -3 are involved in regulating cell migration, although it remains unknown how exactly this relates to their biochemical activity within the lamellipodium. Future work will thus aim at clarifying this issue, and at shedding light on the functions of formins or related factors such as Ena/VASP proteins relative to the proposed dominating role of Arp2/3-complex in actin filament nucleation in the lamellipodium.

5 Summary

In the present work, the contribution of the diaphanous related formins mDia2/Drf3 and FMNL2/3 to the actin-based formation of lamellipodia and filopodia was analysed. Since filopodia formation can occur upon suppression of Arp2/3-complex, filopodial actin filaments may assemble by means of other actin nucleators such as formins. To characterize the role of mDia2/Drf3 in mammalian cells, an EGFP-tagged active Drf3 variant, lacking the C-terminal DAD-domain (Drf3ΔDAD), was generated. Expression of EGFP-Drf3ΔDAD in B16-F1 mouse melanoma cells strongly induced the formation of filopodia tipped by the formin. Interestingly, Drf3ΔDAD–containing filopodia frequently thickened at their tips after protruding beyond the cell periphery. Yet, actin filament spacing in these filopodia was largely independent of filopodial width, as determined by electron microscopy. In addition to that, Drf3ΔDAD levels and F-actin amounts showed a linear correlation in these filopodia tips. Thus, these data demonstrated that thickening of Drf3ΔDAD-induced filopodia tips occurs through *de novo* actin filament nucleation. My results indicate nucleation of actin filaments to be the predominant mechanism of actin filament generation in filopodia, rather than simple elongation of pre-existing lamellipodial filaments. Although clearly involved in this process, Drf3 can be functionally replaced by other formins, as I found its removal to abolish filopodia formation.

For instance, both Drfs FMNL2 and FMNL3 emerged as potential additional regulators of filopodia, but also lamellipodia formation. Active EGFP-tagged FMNL2 was strongly enriched at the tips of protruding lamellipodia and filopodia in B16-F1 cells. FMNL2 and -3 interacted with active Cdc42 and Rac1 *in vitro*. Interestingly, co-expression of Cdc42 but not Rac was sufficient to mediate accumulation of EGFP-tagged FMNL2 and -3 at the tips of lamellipodia and filopodia. In addition, FMNL2 appeared to be regulated by N-terminal myristoylation. Although myristoylation was not essential for interaction of the formin with Cdc42 and proper subcellular targeting, both the lipid modification and active Cdc42 contribute to localisation and activation by counteracting autoinhibition. *In vitro* polymerisation assays indicated that FMNL2 does not promote actin filament nucleation, but instead elongation powered by profilin. *In vivo* the presence of both FMNL2 and -3 was relevant for efficient cell motility, significantly expanding the repertoire of Cdc42 effectors directly promoting actin filament assembly and turnover in migration.

6 Abbreviations

A	Ampere
aa	amino acid
Abi1	Abl interactor1
ADF	actin-depolymerising factor
ATCC	American Type Culture Collection
ATP	Adenosine triphosphate
bp	base pairs
BSA	bovine serum albumin
CC	coiled-coil domain
Cc	critical concentration
cAMP	cyclic adenosin monophosphate
cGMP	cyclic guanosin monophosphate
Cdc42	cell division cycle 42
cDNA	copy DNA
C-terminal	carboxy-terminal
kDa	Kilodalton
DAD	diaphanous autoinhibitory domain
DD	dimerisation domain
DID	diaphanous inhibitory domain
DMSO	dimethylsulfoxide
DNA	desoxyribonucleic acid
Drf3	diaphanous related formin 3
E. coli	Escherichia coli
EDTA	Ethylene diamine tetraacetic acid
EGTA	Ethylene glycol-bis(2-aminoethylether)-tetraacetic acid
EGFP	enhanced green fluorescent protein
ELISA	enzyme-linked immunosorbent assay
et al.	*et alia*
f-actin	filamentous actin
FCS	fetal calf serum
FRAP	Fluorescence recovery after photobleaching
FH1	formin homology 1
FH2	formin homology 2
fw	forward
G-actin	globular actin

GAP	GTPase activating protein
GBD	GTPase-binding domain
GDI	GDP dissociation inhibitor
GDP	Guanosine diphosphate
GEF	guanine nucleotide exchange factor
GTP	Guanosine triphosphate
GFP	green fluorescent protein
HEPES	N-2-Hydroxyethylpiperazine-N'-2-ethane sulfonic acid
IF	immunofluorescence
Ig	immunoglobulin
IP	immunoprecipitation
µ	micro
M	molar
mc	monoclonal
l	liter
mRFP	monomeric red fluorescent protein
mRNA	messenger RNA
Nap1	Nck associated protein1
NMT	N-myristoyltransferase
NPF	nucleation promoting factor
N-terminal	amino terminal
PAGE	polyacrylamide-gel electrophoresis
PBS	phosphate buffered saline
pc	polyclonal
PCR	polymerase chain reaction
PEG	Polyethylene glycol
PI3-K	phosphatidylinositol-3-kinase
PO	peroxidase
Rac1	Ras-related C3 botulinum toxin substrate 1
rev	reverse
RNA	ribonucleic acid
Rho	Ras homolog gene family
RhoA/B/C/G	Ras homolog gene family, member A/B/C/G
RZPD	Deutsches Ressourcenzentrum für Genomforschung GmbH
SDS	sodium dodecyl sulphate
SH2	Src-Homologie-Region2
SH3	Src-Homologie-Region3
Sra-1	specifically Rac associated protein 1

TAE	Tris-Acetate-EDTA-buffer
Toca-1	transducer of Cdc42 dependent actin assembly 1
Tris	Tris-(hydroxymethyl) aminomethane
TIRF	Total Internal Reflection Fluorescense
UK	United Kingdom
USA	United States of America
V	Volt
v/v	volume per volume
x g	times gravity
VASP	Vasodilator stimulated phosphoprotein
WASH	Wiskott-Aldrich Syndrome protein and Scar omolog
WASP	Wiskott-Aldrich Syndrome protein
WAVE	Wiskott-Aldrich Syndrome verprolin homologue protein
WB	Western blot
WHAMM	WASP homolog associated with actin, membranes and microtubules
w/v	weight per volume

7 Danksagungen

Im Laufe der letzten Jahre haben viele Menschen mich in meiner Doktorarbeitszeit unterstützt und die Zeit hier am HZI unvergesslich gemacht.

An erster Stelle möchte ich mich bei Dr. Klemens Rottner bedanken, der mir die Möglichkeit gegeben hat, meine Doktorarbeit in seiner Arbeitsgruppe durchzuführen. Während der gesamten Zeit hat er mit seinem Wissen, seiner Diskussionsbereitschaft und seiner hervorragenden Betreuung maßgeblich dazu beigetragen, dass ich meine Doktorarbeit zum Abschluss bringen konnte. Des Weiteren bedanke ich mich bei Dr. Theresia Stradal, die mir immer hilfreich zur Seite gestanden hat, besonders im Bezug auf Datenbankanalysen und die Herstellung von Expressionskonstrukten.

Mein besonderer Dank gilt Prof. Dr. Jürgen Wehland und Prof. Dr. Martin Korte für die Übernahme des Referats bzw. des Korreferats dieser Arbeit. Prof. Dr. Petra Dersch danke ich für die Übernahme des Prüfungsvorsitzes.

Vielen Dank auch allen jetzigen und ehemaligen Mitgliedern der Arbeitsgruppen SIM, CYD und ZB, die durch ihre herzliche Art ein Arbeitsklima schaffen, in dem man sich jeden Tag wieder auf die Arbeit freut. Ich danke euch allen für wertvolle Diskussionen, unermüdliche Hilfsbereitschaft, erholsame Kaffeepausen und unvergleichliche Partys! Besonders möchte ich mich bei Dr. Malgorzata Szczodrak, Kathrin Schloen, Margit Oelkers, Dr. Jan Hänisch, Dr. Stefanie Weiß und Dr. Frank Lai bedanken: „Ihr seid einfach die Besten“.

Ohne die Unterstützung und Diskussionsbereitschaft unserer Kooperationspartner wäre diese Arbeit unmöglich gewesen. Deshalb bedanke ich mich herzlich bei Dr. Jan Faix und Dennis Breitsprecher (MH, Hannover) für die Durchführung der *in vitro* Experimente, bei Dr. Mathias Geyer (MPI, Dortmund) für seine Unterstützung bezüglich der Myristoylierung von FMNL2, bei Prof. Dr. J. Victor Small, Dr. Stefan Köstler und Edith Urban (IMBA, Wien) für die EM-Daten, bei Dr. Robert Geffers (HZI, Braunschweig) für die Bereitstellung der Affimetrix Daten und bei Dr. Lothar Gröbe und Petra Hagendorff (HZI, Braunschweig) für die Durchführung des FACS Sorting.

Ein stiller Dank geht an Elisabeth Breidbach.

Abschließend möchte ich meinen Eltern, Philipp und Vera und natürlich meinem Freund Jörgen für ihre Unterstützung während der letzten drei Jahre danken!

8 References

Abercrombie M, Heaysman JE, Pegrum SM. (1970). “The locomotion of fibroblasts in culture. II. ‘‘Ruffling’”. Exp. Cell Res. 60, 437–444.

Ahuja R, Pinyol R, Reichenbach N, Custer L, Klingensmith J, Kessels MM, Qualmann B. (2007). “Cordon-bleu is an actin nucleation factor and controls neuronal morphology”. Cell. 131(2):337-50.

Alberts AS. (2001). “Identification of a carboxyl-terminal diaphanous- related formin homology protein autoregulatory domain”. J. Biol. Chem. 276, 2824–2830.

Alberts AS, Bouquin N, Johnston LH, Treisman R. (1998). “Analysis of RhoA-binding proteins reveals an interaction domain conserved in heterotrimeric G protein beta subunits and the yeast response regulator protein Skn7”. J Biol Chem. 273(15):8616-22.

Amann, K. J. and Pollard, T. D. (2001). “Direct real-time observation of actin filament branching mediated by Arp2/3-complex using total internal reflection fluorescence microscopy”. Proc. Natl.Acad. Sci. U.S.A. 98, 15009–15013.

Amano, T., Tanabe, K., Eto, T., Narumiya, S. and Mizuno, K. (2001). “LIMkinase 2 induces formation of stress fibres, focal adhesions and membrane blebs, dependent on its activation by Rho-associated kinase-catalysed phosphorylation at threonine-505”. Biochem J 354, 149-59.

Amatruda, J. F., D. J. Gattermeir, Karpova TS, Cooper JA. (1992). "Effects of null mutations and over-expression of capping protein on morphogenesis, actin distribution and polarized secretion in yeast." J Cell Biol 119(5): 1151-62.

Aspenström P. (2009). “Formin-binding proteins: Modulators of formin-dependent actin polymerization”. Biochim Biophys Acta.

Aspenström P, Richnau N, Johansson AS. (2006). “The diaphanous-related formin DAAM1 collaborates with the Rho-GTPase RhoA and Cdc42, CIP4 and Src in regulating cell morphogenesis and actin dynamics”. Exp Cell Res. 312(12):2180-94.

Aspenström P, Fransson A, Saras J. (2004). “Rho GTPases have diverse effects on the organization of the actin filament system”. Biochem J. 377(Pt 2):327-37.

Bamburg JR, Wiggan OP. (2002). “ADF/cofilin and actin dynamics in disease”.Trends Cell Biol. 12(12):598-605.

Bear JE, Gertler FB. (2009). “Ena/VASP: towards resolving a pointed controversy at the barbed end”. J Cell Sci. 122(Pt 12):1947-53

Bear JE, Loureiro JJ, Libova I, Fässler R, Wehland J, Gertler FB. (2000). “Negative regulation of fibroblast motility by Ena/VASP proteins”. Cell. 101(7):717-28.

Beli P, Mascheroni D, Xu D, Innocenti M. (2008) “WAVE and Arp2/3 jointly inhibit filopodium formation by entering into a complex with mDia2”. Nat Cell Biol. 10(7):849-57.

Benesch S, Lommel S, Steffen A, Stradal TE, Scaplehorn N, Way M, Wehland J, Rottner K. (2002). “Phosphatidylinositol 4,5-biphosphate (PIP2)- induced vesicle movement depends on N-WASP and involves Nck, WIP, and Grb2”. J Biol Chem. 277: 37771-6.

Bernards A. (2003). “GAPs galore! A survey of putative Ras superfamily GTPase activating proteins in man and *Drosophila*”. Biochim. Biophys. Acta 1603:47–82.

Bialkowska A, Zhang XY, Reiser J. (2005). „Improved tagging strategy for protein identification in mammalian cells". BMC Genomics. 6:113.

Biyasheva A, Svitkina T., Kunda P., Baum B. and Borisy G. (2004). "Cascade pathway of filopodia formation downstream of SCAR". J Cell Sci 117: 837–848.

Blanchoin L, Amann KJ, Higgs HN, Marchand JB, Kaiser DA, Pollard TD. (2000). "Direct observation of dendritic actin filament networks nucleated by Arp2/3-complex and WASP/Scar proteins." Nature 404(6781): 1007-11.

Block J, Stradal TE, Hänisch J, Geffers R, Kostler SA, Urban E, Small JV, Rottner K, Faix J. (2008). „Filopodia formation induced by active mDia2/Drf3". J Microsc 231: 506-517

Bosch M, Le KH, Bugyi B, Correia JJ, Renault L, Carlier MF. (2007). "Analysis of the function of Spire in actin assembly and its synergy with formin and profilin". Mol Cell. 28(4):555-68.

Brandt DT, Marion S, Griffiths G, Watanabe T, Kaibuchi K, Grosse R. (2007). "Dia1 and IQGAP1 interact in cell migration and phagocytic cup formation". J Cell Biol. 178(2):193-200. Epub 2007 Jul 9.

Breitsprecher D, Kiesewetter AK, Linkner J, Faix J. (2009). "Analysis of actin assembly by in vitro TIRF microscopy". Methods Mol Biol. 571:401-15.

Breitsprecher D, Kiesewetter AK, Linkner J, Urbanke C, Resch GP, Small JV, Faix J.(2008). „Clustering of VASP actively drives processive, WH2 domain-mediated actin filament elongation". EMBO J. 27(22):2943-54.

Brock R, Hamelers IH, Jovin TM. (1999). "Comparison of fixation protocols for adherent cultured cells applied to a GFP fusion protein of the epidermal growth factor receptor". Cytometry.35(4):353-62.

Bu W, Chou AM, Lim KB, Sudhaharan T, Ahmed S. (2008). „The Toca-1-N-WASP complex links filopodial formation to endocytosis". J Biol Chem. 284(17):11622-36

Burridge K, Wennerberg K. (2004). "Rho and Rac take center stage". Cell. 116(2):167-79.

Byers HR, White GE, Fujiwara K. (1984) "Organization and function of stress fibers in cells in vitro and in situ". Cell and Motility, Vol. 5 (ed. by J.W. Shay), pp. 83–137. Plenum Publishing Corp., New York.

Caldwell JE, Heiss SG, Mermall V, Cooper JA. (1989). "Effects of CapZ, an actin capping protein of muscle, on the polymerization of actin". Biochemistry. 28(21):8506-14.

Carlier MF, Pantaloni D. (1997). "Control of actin dynamics in cell motility". J Mol Biol. 269(4):459-67.

Campellone KG, Webb NJ, Znameroski EA, Welch MD. (2008). "WHAMM is an Arp2/3-complex activator that binds microtubules and functions in ER to Golgi transport". Cell. 134(1):148-61.

Carter RE, Sorkin A. (1998). "Endocytosis of functional epidermal growth factorreceptor-green fluorescent protein chimera." J Biol Chem. 273(52): 35000-7.

Casella JF, Casella SJ, Hollands JA, Caldwell JE, Cooper JA. (1989). "Isolation and characterization of cDNA encoding the alpha subunit of Cap Z(36/32), an actin-capping protein from the Z line of skeletal muscle". Proc Natl Acad Sci USA. 86(15):5800-4.

Castrillon DH, Wasserman SA. (1994). "Diaphanous is required for cytokinesis in Drosophila and shares domains of similarity with the products of the limb deformity gene". Development 120, 3367–3377.

Chang F, Drubin D, Nurse P. (1997). “cdc12p, a protein required for cytokinesis in fission yeast, is a component of the cell division ring and interacts with profilin”. J. Cell Biol. 137, 169–182.

Chereau D, Boczkowska M, Skwarek-Maruszewska A, Fujiwara I, Hayes DB, Rebowski G, Lappalainen P, Pollard TD, Dominguez R. (2008). “Leiomodin is an actin filament nucleator in muscle cells”. Science. 320(5873):239-43.

Chesarone, M., Gould, C. J., Moseley, J. B. & Goode, B. L. (2009). “Displacement of formins from growing barbed ends by Bud14 is critical for actin cable architecture and function”. Dev. Cell 16, 292–302.

Chesarone MA, Goode BL. (2009). “Actin nucleation and elongation factors: mechanisms and interplay”. Curr Opin Cell Biol. 21(1):28-37.

Chhabra ES, Higgs HN. (2007). “The many faces of actin: matching assembly factors with cellular structures”. Nat Cell Biol. 9(10):1110-21.

Chhabra ES, Higgs HN. (2006). “INF2 Is a WASP homology 2 motif-containing formin that severs actin filaments and accelerates both polymerization and depolymerization”. J Biol Chem. 281(36):26754-67

Chrzanowska-Wodnicka M, Burridge K. (1996). “Rho-stimulated contractility drives the formation of stress fibers and focal adhesions”. J Cell Biol.133(6):1403-15.

Cooper JA, Sept D. (2008). “New insights into mechanism and regulation of actin capping protein”. Int Rev Cell Mol Biol. 2008;267:183-206.

Cooper JA. (1987). “Effects of cytochalasin and phalloidin on actin”. J Cell Biol. 105(4):1473-8.

Cooper JA, Walker SB, Pollard TD. (1983). “Pyrene actin: documentation of the validity of a sensitive assay for actin polymerization”. J Muscle Res Cell Motil. 4(2):253-62.

Copeland SJ, Green BJ, Burchat S, Papalia GA, Banner D, Copeland JW. (2007). The diaphanous inhibitory domain/diaphanous autoregulatory domain interaction is able to mediate heterodimerisation between mDia1 and mDia2. J Biol Chem 282:30120-30130.

Copeland JW, Treisman R. (2002). “The diaphanous-related formin mDia1 controls serum response factor activity through its effects on actin polymerization”. Mol Biol Cell.13(11):4088-99.

Czuchra A, Wu X, Meyer H, van Hengel J, Schroeder T, Geffers R, Rottner K, Brakebusch C. (2005). “Cdc42 is not essential for filopodium formation, directed migration, cell polarization, and mitosis in fibroblastoid cells”. Mol Biol Cell.16(10):4473-84.

Dent EW, Kwiatkowski AV, Mebane LM, Philippar U, Barzik M, Rubinson DA, Gupton S, Van Veen JE, Furman C, Zhang J, Alberts AS, Mori S, Gertler FB. (2007). “Filopodia are required for cortical neurite initiation”. Nat Cell Biol. 9(12):1347-59.

DerMardirossian C, Bokoch GM. (2005). “GDIs: central regulatory molecules in Rho GTPase activation”. Trends Cell Biol. 15(7):356-63.

DerMardirossian C, Schnelzer A, Bokoch GM. (2004) “Phosphorylation of RhoGDI by Pak1 mediates dissociation of Rac GTPase”. Mol Cell.15(1):117-27.

Derivery E, Lombard B, Loew D, Gautreau A. (2009). “The Wave complex is intrinsically inactive”. Cell Motil Cytoskeleton. 66(10):777-90.

DeWard AD, Alberts AS. (2009). “Ubiquitin-mediated degradation of the formin mDia2 upon completion of cell division”. J Biol Chem. 284(30):20061-9.

Brandt DT, Marion S, Griffiths G, Watanabe T, Kaibuchi K, Grosse R. (2007) "Dia1 and IQGAP1 interact in cell migration and phagocytic cup formation**".** J Cell Biol.**,** 178 (2): 193–200.

dos Remedios CG, Chhabra D, Kekic M, Dedova IV, Tsubakihara M, Berry DA, Nosworthy NJ. (2003). "Actin binding proteins: regulation of cytoskeletal microfilaments". Physiol Rev. 83(2):433-73.

Dovas A, Couchman JR. (2005). "RhoGDI: multiple functions in the regulation of Rho family GTPase activities". Biochem J. 390(Pt 1):1-9.

Dvorsky R, Ahmadian MR. (2004) "Always look on the bright site of Rho: structural implications for a conserved intermolecular interface". EMBO Rep. 5(12):1130-6.

Eden S, Rohatgi R, Podtelejnikov AV, Mann M, Kirschner MW. (2002). "Mechanism of regulation of WAVE1-induced actin nucleation by Rac1 and Nck". Nature 418, 790–793.

Egile C, Rouiller I, Xu XP, Volkmann N, Li R, Hanein D. (2005). "Mechanism of filament nucleation and branch stability revealed by the structure of the Arp2/3-complex at actin branch junctions." PLoS Biol 3(11): e383.

Egile C, Loisel TP, Laurent V, Li R, Pantaloni D, Sansonetti PJ, Carlier MF.(1999). "Activation of the CDC42 effector N-WASP by the Shigella flexneri IcsA protein promotes actin nucleation by Arp2/3 complex and bacterial actin-based motility". J Cell Biol. 146(6):1319-32.

Eisenmann KM, West RA, Hildebrand D, Kitchen SM, Peng J, Sigler R, Zhang J, Siminovitch KA, Alberts AS. (2007). "T cell responses in mammalian diaphanous-related formin mDia1 knock-out mice". J Biol Chem.282(34):25152-8.

Ellis, S. and Mellor, H. (2000). "The novel Rho-family GTPase rif regulates coordinated actin-based membrane rearrangements". Curr Biol 10, 1387-90.

Esue O, Harris ES, Higgs HN, Wirtz D. (2008) "The filamentous actin cross-linking/bundling activity of mammalian formins". J Mol Biol. 384(2):324-34.

Evangelista, M., Pruyne, D., Amberg, D. C., Boone, C. & Bretscher, A. (2002). "Formins direct Arp2/3-independent actin filament assembly to polarize cell growth in yeast". Nature Cell Biol*.* 4: 32–41 .

Faix J, Breitsprecher D, Stradal TE, Rottner K. (2009) "Filopodia: Complex models for simple rods". Int J Biochem Cell Biol. 41(8-9):1656-64.

Faix J, Grosse R. (2006). "Staying in shape with formins." Dev. Cell 10: 693–706

Faix J, Rottner K. (2006). "The making of filopodia". Curr Opin Cell Biol.18(1):18-25.

Feig LA. (1999). "Tools of the trade: use of dominant-inhibitory mutants of Ras-family GTPases". Nat Cell Biol.1(2):E25-7.

Ferron F, Rebowski G, Lee SH, Dominguez R. (2007). "Structural basis for the recruitment of profilin-actin complexes during filament elongation by Ena/VASP". EMBO J. 26(21):4597-606.

Frischknecht F, Moreau V, Röttger S, Gonfloni S, Reckmann I, Superti-Furga G, Way M. (1999). "Actin-based motility of vaccinia virus mimics receptor tyrosine kinase signalling". Nature. 401(6756):926-9.

Galbraith CG, Yamada KM, Galbraith JA. (2007). "Polymerizing actin fibers position integrins primed to probe for adhesion sites". Science. 315, 992–995.

Gallo G, Letourneau PC. (2004). "Regulation of growth cone actin filaments by guidance cues". J. Neurobiol. 58, 92–102.

Gasteier JE, Madrid R, Krautkrämer E, Schröder S, Muranyi W, Benichou S, Fackler OT. (2003). “Activation of the Rac-binding partner FHOD1 induces actin stress fibers via a ROCK-dependent mechanism”. J Biol Chem. 278(40):38902-12.

Gautreau A, Ho HY, Li J, Steen H, Gygi SP, Kirschner MW. (2004). “Purification and architecture of the ubiquitous Wave complex“. Proc. Natl.Acad. Sci. USA 101, 4379–4383.

Gazman S., Kalaidzidis Y., Zerial M. (2003). “RhoD regulates endosome dynamics through Diaphanous-related Formin and Src tyrosine kinase”. Nature cell Biol. 5 (7):195-204

Gertler FB, Niebuhr K, Reinhard M, Wehland J, Soriano P. (1996). “Mena, a relative of VASP and Drosophila Enabled, is implicated in the control of microfilament dynamics”. Cell. 87(2):227-39.

Glacy SD. (1983). "Subcellular distribution of rhodamine-actin microinjected into living fibroblastic cells." J Cell Biol 97(4): 1207-13.

Goldschmidt-Clermont PJ, Furman MI, Wachsstock D, Safer D, Nachmias VT, Pollard TD. (1992). “The control of actin nucleotide exchange by thymosin b 4 and profilin. A potential regulatory mechanism for actin polymerization in cells”. Mol. Biol. Cell 3, 1015–1024

Goley ED, Welch MD. (2006). “The Arp2/3-complex: an actin nucleator comes of age”. Nat Rev Mol Cell Biol. 7(10):713-26.

Goley ED, Rodenbusch SE, Martin AC, Welch MD. (2004). “Critical conformational changes in the Arp2/3-complex are induced by nucleotide and nucleation promoting factor”. Mol Cell. 16(2):269-79.

Gomez TS, Kumar K, Medeiros RB, Shimizu Y, Leibson PJ, Billadeau DD (2007). “Formins regulate the actin-related protein 2/3 complex-independent polarization of the centrosome to the immunological synapse”. Immunity 26: 177–90.

Goode BL, Rodal AA, Barnes G, Drubin DG. (2001). „Activation of the Arp2/3-complex by the actin filament binding protein Abp1p”. J. Cell Biol. 153:627–34.

Goulimari P, Kitzing TM, Knieling H, Brandt DT, Offermanns S, Grosse R. (2005) “Galpha12/13 is essential for directed cell migration and localized Rho-Dia1 function”. J Biol Chem. 23;280(51):42242-51

Gupton, S. L. and F. B. Gertler (2007). "Filopodia: the fingers that do the walking." Sci STKE (400): re5.

Habas R, Kato Y, He X. (2001). “Wnt/Frizzled activation of Rho regulates vertebrate gastrulation and requires a novel Formin homology protein Daam1”. Cell. 107(7):843-54.

Hahne P, Sechi A, Benesch S, Small JV.(2001). “Scar/WAVE is localised at the tips of protruding lamellipodia in living cells”. FEBS Lett. 492(3):215-20.

Han, Y., Eppinger, E., Schuster, I.G., Weigand, L.U., Liang, X., Kremmer, E., Peschel, C. and Krackhardt, A.M. (2009). “Formin-like 1 (FMNL1) is regulated by N-terminal myristoylation and induces polarized membrane blebbing”. J Biol Chem. 284(48):33409-17

Harris ES, Rouiller I, Hanein D, Higgs HN.(2006a). “Mechanistic differences in actin bundling activity of two mammalian formins, FRL1 and mDia2”. J Biol Chem.;281(20):14383-92.

Harris ES, Higgs HN. (2006). “Biochemical analysis of mammalian formin effects on actin dynamics”. Methods Enzymol. 406:190-214.

Harris ES, Li F, Higgs HN. (2004). “The mouse formin, FRLalpha, slows actin filament barbed end elongation, competes with capping protein, accelerates polymerization from monomers, and severs filaments”. J Biol Chem. 279(19):20076-87.

Higashida C, Miyoshi T, Fujita A, Oceguera-Yanez F, Monypenny J, Andou Y, Narumiya S, Watanabe N. (2004). “Actin polymerization-driven molecular movement of mDia1 in living cells”. Science. 303(5666):2007-10.

Higgs HN, Pollard TD. (1999). "Regulation of actin polymerization by Arp2/3-complex and WASp/Scar proteins." J Biol Chem 274(46): 32531-4.

Higgs HN, Peterson KJ. (2005) “Phylogenetic analysis of the formin homology 2 domain”. Mol Biol Cell. 16(1):1-13

Ho HY, Rohatgi R, Lebensohn AM, Le Ma Li J, Gygi SP, Kirschner M. (2004). “Toca-1 mediates Cdc42-dependent actin nucleation by activating the N-WASP-WIP complex”. Cell 118, 203-216.

Homem CC, Peifer M. (2009). “Exploring the roles of diaphanous and enabled activity in shaping the balance between filopodia and lamellipodia”. Mol Biol Cell. 20(24):5138-55

Hotulainen P, Lappalainen P. (2006). “Stress fibers are generated by two distinct actin assembly mechanisms in motile cells”. J Cell Biol.173(3):383-94.

Hug C, Jay PY, Reddy I, McNally JG, Bridgman PC, Elson EL, Cooper JA. (1995). “Capping protein levels influence actin assembly and cell motility in *Dictyostelium*”. Cell 81:591–600.

Hüfner K, Higgs HN, Pollard TD, Jacobi C, Aepfelbacher M, Linder S. (2001). The verprolin-like central (VC) region of Wiskott- Aldrich syndrome protein induces Arp2/3-complex-dependent actin nucleation. J. Biol. Chem. 276:35761–67.

Huxley HE. (1963). “Electron microscope studies of the structure of natural and synthetic protein filaments from muscle”. J. Mol. Biol. 7 pp. 281–308.

Imamura H, Tanaka K, Hihara T, Umikawa M, Kamei T, Takahashi K, Sasaki T, Takai Y. (1997). “Bni1p and Bnr1p: downstream targets of the Rho family small G-proteins which interact with profilin and regulate actin cytoskeleton in saccharomyces cerevisiae”. EMBO J. 16, 2745–2755.

Ingram VM. (1969). “A side view of moving fibroblasts”. Nature. 222(5194):641-4.

Innocenti, M., Zucconi, A., Disanza, A., Frittoli, E., Areces, L.B., Steffen, A., Stradal, T.E., Di Fiore, P.P., Carlier, M.F. and Scita, G. (2004). “Abi1 is essential for the formation and activation of a WAVE2 signalling complex”. Nat Cell Biol 6: 319-327.

Ismail AM, Padrick SB, Chen B, Umetani J, Rosen MK. (2009). “The WAVE regulatory complex is inhibited”. Nat Struct Mol Biol. 16(5):561-3.

Iwasa JH, Mullins RD. (2007). “Spatial and temporal relationships between actin-filament nucleation, capping, and disassembly”. Curr Biol 17:395–406.

Izzard, C. S. and L. R. Lochner (1976). "Cell-to-substrate contacts in living fibroblasts: an interference reflexion study with an evaluation of the technique." J Cell Sci 21(1): 129-59.

Jaffe AB, Hall A. (2005). “Rho GTPases: biochemistry and biology”. Annu Rev Cell Dev Biol. 21:247-69.

Jarvik JW, Fisher GW, Shi C, Hennen L, Hauser C, Adler S, Berget PB. (2002). “In vivo functional proteomics: mammalian genome annotation using CD-tagging”. Biotechniques. 33(4):852-4, 856, 858-60 passim.

Kaiser DA, Vinson VK, Murphy DB, Pollard TD. (1999). “Profilin is predominantly associated with monomeric actin in Acanthamoeba”. J Cell Sci. 112 (Pt 21):3779-90.

Katoh, M. , Katoh M. (2003). “Identification and characterization of human FMNL1, FMNL2 and FMNL3 genes in silico”. Int J Oncol 22, 1161-1168.

Katoh H, Negishi M. (2003). “RhoG activates Rac1 by direct interaction with the Dock180-binding protein Elmo”. Nature. 2003 Jul 24;424(6947):461-4.

Kato, T., Watanabe, N., Morishima, Y., Fujita, A., Ishizaki, T. and Narumiya, S. (2001). “Localization of a mammalian homolog of diaphanous, mDia1, to the mitotic spindle in HeLa cells”. J. Cell Sci. 114, 775-784.

Keller PJ, Fiordalisi JJ, Berzat AC, Cox AD. (2005). “Visual monitoring of post-translational lipid modifications using EGFP-GTPase probes in live cells”. Methods. 37(2):131-37.

Kelleher, J. F., Atkinson, S. J. & Pollard, T. D. (1995). “Sequences, structural models, and cellular localization of the actin-related proteins Arp2 and Arp3 from *Acanthamoeba*”. J. Cell Biol. 131, 385–397.

Kim Y, Sung JY, Ceglia I, Lee KW, Ahn JH, Halford JM, Kim AM, Kwak SP, Park JB, Ho Ryu S, Schenck A, Bardoni B, Scott JD,Nairn AC, Greengard P. (2006). “Phosphorylation of WAVE1 regulates actin polymerization and dendritic spine morphology”. Nature 442(7104):814–817.

Kim AS, Kakalis LT, Abdul-Manan N, Liu GA, Rosen, M. K. (2000). Autoinhibition and activation mechanisms of the Wiskott-Aldrich syndrome protein. Nature .404, 151-158.

Kimura K, Ito M, Amano M, Chihara K, Fukata Y, Nakafuku M, Yamamori B, Feng J, Nakano T, Okawa K, Iwamatsu A, Kaibuchi K. (1996). “Regulation of myosin phosphatase by Rho and Rho-associated kinase (Rho-kinase)“. Science. 273(5272):245-8.

Kirschner MW. (1980). "Implications of treadmilling for the stability and polarity of actin and tubulin polymers in vivo." J Cell Biol 86(1): 330-4.

Kitzing TM, Sahadevan AS, Brandt DT, Knieling H, Hannemann S, Fackler OT, Grosshans J, Grosse R. (2007). “Positive feedback between Dia1, LARG, and RhoA regulates cell morphology and invasion”. Genes Dev.21(12):1478-83.

Kopecki Z., Luchetti M. M., Adams D. H., Strudwick X., Mantamadiotis T., Stoppacciaro A., Gabrielli A., Ramsay R. G., Cowin A. J. (2007). “Collagen loss and impaired wound healing is associated with c-Myb deficiency”. J. Pathol. 211:351–361.

Koestler SA, Auinger S, Vinzenz M, Rottner K, Small JV. (2008). "Differentially oriented populations of actin filaments generated in lamellipodia collaborate in pushing and pausing at the cell front." Nat Cell Biol. 10(3): 306-13.

Koka S, Neudauer CL, Li X, Lewis RE, McCarthy JB, Westendorf JJ. (2003) “The formin-homology-domain-containing protein FHOD1 enhances cell migration”. J Cell Sci 116: 1745–1755.

Korn ED, Carlier MF, Pantaloni D. (1987). "Actin polymerization and ATP hydrolysis." Science 238(4827): 638-44.

Korobova F, Svitkina T. (2008). “Arp2/3-complex is important for filopodia formation, growth cone motility, and neuritogenesis in neuronal cells”. Mol Biol Cell 19:1561–74.

Kovar DR. (2006). “Cell polarity: formin on the move”. Curr Biol. 16(14):R535-8.

Kovar DR, Harris ES, Mahaffy R, Higgs HN, Pollard TD. (2006). “Control of the assembly of ATP- and ADP-actin by formins and profilin”. Cell 124:423–435.

Kovar DR, Pollard TD. (2004). “Insertional assembly of actin filament barbed ends in association with formins produces piconewton forces”. Proc Natl Acad Sci USA 01:14725–14730.

Kovar DR, Kuhn JR, Tichy AL, Pollard TD. (2003). “The fission yeast cytokinesis formin Cdc12p is a barbed end actin filament capping protein gated by profiling”. J Cell Biol 61:875– 887.

Krause M, Dent EW, Bear JE, Loureiro JJ, Gertler FB. (2003). “Ena/VASP proteins: regulators of the actin cytoskeleton and cell migration”. Annu Rev Cell Dev Biol. 19:541-64.

Kunda P, Craig G, Dominguez V, Baum B. (2003). “Abi, Sra1, and Kette control the stability and localization of SCAR/WAVE to regulate the formation of actin-based protrusions”. Curr Biol. 13(21):1867-75.

Kursula P, Kursula I, Massimi M, Song YH, Downer J, Stanley WA, Witke W, Wilmanns M. (2008). “High-resolution structural analysis of mammalian profilin 2a complex formation with two physiological ligands: the formin homology 1 domain of mDia1 and the proline-rich domain of VASP”. J Mol Biol. 375(1):270-90.

Kwiatkowski AV, Rubinson DA, Dent EW, Edward van Veen J, Leslie JD, Zhang J, Mebane LM, Philippar U, Pinheiro EM, Burds AA, Bronson RT, Mori S, Fässler R, Gertler FB. (2007). “Ena/VASP Is Required for neuritogenesis in the developing cortex”.Neuron. 56(3):441-55.

Ladwein M, Rottner K. (2008). “On the Rho'd: the regulation of membrane protrusions by Rho-GTPases”. FEBS Lett. 582(14):2066-74.

Laemmli UK. (1970). "Cleavage of structural proteins during the assembly of the head of bacteriophage T4." Nature 227(5259): 680-5.

Lai FP, Szczodrak M, Block J, Faix J, Breitsprecher D, Mannherz HG, Stradal TE, Dunn GA, Small JV, Rottner K. (2008). "Arp2/3-complex interactions and actin network turnover in lamellipodia." EMBO J 27(7): 982-92.

Lammers M, Meyer S, Kühlmann D, Wittinghofer A. (2008) “Specificity of interactions between mDia isoforms and Rho proteins”. J Biol Chem. 283(50):35236-46.

Lammers M, Rose R, Scrima A, Wittinghofer A. (2005). “The regulation of mDia1 by autoinhibition and its release by Rho*GTP”. EMBO J. 24(23):4176-87.

Laurent V, Loisel TP, Harbeck B, Wehman A, Gröbe L, Jockusch BM, Wehland J, Gertler FB, Carlier MF. (1999). “Role of proteins of the Ena/VASP family in actin-based motility of Listeria monocytogenes”. J Cell Biol. 144(6):1245-58.

Lebensohn AM, Kirschner MW. (2009). “Activation of the WAVE complex by coincident signals controls actin assembly”. Mol Cell. 36(3):512-24.

LeClaire LL 3rd, Baumgartner M, Iwasa JH, Mullins RD, Barber DL. (2008). “Phosphorylation of the Arp2/3-complex is necessary to nucleate actin filaments”. J Cell Biol. 182(4):647-54.

Lewis WH, Lewis MR. (1924) “Behavior of cells in tissue cultures”.General Cytology (ed. by E.V. Cowdry), pp. 385–447. The University of Chicago Press, Chicago, IL.

Li F, Higgs HN. (2003). The mouse Formin mDia1 is a potent actin nucleation factor regulated by autoinhibition. Curr. Biol. 13, 1335–1340.

Linardopoulou EV, Parghi SS, Friedman C, Osborn GE, Parkhurst SM, Trask BJ. (2007). “Human subtelomeric WASH genes encode a new subclass of the WASP family”. PLoS Genet. 3(12):e237.

Linder S, Hufner K, Wintergerst U, Aepfelbacher M. (2000). „Microtubule-dependent formation of podosomal adhesion structures in primary human macrophages". J Cell Sci .113 Pt 23, 4165-76.

Lizárraga F, Poincloux R, Romao M, Montagnac G, Le Dez G, Bonne I, Rigaill G, Raposo G, Chavrier P. (2009). "Diaphanous-related formins are required for invadopodia formation and invasion of breast tumor cells". Cancer Res. 69(7):2792-800.

Loisel TP, Boujemaa R, Pantaloni D, Carlier MF. (1999). "Reconstitution of actin-based motility of Listeria and Shigella using pure proteins". Nature. 401:613-6.

Lommel S, Benesch S, Rohde M, Wehland J, Rottner K. (2004). "Enterohaemorrhagic and enteropathogenic Escherichia coli use different mechanisms for actin pedestal formation that converge on N-WASP". Cell Microbiol. 6(3):243-54.

Lommel S, Benesch S, Rottner K, Franz T, Wehland J, Kuhn R. (2001). "Actin pedestal formation by enteropathogenic Escherichia coli and intracellular motility of Shigella flexneri are abolished in N-WASP-defective cells". EMBO Rep 2, 850-857.

Machesky LM, Mullins RD, Higgs HN, Kaiser DA, Blanchoin L, May RC, Hall ME, Pollard TD. (1999). "Scar, a WASp-related protein, activates nucleation of actin filaments by the Arp2/3-complex". Proc Natl Acad Sci U S A. 96(7):3739-44.

Machesky LM, Atkinson SJ, Ampe C, Vandekerckhove J, Pollard TD. (1994). "Purification of a cortical complex containing two unconventional actins from *Acanthamoeba* by affinity chromatography on profilin-agarose". J. Cell Biol. 127, 107–115.

Mahoney NM, Rozwarski DA, Fedorov E, Fedorov AA, Almo SC. (1999). "Profilin binds proline-rich ligands in two distinct amide backbone orientations". Nat Struct Biol. 6(7):666-71.

Mahoney NM, Janmey PA, Almo SC. (1997). "Structure of the profilin-poly-L-proline complex involved in morphogenesis and cytoskeletal regulation". Nat Struct Biol.4(11):953-60. Erratum in: Nat Struct Biol 4(12):1047.

Marchand JB, Kaiser DA, Pollard TD, Higgs HN. (2001). "Interaction of WASP/Scar proteins with actin and vertebrate Arp2/3-complex". Nat. Cell Biol. 3:76–82

Martin SG, Rincón SA, Basu R, Pérez P, Chang F. (2007). "Regulation of the formin for3p by cdc42p and bud6p". Mol Biol Cell. 18(10):4155-67

Martin SG, Chang F. (2006). "Dynamics of the formin for3p in actin cable assembly". Curr. Biol. 16, 1161–1170

Martinez-Quiles N, Rohatgi R, Antón IM, Medina M, Saville SP, Miki H, Yamaguchi H, Takenawa T, Hartwig JH, Geha RS, Ramesh N. (2001). "WIP regulates N-WASP-mediated actin polymerization and filopodium formation". Nat Cell Biol. 3(5):484-91.

Matusek T, Gombos R, Szécsényi A, Sánchez-Soriano N, Czibula A, Pataki C, Gedai A, Prokop A, Raskó I, Mihály J. (2008). "Formin proteins of the DAAM subfamily play a role during axon growth". J Neurosci. 28(49):13310-9.

Maurer-Stroh S, Eisenhaber B, Eisenhaber F. (2002). N-terminal N-myristoylation of proteins: prediction of substrate proteins from amino acid sequence. J Mol Biol 317**,** 541-557.

Mejillano MR, Kojima S, Applewhite DA, Gertler FB, Svitkina TM, Borisy GG. (2004). "Lamellipodial versus filopodial mode of the actin nanomachinery; pivotal role of the filament barbed end". Cell 3:363–373.

Maekawa M, Ishizaki T, Boku S, Watanabe N, Fujita A, Iwamatsu A,Obinata T, Ohashi, K, Mizuno K, Narumiya S. (1999). “Signaling from Rho tothe actin cytoskeleton through protein kinases ROCK and LIM-kinase”. Science 285,895-8.

Millard TH, Behrendt B, Launay S, Fütterer K, Machesky LM. (2002). “Identification and characterisation of a novel human isoform of Arp2/3-complex subunit p16-ARC/ARPC5”. Cell Motil Cytoskeleton.54(1):81-90.

Mullins RD, Heuser JA, Pollard TD. (1998). “The interaction of Arp2/3-complex with actin: nucleation, high affinity pointed end capping, and formation of branching networks of actin filaments”. Proc. Natl Acad. Sci. USA 95, 6181–6186.

Mockrin SC, Korn ED. (1980). “Acanthamoeba profilin interacts with G-actin to increase the rate of exchange of actin-bound adenosine 50-triphosphate”. Biochemistry 19, 5359–5362.

Monypenny J, Zicha D, Higashida C, Oceguera-Yanez F, Narumiya S, Watanabe N. (2009). “Cdc42 and Rac family GTPases regulate mode and speed but not direction of primary fibroblast migration during platelet-derived growth factor-dependent chemotaxis”. Mol Cell Biol. 29(10):2730-47.

Moseley JB, Maiti S, Goode BL. (2006). “Formin proteins: purification and measurement of effects on actin assembly”. Methods Enzymol. 406:215-34.

Neidt EM, Scott BJ, Kovar DR. (2009). “Formin differentially utilizes profilin isoforms to rapidly assemble actin filaments”. J Biol Chem. 284(1):673-84.

Nemethova M, Auinger S, Small JV. (2008). “Building the actin cytoskeleton: filopodia contribute to the construction of contractile bundles in the lamella”. J Cell Biol. 180(6):1233-44.

Neumann-Giesen C, Falkenbach B, Beicht P, Claasen S, Lüers G, Stuermer CA, Herzog V, Tikkanen R. (2004). “Membrane and raft association of reggie-1/flotillin-2: role of myristoylation, palmitoylation and oligomerization and induction of filopodia by over-expression”. Biochem J. 378(Pt 2):509-18.

Nezami AG, Poy F, Eck MJ. (2006). “Structure of the autoinhibitory switch in formin mDia1”. Structure. 14(2):257-63.

Nicholson-Dykstra SM, Higgs HN. (2009) ”Arp2 Depletion Inhibits Sheet-Like Protrusions but not Linear Protrusions of Fibroblasts and Lymphocytes”. Cell Motil Cytoskeleton. 65(11):904-22.

Nobes CD and Hall A (1999). “Rho-GTPase control polarity, protrusion, and adhesion during cell movement”. J. Cell Biol. 144, 1235–1244.

Nobes CD and Hall A. (1995). "Rho, rac, and cdc42 GTPases regulate the assembly of multimolecular focal complexes associated with actin stress fibers, lamellipodia, and filopodia". Cell 81(1): 53-62.

Nolen BJ, Littlefield RS, Pollard TD. (2004). “Crystal structures of actin-related protein 2/3 complex with bound ATP or ADP”. Proc. Natl Acad. Sci. USA 101, 15627–15632.

Ohta Y, Hartwig JH, Stossel TP. (2006). “FilGAP, a Rho- and ROCK-regulated GAP for Rac binds filamin A to control actin remodelling”. Nat Cell Biol. 8(8):803-14.

Otomo T, Otomo C, Tomchick DR, Machius M, Rosen MK. (2005). “Structural basis of Rho GTPase-mediated activation of the formin mDia1”. Mol Cell. 18(3):273-81.

Otomo T, Tomchick DR, Otomo C, Panchal SC, Machius M, Rosen MK. (2005b). “Structural basis of actin filament nucleation and processive capping by a formin homology 2 domain”. Nature. 433:488–494.

Ozaki-Kuroda K, Yamamoto Y, Nohara H, Kinoshita M, Fujiwara T, Irie K, Takai Y. (2001). “Dynamic localization and function of Bni1p at the sites of directed growth in Saccharomyces cerevisiae”. Mol Cell Biol. 21(3):827-39.

Padrick SB, Cheng HC, Ismail AM, Panchal SC, Doolittle LK, Kim S, Skehan BM, Umetani J, Brautigam CA, Leong JM, Rosen MK. (2008). “Hierarchical regulation of WASP/WAVE proteins”. Mol Cell. 32(3):426-38.

Pallari HM, Eriksson JE. (2006). “Intermediate filaments as signaling platforms”. Sci STKE. (366):pe53.

Pankov R, Endo Y, Even-Ram S, Araki M, Clark K, Cukierman E, Matsumoto K, Yamada KM. (2005). “A Rac switch regulates random versus directionally persistent cell migration”. J. Cell Biol.170:793–802.

Pantaloni D, Le Clainche C, Carlier MF. (2001). "Mechanism of actin-based motility". Science 292(5521): 1502-6.

Paul AS, Pollard TD. (2009). “Review of the mechanism of processive actin filament elongation by formins”. Cell Motil Cytoskeleton.66(8):606-17.

Paul AS, Pollard TD. (2008). “The role of the FH1 domain and profilin in formin-mediated actin-filament elongation and nucleation”. Curr Biol.18(1):9-19.

Pechlivanis M, Samol A, Kerkhoff E. (2009). “Identification of a short Spir interaction sequence at the C-terminal end of formin subgroup proteins”. J Biol Chem. 284(37):25324-33

Pellegrin S, Mellor H. (2005). “The Rho family GTPase Rif induces filopodia through mDia2”. Curr Biol. 15(2):129-33.

Peng J, Wallar BJ, Flanders A, Swiatek PJ, Alberts AS. (2003). ”Disruption of the Diaphanous-related formin Drf1 gene encoding mDia1 reveals a role for Drf3 as an effector for Cdc42”. Curr Biol.13(7):534-45.

Perez M, Greenwald DL, de la Torre JC. (2004). “Myristoylation of the RING finger Z protein is essential for arenavirus budding”. J Virol. 78(20):11443-8.

Petersen J, Nielsen O, Egel R, Hagan IM. (1998). “FH3, a domain found in formins, targets the fission yeast formin Fus1 to the projection tip during conjugation”. J. Cell Biol. 141, 1217-1228.

Petrella EC, Machesky LM, Kaiser DA, Pollard TD. (1996). “Structural requirements and thermodynamics of the interaction of proline peptides with profilin”. Biochemistry. 35(51):16535-43.

Pollard TD, Blanchoin L, Mullins RD. (2000). “Molecular mechanisms controlling actin filament dynamics in nonmuscle cells”. Annu Rev Biophys Biomol Struct. 29:545-76.

Pollard TD. (1986). "Rate constants for the reactions of ATP- and ADP-actin with the ends of actin filaments". J Cell Biol. 103(6 Pt 2): 2747-54.

Pollard TD, Cooper JA. (1984). “Quantitative analysis of the effect of Acanthamoeba profilin on actin filament nucleation and elongation”. Biochemistry. 23(26):6631-41.

Prehoda KE, Lee DJ, Lim WA. (2000). “Integration of multiple signals through cooperative regulation of the N-WASP-Arp2/3-complex” . Science. 290(5492):801-6.

Pritchard CA, Hayes L, Wojnowski L, Zimmer A, Marais RM and Norman JC. (2004). “B-Raf acts via the ROCKII/LIMK/cofilin pathway to maintain actin stress fibers in fibroblasts”. Mol Cell Biol 24, 5937-52.

Pruyne D, Evangelista M, Yang C, Bi E, Zigmond S, Bretscher A, Boone C. (2002). “Role of formins in actin assembly: nucleation and barbed-end association”. Science. 297(5581):612-5.

Quinlan ME, Hilgert S, Bedrossian A, Mullins RD, Kerkhoff E. (2007). "Regulatory interactions between two actin nucleators, Spire and Cappuccino". J Cell Biol. 179(1):117-28.

Quinlan ME, Heuser JE, Kerkhoff E, Mullins RD. (2005). "Drosophila Spire is an actin nucleation factor". Nature. 433(7024):382-8.

Raftopoulou M and Hall A. (2004). "Cell migration: Rho GTPases lead the way". Dev Biol 265, 23-32.

Ramesh N, Antón IM, Hartwig JH and Geha RS. (1997). "WIP, a protein associated with wiskott-aldrich syndrome protein, induces actin polymerization and redistribution in lymphoid cells". Proc. Natl. Acad. Sci. USA .94, 14671-14676.

Reinhard M, Halbrügge M, Scheer U, Wiegand C, Jockusch BM, Walter U. (1992). "The 46/50 kDa phosphoprotein VASP purified from human platelets is a novel protein associated with actin filaments and focal contacts". EMBO J.11(6):2063-70.

Resh MD. (1999). "Fatty acylation of proteins: new insights into membrane targeting of myristoylated and palmitoylated proteins". Biochim Biophys Acta. 1451(1):1-16.

Resh MD. (2006). "Trafficking and signaling by fatty-acylated and prenylated proteins". Nat Chem Biol 2, 584-590.

Ridley AJ. (2006). "Rho-GTPase and actin dynamics in membrane protrusions and vesicle trafficking". Trends Cell Biol. 16(10):522-9.

Ridley AJ. (2001). "Rho GTPases and cell migration". J Cell Sci. 114(Pt 15):2713-22.

Ridley AJ, Paterson HF, Johnston CL, Diekmann D, Hall A. (1992). "The small GTP-binding protein rac regulates growth factor-induced membrane ruffling". Cell 70**,** 401-410.

Rivero F, Muramoto T, Meyer AK, Urushihara H, Uyeda TQ, Kitayama C. (2005) "A comparative sequence analysis reveals a common GBD/FH3-FH1-FH2-DAD architecture in formins from Dictyostelium, fungi and metazoan". BMC Genomics. 6(1):28.

Robinson RC, Turbedsky K, Kaiser DA, Marchand JB, Higgs HN, Choe S, Pollard TD. (2001). "Crystal structure of Arp2/3-complex". Science*.* 294:1679-1684

Rodal AA, Sokolova O, Robins DB, Daugherty KM, Hippenmeyer S, Riezman H, Grigorieff N, Goode BL. (2005). "Conformational changes in the Arp2/3-complex leading to actin nucleation". Nat Struct Mol Biol. 12(1):26-31.

Rohatgi R, Ma L, Miki H, Lopez M, Kirchhausen T, Takenawa T, Kirschner MW. (1999). "The interaction between N-WASP and the Arp 2/3 complex links Cdc42-dependent signals to actin assembly". Cell 97: 221-231.

Romero S, Le Clainche C, Didry D, Egile C, Pantaloni D, Carlier MF. (2004). "Formin is a processive motor that requires profilin to accelerate actin assembly and associated ATP hydrolysis". Cell 119:419–429.

Rose R, Wittinghofer A, Weyand M. (2005a). "The purification and crystallization of mDia1 in complex with RhoC". Acta Crystallogr Sect F Struct Biol Cryst Commun. 61(Pt 2):225-7.

Rose R, Weyand M, Lammers M, Ishizaki T, Ahmadian MR, Wittinghofer A. (2005b). "Structural and mechanistic insights into the interaction between Rho and mammalian Dia". Nature. 26;435(7041): 513-8

Rossman KL, Der CJ, Sondek J. (2005). "GEF means go: turning on RHO GTPases with guanine nucleotide-exchange factors". Nat Rev Mol Cell Biol 6, 167-80.

Rottner K, Behrendt B, Small JV, Wehland J. (1999a). “VASP dynamics during lamellipodia protrusion”. Nat Cell Biol. 1(5):321-2.

Rottner K, Hall A, Small JV.(1999b). “Interplay between Rac and Rho in the control of substrate contact dynamics”. Curr Biol.9(12):640-8.

Sagot I, Rodal AA, Moseley J, Goode BL, Pellman D. (2002a). “An actin nucleation mechanism mediated by Bni1 and profilin”. Nat Cell Biol. 4(8):626-31.

Sagot I, Klee SK, Pellman D. (2002b). “Yeast formins regulate cell polarity by controlling the assembly of actin cables”. Nat Cell Biol. 4(1):42-50.

Sarmiento C, Wang W, Dovas A, Yamaguchi H, Sidani M, El-Sibai M, Desmarais V, Holman HA, Kitchen S, Backer JM, Alberts A, Condeelis J. (2008). “WASP family members and formin proteins coordinate regulation of cell protrusions in carcinoma cells”. J Cell Biol. 180(6):1245-60.

Satoh S, Tominaga T. (2001). “mDia-interacting protein acts downstream of Rho-mDia and modifies Src activation and stress fiber formation”. J Biol Chem. 276(42):39290-4

Schirenbeck A, Arasada R, Bretschneider T, Stradal TE, Schleicher M, Faix J. (2006). “The bundling activity of vasodilator-stimulated phosphoprotein is required for filopodium formation”. Proc Natl Acad Sci U S A. 103(20):7694-9.

Schirenbeck A, Bretschneider T, Arasada R, Schleicher M, Faix J. (2005). “The Diaphanous-related formin dDia2 is required for the formation and maintenance of filopodia”. Nat. Cell Biol. 7: 619– 625.

Schumacher N, Borawski JM, Leberfinger CB, Gessler M, Kerkhoff E. (2004). “Overlapping expression pattern of the actin organizers Spir-1 and formin-2 in the developing mouse nervous system and the adult brain”. Gene Expr Patterns. 4(3):249-55.

Seth A, Otomo C, Rosen MK. (2006) “Autoinhibition regulates cellular localization and actin assembly activity of the diaphanous related formins FRLalpha and mDia1”. J. Cell Biol. 174: 701–713.

Sharpless KE, Harris SD. (2002). “Functional characterization and localization of the Aspergillus nidulans formin SEPA”. Mol. Biol. Cell 13, 469-479.

Shimada A, Nyitrai M, Vetter IR, Kühlmann D, Bugyi B, Narumiya S, Geeves MA, Wittinghofer A. (2004). “The core FH2 domain of diaphanous-related formins is an elongated actin binding protein that inhibits polymerization”. Mol Cell. 13(4):511-22.

Skoble J, Portnoy DA, Welch MD. (2000). “Three regions within ActA promote Arp2/3-complex-mediated actin nucleation and *Listeria monocytogenes* motility”. J. Cell Biol. 150:527–38.

Small JV, Auinger S, Nemethova M, Koestler S, Goldie KN, Hoenger A, Resch GP. (2008). "Unravelling the structure of the lamellipodium." J Microsc 231(3): 479-85.

Small JV, Isenberg G, Celis JE (1978). “Polarity of actin at the leading edge of cultured cells”. Nature 272: 638–639.

Snapper SB, Takeshima F, Anton I, Liu CH, Thomas SM, Nguyen D, Dudley D, Fraser H, Purich D, Lopez-Ilasaca M, Klein C, Davidson L, Bronson R, Mulligan RC, Southwick F, Geha R, Goldberg MB, Rosen FS, Hartwig JH, Alt FW. (2001). “N-WASP deficiency reveals distinct pathways for cell surface projections and microbial actin-based motility”. Nat Cell Biol 3, 897-904.

Steffen A, Faix J, Resch GP, Linkner J, Wehland J, Small JV, Rottner K, Stradal TE. (2006). “Filopodia formation in the absence of functional WAVE- and Arp2/3-complexes”. Mol Biol Cell 17**:** 2581-2591.

Steffen A, Rottner K, Ehinger J, Innocenti M, Scita G, Wehland J, Stradal TE. (2004) “Sra-1 and Nap1 link Rac to actin assembly driving lamellipodia formation”. EMBO J. 23: 749–759.

Stradal TE, Rottner K, Disanza A, Confalonieri S, Innocenti M, Scita G. (2004). “Regulation of actin dynamics by WASP and WAVE family proteins”. Trends Cell Biol.14(6):303-11

Stradal TE, Courtney KD, Rottner K, Hahne P, Small JV, Pendergast AM. (2001). “The Abl interactor proteins localize to sites of actin polymerization at the tips of lamellipodia and filopodia”. Curr.Biol. 11: 891–895.

Svitkina TM, Bulanova EA, Chaga OY, Vignjevic DM, Kojima S, Vasiliev JM, Borisy GG. (2003).”Mechanism of filopodia initiation by reorganization of a dendritic network”. J Cell Biol. 160(3):409-21

Svitkina TM, Borisy GG. (1999). "Arp2/3-complex and actin depolymerizing factor/cofilin in dendritic organization and treadmilling of actin filament array in lamellipodia". J Cell Biol 145(5): 1009-26.

Swan KA, Severson AF, Carter JC, Martin PR, Schnabel H, Schnabel R, Bowerman B. (1998). “cyk-1: a C. elegans FH gene required for a late step in embryonic cytokinesis”. J. Cell Sci. 111, 2017–2027.

Swierczynski SL, Blackshear PJ. (1996). “Myristoylation-dependent and electrostatic interactions exert independent effects on the membrane association of the myristoylated alanine-rich protein kinase C substrate protein in intact cells”. J Biol Chem 271:23424–23430.

Takenawa T, Miki H. (2001). “WASP and WAVE family proteins: key molecules for rapid rearrangement of cortical actin filaments and cell movement”. J Cell Sci 114, 1801-9.

Takeya R, Taniguchi K, Narumiya S, Sumimoto H. (2008). “The mammalian formin FHOD1 is activated through phosphorylation by ROCK and mediates thrombin-induced stress fibre formation in endothelial cells”. EMBO J. 27(4):618-28.

Tang BL, Teng FYH. (2004). “Concepts of protein sorting or targeting signals and membrane topology in undergraduate teaching”. Biochem Mol Biol Educ. 33:188-193

Taniguchi K, Takeya R, Suetsugu S, Kan-O M, Narusawa M, Shiose A, Tominaga R, Sumimoto H. (2009). ”Mammalian formin fhod3 regulates actin assembly and sarcomere organization in striated muscles”. J Biol Chem. 284(43):29873-81.

Tarasova NI, Stauber RH, Choi JK, Hudson EA, Czerwinski G, Miller JL, Pavlakis GN, Michejda CJ, Wank SA. (1997). "Visualization of G protein-coupled receptor trafficking with the aid of the green fluorescent protein. Endocytosis and recycling of cholecystokinin receptor type A". J Biol Chem 272(23): 14817-24.

Tominaga T, Sahai E, Chardin P, McCormick F, Courtneidge SA, Alberts AS. (2000) “Diaphanous-related formins bridge Rho GTPase and Src tyrosine kinase signaling“. Mol. Cell 5: 13–25.

Trichet L, Sykes C, Plastino J. (2008). “Relaxing the actin cytoskeleton for adhesion and movement with Ena/VASP”. J Cell Biol. 181(1):19-25.

Uetz P, Fumagalli S, James D, Zeller R. (1996). “Molecular interaction between limb deformity proteins (formins) and Src family kinases”. J Biol Chem. 271(52):33525-30.

Uruno T, Liu J, Zhang P, Fan Yx, Egile C, Li R, Mueller SC, Zhan X. (2001). “Activation of Arp2/3-complex mediated actin polymerization by cortactin”. Nat. Cell Biol. 3:259–66.

Vaillant DC, Copeland SJ, Davis C, Thurston SF, Abdennur N, Copeland JW. (2008). “Interaction of the N- and C-terminal autoregulatory domains of FRL2 does not inhibit FRL2 activity”. J Biol Chem. 283(48):33750-62.

Vallen EA, Caviston J, Bi E. (2000). “Roles of Hof1p, Bni1p, Bnr1p, and Myo1p in cytokinesis in Saccharomyces cerevisiae”. Mol. Biol. Cell 11**,** 593–611.

Van Troys M, Huyck L, Leyman S, Dhaese S, Vandekerkhove J, Ampe C (2008). “Ins and outs of ADF/cofilin activity and regulation”. Eur J Cell Biol. 87(8-9):649-67.

Vasioukhin V, Bauer C, Yin M, Fuchs E (2000). ”Directed actin polymerization is the driving force for epithelial cell–cell adhesion”. Cell 100, 209–219.

Vavylonis D, Kovar DR, O’Shaughnessy B, Pollard TD. (2006). “Model of formin-associated actin filament elongation”. Mol. Cell 21, 455–466.

Vignjevic D, Kojima S, Aratyn Y, Danciu O, Svitkina T, Borisy GG. (2006). ”Role of fascin in filopodial protrusion”. J Cell Biol. 174(6):863-75.

Wade RH, Hyman AA.(1997). “Microtubule structure and dynamics”. Curr Opin Cell Biol. 9(1):12-7.

Wallar BJ, Stropich BN, Schoenherr JA, Holman HA, Kitchen SM, Alberts AS. (2006) “The basic region of the diaphanous-autoregulatory domain (DAD) is required for autoregulatory interactions with the diaphanous-related formin inhibitory domain”. J Biol Chem. 281(7):4300-7.

Wang YL. (1985). “Exchange of actin subunits at the leading edge of living fibroblasts: possible role of treadmilling”. J. Cell Biol. *101*, 597–602.

Watanabe S, Ando Y, Yasuda S, Hosoya H, Watanabe N, Ishizaki T, Narumiya S.(2008). “mDia2 induces the actin scaffold for the contractile ring and stabilizes its position during cytokinesis in NIH 3T3 cells”. Mol Biol Cell. 19(5):2328-38.

Watanabe N, Kato T, Fujita A, Ishizaki T, Narumiya S. (1999). “Cooperation between mDia1 and ROCK in Rho-induced actin reorganization”. Nature Cell Biol. 1, 136–-143.

Watanabe N, Madaule P, Reid T, Ishizaki T, Watanabe G, Kakizuka A, Saito Y, Nakao K, Jockusch BM, Narumiya S. (1997). “p140mDia, a mammalian homolog of *Drosophila* diaphanous, is a target protein for Rho small GTPase and is a ligand for profilin”. EMBO J. 16: 3044– 3056.

Weaver AM, Karginov AV, Kinley AW, Weed SA, Li Y, Parsons JT, Cooper JA. (2001). “Cortactin promotes and stabilizes Arp2/3-induced actin filament network formation”. Curr. Biol. 11:370–74.

Weaver AM, Heuser JE, Karginov AV, Lee WL, Parsons JT, Cooper JA. (2002). "Interaction of cortactin and N-WASp with Arp2/3-complex". Curr Biol 12(15): 1270-8.

Wegner A. (1977). "The mechanism of ATP hydrolysis by polymer actin". Biophys Chem 7(1): 51-8.

Wegner A. (1976). "Head to tail polymerization of actin". J Mol Biol 108(1): 139-50.

Welch MD, Iwamatsu A, Mitchison TJ. (1997). "Actin polymerization is induced by Arp2/3 protein complex at the surface of Listeria monocytogenes". Nature 385(6613): 265-9.

Wheeler AP, Wells CM, Smith SD, Vega FM, Henderson RB, Tybulewicz VL, Ridley AJ. (2006). “Rac1 and Rac2 regulate macrophage morphology but are not essential for migration”. J Cell Sci. 119(Pt 13):2749-57

Wiesner, S., E. Helfer, D. Didry, G. Ducouret, F. Lafuma, M.F. Carlier, and D. Pantaloni. (2003). “A biomimetic motility assay provides insight into the mechanism of actin-based motility”. J Cell Biol. 160:387-98.

Westendorf, J. J. (2001). “The Formin/Diaphanous-related protein, FHOS, interacts with Rac1 and activates transcription from the serum response element”. J. Biol. Chem. 276, 46453-46459.

Winter D, Lechler T, Li R. (1999). “Activation of the yeast Arp2/3-complex by Bee1p, a WASP-family protein”. Curr Biol. 9(9):501-4.

Wood W, Jacinto A, Grose R, Woolner S, Gale J, Wilson C, Martin P. (2002). “Wound healing recapitulates morphogenesis in Drosophila embryos”. Nat Cell Biol. 4(11):907-12.

Woychik RP, Maas RL, Zeller R, Vogt TF, Leder P. (1990). “'Formins': proteins deduced from the alternative transcripts of the limb deformity gene”. Nature. 346(6287):850-3.

Wu YI, Frey D, Lungu OI, Jaehrig A, Schlichting I, Kuhlman B, Hahn KM. (2009). “A genetically encoded photoactivatable Rac controls the motility of living cells”. Nature. 461(7260):104-8.

Xu Y, Moseley JB, Sagot I, Poy F, Pellman D, Goode BL, Eck MJ. (2004). ”Crystal structures of a formin homology-2 domain reveal a tethered dimer architecture”. Cell 116:711–723.

Yamana N, Arakawa Y, Nishino T, Kurokawa K, Tanji M, Itoh RE, Monypenny J, Ishizaki T, Bito H, Nozaki K, Hashimoto N, Matsuda M, Narumiya S. (2006). “The Rho-mDia1 pathway regulates cell polarity and focal adhesion turnover in migrating cells through mobilizing Apc and c-Src”. Mol Cell Biol. 26(18):6844-58.

Yamashita M, Higashi T, Suetsugu S, Sato Y, Ikeda T, Shirakawa R, Kita T, Takenawa T, Horiuchi H, Fukai S, Nureki O. (2007). “Crystal structure of human DAAM1 formin homology 2 domain”. Genes Cells.12(11):1255-65.

Yamashita A, Maéda K, Maéda Y. (2003). “Crystal structure of CapZ: Structural basis for actin filament barbed end capping”. EMBO J 7:1529–1538.

Yang C, Czech L, Gerboth S, Kojima S, Scita G, Svitkina T. (2007). “Novel roles of formin mDia2 in lamellipodia and filopodia formation in motile cells”. PLoS Biol. 5(11), e317.

Yarar D, To W, Abo A, Welch MD.(1999). “The Wiskott-Aldrich syndrome protein directs actin-based motility by stimulating actin nucleation with the Arp2/3-complex”. Curr Biol. 9(10):555-8.

Yayoshi-Yamamoto S, Taniuchi I, Watanabe T (2000). “FRL, a novel formin related protein, binds to Rac and regulated cell motility and survival of macrophages”. Mol Cell Biol 20: 6872–6881.

Zaidel-Bar R, Ballestrem C, Kam Z, Geiger B. (2003). "Early molecular events in the assembly of matrix adhesions at the leading edge of migrating cells". J Cell Sci 116(Pt 22): 4605-13.

Zalevsky J, Grigorova I, Mullins RD. (2001a). “Activation of the Arp2/3-complex by the *Listeria* acta protein. acta binds two actin monomers and three subunits of the Arp2/3-complex”. J. Biol. Chem. 276:3468–75.

Zalevsky J, Lempert L, Kranitz H, Mullins RD. (2001b). “Different WASP family proteins stimulate different Arp2/3-complex dependent actin-nucleating activities”. Curr.Biol. 11:1903–13.

Zhu XL, Liang L, Ding YQ (2008) “Over-expression of FMNL2 is closely related to metastasis of colorectal cancer”. Int J Colorectal Dis. 23(11):1041-7

Zhou W, Parent LJ, Wills JW, Resh MD. (1994). “Identification of a membrane-binding domain within the amino-terminal region of human immunodeficiency virus type 1 Gag protein which interacts with acidic phospholipids”. J Virol. 68(4):2556-69.

Zigmond SH, Evangelista M, Boone C, Yang C, Dar AC, Sicheri F, Forkey J, Pring M. (2003). “Formin leaky cap allows elongation in the presence of tight capping proteins”. Curr Biol. 13(20):1820-3.

Zuchero JB, Coutts AS, Quinlan ME, Thangue NB, Mullins RD. (2009). “p53-cofactor JMY is a multifunctional actin nucleation factor”. Nat Cell Biol.11(4):451-9

Zuniga A, Michos O, Spitz F, Haramis AP, Panman L, Galli A, Vintersten K, Klasen C, Mansfield W, Kuc S, Duboule D, Dono R, Zeller R. (2004). “Mouse limb deformity mutations disrupt a global control region within the large regulatory landscape required for Gremlin expression”. Genes Dev. 8(13):1553-64.

9 Appendix

9.1 Video Legends (Supplementary material available on CD)

Movie1. B16-F1 cell moving on laminin and expressing EGFP-tagged full-length human Drf3. Display rate is 330-fold. Bar is 10 µm.

Movie 2. B16-F1 cell over-expressing EGFP-tagged, active Drf3. Display rate is 330-fold. Bar is 10 µm.

Movie 3. Control siRNA-treated (Control RNAi) VA-13 fibroblast cell (Steffen *et al.*, 2006) transiently transfected with Drf3ΔDAD. Display rate is 330-fold. Bar is 10 µm.

Movie 4. Nap1 knockdown VA-13 fibroblast (Nap1 RNAi) transiently expressing Drf3ΔDAD. Note prominent formation of filopodia tipped by EGFP-tagged Drf3ΔDAD in spite of WAVE-complex loss of function and coincident lack of lamellipodia (Steffen *et al.*, 2004). Display rate is 330-fold. Bar is 10 µm.

Movie 5. B16-F1 cell moving on laminin and expressing EGFP-tagged, active Drf3. Note the accumulation of Drf3 at the tips of both filopodia and lamellipodia-like structures. Display rate is 330-fold. Bar is 10µm.

Movie 6: B16-F1 cell moving on laminin and expression EGFP-tagged full length human FMNL2A. Time as indicated. Bar is 10µm.

Movie 7: B16-F1 cell over-expressing EGFP-tagged full length human FMNL2B. Time as indicated. Bar is 10µm.

Movie 8: Migrating B16-F1 cell expressing EGFP-tagged full length human FMNL2C. Note weak localisation of this splice variant to the lamellipodium in contrast to EGFP-tagged full length human FMNL2A and FMNL2B. Display rate is 330-fold. Bar equals 10µm.

Movie 9: B16-F1 cells moving on laminin and expressing EGFP-tagged, active FMNL2. Note prominent accumulation at the lamellipodium and tips of filopodia. Time as indicated. Bar equals 10µm.

9.2 List of Figures

9.3 List of Tables

10 Lebenslauf

Name: Jennifer Block

email: Jennifer.Block@helmholtz-hzi.de

Geburtsdatum: 04.01.1982

Geburtsort: Friesoythe

Staatsangehörigkeit: Deutsch

Ausbildung:

November 2006 bis heute:	Doktorarbeit in der Arbeitsgruppe für Zytoskelettdynamik am Helmholtz-Zentrum für Infektionsforschung in Braunschweig, Deutschland
Januar 2006- Oktober 2006:	Diplomarbeit „Dynamik und `Turnover´ von Aktinmonomeren in migrierenden Zellen“ in der Arbeitsgruppe für Zytoskelettdynamik am Helmholtz-Zentrum für Infektionsforschung in Braunschweig, Deutschland
Oktober 2001- Oktober 2006:	Diplomstudiengang Biologie an der Technischen Universität Carolo-Wilhelmina zu Braunschweig

Schullaufbahn:

1994-2001:	Albertus-Magnus Gymnasium in Friesoythe, Schulabschluss mit dem Abitur
1992-1994:	Orientierungsstufe Friesoythe
1988-1992:	St. Ludgeri Grundschule Friesoythe